



Phys. Lett. B 803 (2020) 135341
DOI: [10.1016/j.physletb.2020.135341](https://doi.org/10.1016/j.physletb.2020.135341)

CERN-EP-2019-206
16th April 2020

Evidence for electroweak production of two jets in association with a $Z\gamma$ pair in pp collisions at $\sqrt{s} = 13$ TeV with the ATLAS detector

The ATLAS Collaboration

Evidence for electroweak production of two jets in association with a $Z\gamma$ pair in $\sqrt{s} = 13$ TeV proton–proton collisions at the Large Hadron Collider is presented. The analysis uses data collected by the ATLAS detector in 2015 and 2016 that corresponds to an integrated luminosity of 36.1 fb^{-1} . Events that contain a Z boson candidate decaying leptonically into either e^+e^- or $\mu^+\mu^-$, a photon, and two jets are selected. The electroweak component is measured with observed and expected significances of 4.1 standard deviations. The fiducial cross-section for electroweak production is measured to be $\sigma_{Z\gamma jj-\text{EW}} = 7.8 \pm 2.0 \text{ fb}$, in good agreement with the Standard Model prediction.

1 Introduction

At the Large Hadron Collider (LHC), the electroweak (EW) sector of the Standard Model (SM) can be probed by studying the self-coupling of vector bosons, which is precisely predicted through the $SU(2)_L \times U(1)_Y$ gauge symmetry. Vector-boson scattering (VBS), $VV \rightarrow VV$ with $V = W/Z/\gamma$, is one of the most interesting processes to look at to study such effects, as it is sensitive to both the triple and the quartic gauge boson couplings, where physics beyond the SM can significantly alter the SM predictions [1–3].

In hadron collisions, VBS events are characterised by the presence of two bosons and two jets, $VVjj$, that are created in a purely electroweak process [4], through the interaction of bosons that have been radiated from the initial-state quarks. For such events, the scattered quarks are not colour-connected and little hadronic activity is expected in the gap between the two jets. These events are also characterised by a large invariant mass of the dijet system and a large separation of the two jets in rapidity, while the decay products of the bosons are typically produced in the central region.

The $VVjj$ final states, however, are produced mainly through a combination of strong and electroweak interactions in pp collisions. The former are of order $\alpha_S^2 \alpha_{EW}^2$ at the Born level, where α_S is the strong coupling constant and α_{EW} is the electroweak coupling constant. In the following, such processes are referred to as QCD-induced backgrounds, $Z\gamma jj$ –QCD. The production of $VVjj$ events through pure α_{EW}^4 interactions at the Born level are more rare; they are referred to as electroweak processes, $Z\gamma jj$ –EW, in the following. It is not possible to study VBS diagrams independently from other electroweak processes as only the ensemble is gauge invariant [5]. There is also interference between the SM electroweak and QCD-induced processes. Some example Feynman diagrams for these processes are shown in Figure 1.

Among all the possible electroweak production modes, only the $W^\pm W^\pm jj$ and $WZjj$ production processes have been observed [6–9]. Evidence for the $Z\gamma jj$ channel has been reported [10], while limits on electroweak cross-sections have been reported for the $ZZjj$ channel [11], the $W\gamma jj$ channel [12], and the VV channel [13, 14] where at most one of the two bosons decays to two jets.

The $Z\gamma jj$ channel [15] is particularly interesting to study since it allows the measurement of the neutral quartic gauge couplings, as for the ZZ final state but with a larger expected cross-section. The $Z\gamma jj$ cross-sections have been computed at next-to-leading order (NLO) in α_S for both the QCD-induced backgrounds [16] and the electroweak signal [17]. The NLO QCD corrections are not included in the following for either the electroweak signal or the QCD-induced background, as they were not evaluated for the phase space used in this paper.

This Letter reports the evidence for, and the most precise measurements to date of, electroweak $Z\gamma jj$ production, where the Z boson decays leptonically into either e^+e^- or $\mu^+\mu^-$, exploiting the data collected with the ATLAS detector in 2015 and 2016 at a centre-of-mass energy of $\sqrt{s} = 13$ TeV, and corresponding to an integrated luminosity of 36.1 fb^{-1} .

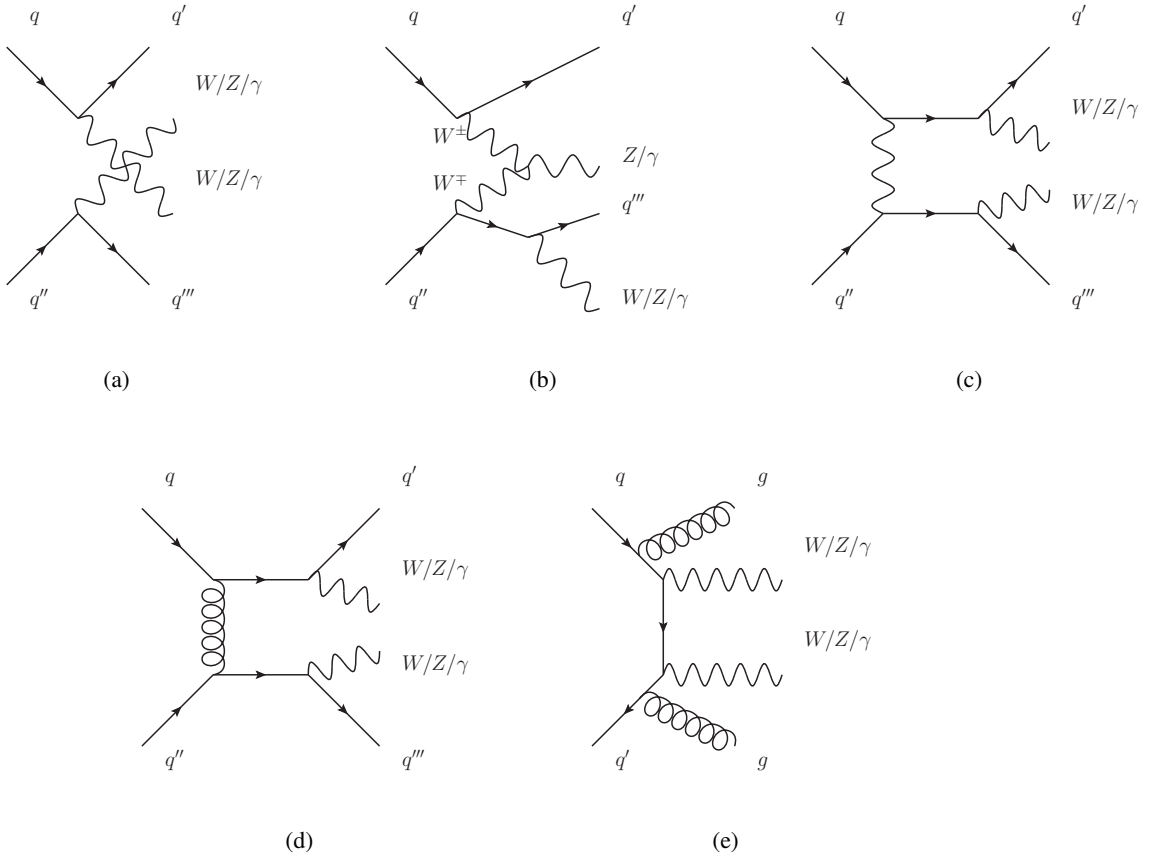


Figure 1: Representative Feynman diagrams of the processes relevant to this analysis: (a) quartic gauge coupling VBS signal, (b) triple gauge coupling, (c) electroweak non-VBS signal, QCD-induced backgrounds with (d) gluon exchange or (e) gluon radiation.

2 ATLAS detector

The ATLAS detector [18–20] is a multipurpose detector with a cylindrical geometry¹ and nearly 4π coverage in solid angle.

The collision point is surrounded by inner tracking detectors, collectively referred to as the inner detector (ID), located within a superconducting solenoid providing a 2 T axial magnetic field, followed by a calorimeter system and a muon spectrometer (MS).

The inner detector provides precise measurements of charged-particle tracks in the pseudorapidity range $|\eta| < 2.5$. It consists of three subdetectors arranged in a coaxial geometry around the beam axis: a silicon pixel detector, a silicon microstrip detector and a transition radiation tracker.

¹ ATLAS uses a right-handed coordinate system with its origin at the nominal interaction point (IP) in the centre of the detector and the z -axis along the beam direction. The x -axis points from the IP to the centre of the LHC ring, and the y -axis points upward. Cylindrical coordinates (r, ϕ) are used in the transverse (x, y) plane, ϕ being the azimuthal angle around the beam direction. The pseudorapidity is defined in terms of the polar angle θ as $\eta = -\ln[\tan(\theta/2)]$.

The electromagnetic (EM) calorimeter covers the region $|\eta| < 3.2$ and is based on high-granularity, lead/liquid-argon (LAr) sampling technology. The hadronic calorimeter uses a steel/scintillator-tile detector in the region $|\eta| < 1.7$ and a copper/LAr detector in the region $1.5 < |\eta| < 3.2$. The most forward region of the detector, $3.1 < |\eta| < 4.9$, is equipped with a forward calorimeter, measuring electromagnetic and hadronic energies in copper/LAr and tungsten/LAr modules, respectively.

The muon spectrometer comprises separate trigger and high-precision tracking chambers to measure the deflection of muons in a magnetic field generated by three large superconducting toroidal magnets arranged with an eightfold azimuthal coil symmetry around the calorimeters. The high-precision chambers cover the range $|\eta| < 2.7$. The muon trigger system covers the range $|\eta| < 2.4$ with resistive-plate chambers in the barrel and thin-gap chambers in the endcap regions.

A two-level trigger system [21] is used to select events in real time. It consists of a hardware-based first-level (L1) trigger and a software-based high-level trigger. The latter employs algorithms similar to those used offline to identify electrons, muons, photons and jets.

3 Signal and background simulation

Signal and background processes are modelled using Monte Carlo (MC) simulations. All MC events were passed through the GEANT4-based [22] ATLAS detector simulation [23]. They are reconstructed and analysed using the same algorithm chain as the data. These events also include additional proton–proton interactions (pile-up) generated with PYTHIA 8.186 [24] using the MSTW2008LO [25] parton distribution functions (PDFs) and the A2 set of tuned parameters [26] (A2 tune). The simulated events are reweighted to reproduce the mean number of interactions per bunch crossing observed during 2015 and 2016 data-taking. The average number of pp interactions per bunch crossing is found to be around 13 in 2015 and 25 in 2016. Scale factors are applied to simulated events to correct for the differences observed between data and MC simulation in the trigger, reconstruction, identification, isolation and impact parameter efficiencies of photons, electrons and muons [27, 28]. The photon energy, electron energy and muon momentum in simulated events are smeared to account for differences in resolution between data and MC simulation [28, 29].

In this analysis, the signal is the electroweak production of $Z(\rightarrow \ell\ell)\gamma jj$ (with $\ell = e, \mu$), with jets originating from the fragmentation of partons arising from electroweak vertices. Signal events ($\ell\ell\gamma jj$) were generated [30] at leading-order (LO) accuracy (at order α_{EW}^5) using MADGRAPH5_AMC@NLO 2.3.3 [31] with no extra parton in the final state. The nominal renormalisation and factorisation scales were set to the transverse mass of the diboson system. The NNPDF30 LO PDF set [32] was used for the generation of the events, and the hadronisation and parton shower of the events was modelled using PYTHIA 8.212 with the A14 tune [33]. An alternative model of hadronisation and parton shower is obtained by re-showering events with Herwig 7.0.1 [34, 35] using the UEEE-5 tune that is based on the models discussed in Ref. [36, 37] in conjunction with the CTEQ6L1 LO PDF set [38].

An alternative sample of simulated events at LO accuracy was generated using SHERPA 2.2.4 [39] with Comix [40] and merged with the SHERPA parton shower [41]. The factorisation and renormalisation scales were set to the invariant mass of the diboson system. The NNPDF30 next-to-next-to-leading order (NNLO) PDF set [32] was used for the generation of this sample.

The main background comes from the QCD-induced production of the $Z(\rightarrow \ell\ell)\gamma jj$ final state, which is estimated at leading order, i.e. at order $\alpha_S^2 \alpha_{EW}^3$. The MC sample used to model this background was

obtained with the **SHERPA** 2.2.2 event generator for the $\ell\ell\gamma$ process with up to one parton at NLO generated with **OpenLoops** [42] and up to three partons at LO using **Comix**. The different final-state multiplicities were merged with the **SHERPA** parton shower using the ME+PS@NLO prescription [43]. This sample was generated using the NNPDF30 NNLO PDF set.

An alternative QCD sample was used to study the dependence of the kinematic distributions on the matrix-element generator. This sample was obtained with **MADGRAPH5_AMC@NLO** 2.3.3 with up to one parton at NLO for the $\ell\ell\gamma$ process. The second jet is obtained from the real emission at matrix-element level, i.e. with LO accuracy. The event generator was interfaced to **PYTHIA** 8.212 for the inclusion of the parton shower and hadronisation of the events; the FxFx merging prescription was used [44] with a merging scale of 20 GeV. The NNPDF30 NLO PDF set and the A14 tune were used for the generation.

Interference between the electroweak and QCD processes was estimated at LO accuracy in QCD using the **MADGRAPH5_AMC@NLO** 2.3.3 MC event generator with the NNPDF30 LO PDF set including only contributions to the squared matrix-element at order $\alpha_S \alpha_{EW}^4$. The event generator was interfaced to **PYTHIA** 8.212 for the parton showers and hadronisation of the events with the A14 tune. These interference effects are found to be positive and are of the order of 3% of the $Z\gamma jj$ –EW cross-section in the fiducial phase space studied by this analysis.

The second-largest background in this analysis is due to Z +jets processes. In this case, one of the jets is misidentified as a photon. This contribution is estimated using a data-driven method, as explained in Section 5. Cross-checks are performed using a **SHERPA** 2.2.1 MC sample [45], produced with up to two jets at NLO accuracy and up to four jets at LO accuracy, using **Comix** and **OpenLoops**, and merged with the **SHERPA** parton shower according to the ME+PS@NLO prescription. The NNPDF30 NNLO PDF set was used for the generation of this sample. This sample is scaled to the NNLO predictions for inclusive Z production using a normalisation factor [45] derived from **FEWZ** [46] and the **MSTW2008NNLO** PDF set [25].

The third-largest background affecting this analysis is from $t\bar{t} + \gamma$ events. These events were generated at LO accuracy using the **MADGRAPH5_AMC@NLO** 2.3.3 generator interfaced to **PYTHIA** 8.212 for the parton showering and hadronisation. The NNPDF23 LO PDF set and the A14 tune were used for the generation. The normalisation of the predictions is corrected for NLO QCD effects [47].

All other backgrounds are smaller and are obtained from MC simulations. The most important of these are the WZ background, which was simulated with **SHERPA** 2.2.1 and the NNPDF30 NNLO PDF set, and the Wt background, which was simulated with the **POWHEG-Box** [48–50] generator interfaced to **PYTHIA** 6.428 [51] and the **PERUGIA** 2012 tune [52]. The CT10 NLO PDF set [53] was used for the generation of this sample.

4 Event selection

Events are selected if they were recorded during stable beam conditions and if they satisfy detector and data quality requirements, which include all relevant subdetectors functioning normally. Events were collected using single-lepton or dilepton triggers [21, 54] that require, respectively, at least one or two electrons or muons.

For single-lepton triggers, the transverse momentum (p_T) threshold in 2015 was 24 GeV for electrons and 20 GeV for muons satisfying a loose isolation requirement based only on ID track information. In 2016,

due to the higher instantaneous luminosity, these thresholds were increased to 26 GeV for both the electrons and muons, and tighter isolation requirements were applied. Inefficiencies for leptons with large transverse momenta were reduced by including additional electron and muon triggers that do not include any isolation requirements; these had transverse momentum thresholds of 60 GeV and 50 GeV, respectively. Finally, a single-electron trigger requiring $p_T > 120$ GeV with less restrictive electron identification criteria was used to increase the selection efficiency for high- p_T electrons. The threshold was increased to 140 GeV in 2016. In 2015, the dilepton trigger p_T threshold was 12 GeV for electrons, and either 10 GeV for muons in conjunction with two muons producing L1 triggers, or 18 GeV and 8 GeV in the case that only one of the two muons produced an L1 trigger. In 2016, these thresholds were raised to 17 GeV for electrons, 14 GeV for the symmetric dimuon trigger, and 22 GeV and 8 GeV for the asymmetric muon trigger. The combined efficiency of these triggers is close to 100% for the events that pass the kinematic requirements described below. To ensure that the trigger efficiency is well determined, the lepton candidates must be matched to the leptons that are selected by the trigger and have a transverse momentum at least 1 GeV above the online threshold.

Events must have a primary vertex with at least two charged-particle tracks which must be compatible with the pp interaction region. In cases where multiple vertices are reconstructed in a single event, the vertex with the highest sum of the p_T^2 of the associated tracks is selected as the production vertex of the $Z\gamma$ system.

Muons are reconstructed by matching tracks in the muon spectrometer to tracks in the inner detector. Candidate muons are required to satisfy the ‘medium’ set of identification criteria [28] based on the number of detector hits and p_T measurements in the ID and the MS. The efficiency of selecting such muons averaged over p_T and η is larger than 98%. Both the ID and MS measurements are used to compute the muon momentum. The measurement also takes into account the energy loss in the calorimeters. Muons are used in the analysis if they satisfy $p_T > 20$ GeV and $|\eta| < 2.5$.

Electrons are reconstructed by matching energy clusters in the electromagnetic calorimeter to an ID track. Candidate electrons are required to pass a ‘medium’ likelihood requirement that is built from information about the electromagnetic shower shape in the calorimeter, track properties and the track-to-cluster matching [27]. The efficiency of selecting such electrons is of about 90%. Calorimeter energy and the track’s direction are combined to compute the electron momentum. Electrons are required to satisfy $p_T > 20$ GeV and $|\eta| < 2.47$.

To ensure that electron and muon candidates originate from the primary vertex, the significance of the track’s transverse impact parameter relative to the beam line must satisfy $|d_0/\sigma_{d_0}| < 3$ (5) for muons (electrons), and the longitudinal impact parameter z_0 , the difference between the value of z at the point on the track at which d_0 is defined and the longitudinal position of the primary vertex, is required to satisfy $|z_0 \cdot \sin(\theta)| < 0.5$ mm.

Electrons and muons are required to be isolated from hadronic activity by imposing maximum energy requirements in cones in the η – ϕ plane, defined using the $\Delta R = \sqrt{(\Delta\eta)^2 + (\Delta\phi)^2}$ distance, around their direction of flight, using calorimeter-cluster and ID-track information, excluding the electron or muon momentum. They are selected following the ‘gradient loose’ requirements [27, 28]. The muon isolation criterion imposes a fixed upper limit in a cone of size $\Delta R = 0.2$ for calorimeter-based isolation and in a cone of size $\Delta R = 0.3$ for ID-based isolation, with a selection efficiency above 90% for $p_T > 20$ GeV and at least 99% for $p_T > 60$ GeV. For electrons, the requirements vary with p_T , allowing a selection efficiency of at least 90% for $p_T > 25$ GeV and at least 99% for $p_T > 60$ GeV. For electrons, both isolation variables are evaluated with a cone of size $\Delta R = 0.2$.

Photon candidates are reconstructed from clusters of energy deposited in the electromagnetic calorimeter and are classified as unconverted (clusters without a matching track or matching reconstructed conversion vertex in the ID) or converted (clusters with a matching reconstructed conversion vertex or a matching track consistent with originating from a photon conversion). Photons are identified using a cut-based selection relying on shower shapes measured with the electromagnetic calorimeter. Nine discriminating variables are used, built from the distribution of energy in different layers of the EM calorimeter and information about energy leaking into the hadronic calorimeter. The shower shape values in the simulation are corrected to improve their agreement with the shower shapes in data. Photons must satisfy a ‘tight’ requirement [55]. Photons selected in this analysis must satisfy $E_T > 15$ GeV, where E_T is the photon transverse energy, and the pseudorapidity of the cluster must be in the range $|\eta| < 1.37$ or $1.52 < |\eta| < 2.37$, to avoid the transition region between barrel and endcap calorimeters. Photon candidates are required to be isolated according to calorimeter-cluster and ID-track information in a cone of size $\Delta R = 0.2$, excluding the photon energy. The requirement varies with E_T following the ‘fixed loose’ requirement [55], providing an average efficiency of about 95%. The calorimetric photon isolation is corrected to account for leakage and the contribution from the underlying event and pile-up transverse energy [27].

Jets are reconstructed from clusters of energy depositions in the calorimeter [56] using the anti- k_t algorithm [57, 58] with a radius parameter $R = 0.4$. Calibration of the jet energy is based on simulation and *in situ* methods from data [59]. Jets originating from non-collision backgrounds or detector noise are removed [60]. Pile-up jets are suppressed using a multivariate combination of track-based variables in the ID acceptance ($|\eta| < 2.5$) [61]. All jets considered must have $p_T > 25$ GeV and must be reconstructed in the pseudorapidity range $|\eta| < 4.5$.

Jets containing a b -hadron are identified in the ID volume using a multivariate algorithm [62, 63] that uses the impact parameters and secondary vertices of the tracks contained in the jet. The selection is done using a working point chosen to provide a 70% selection efficiency for b -jets in an inclusive $t\bar{t}$ MC sample. The 70% working point has rejection factors of 10 and 400 for charm and light-flavour jets, respectively. Correction factors are applied to the simulated event samples to compensate for differences between data and simulation in the flavour-tagging efficiencies for b -jets, c -jets and light-flavour jets. The correction for b -jets is derived from $t\bar{t}$ events with final states containing two leptons, and the corrections are consistent with unity with uncertainties at the level of a few percent over most of the jet p_T range.

To avoid cases in which a lepton, photon, or jet is reconstructed as two separate final-state objects, several steps are followed to remove such overlaps. Bremsstrahlung radiation by a muon can result in ID tracks and a calorimeter energy deposit that are reconstructed as an electron candidate. Therefore, in cases for which an electron candidate and a muon candidate share an ID track, the object is considered to be a muon, and the electron candidate is rejected. The overlap of objects is measured using the ΔR distance. Due to the isolation requirements placed on electron candidates, any jets that closely overlap an electron candidate within a conical region $\Delta R < 0.2$ are likely to be reconstructions of the electron and so are rejected. When jets and electrons are found within a larger hollow conical region $0.2 < \Delta R < 0.4$, it is more likely that a real hadronic jet is present and that the electron is a non-prompt constituent of the jet, arising from the decay of a heavy-flavour hadron. Hence an electron candidate found within $\Delta R < 0.4$ of any remaining jet is rejected. Muons can be accompanied by a hard photon due to bremsstrahlung or collinear final-state radiation, and the muon–photon system can then be reconstructed as both a jet and a muon candidate. Non-prompt muons can arise from decays of hadrons in jets; however, these muons are associated with a higher ID track multiplicity than those accompanied by hard photons. In order to resolve these ambiguities between nearby jet and muon candidates, first any jets having fewer than three ID tracks and within $\Delta R < 0.4$ of any muon candidate are rejected, then any muon candidates within $\Delta R < 0.4$ of

any remaining jet are rejected. The ambiguity between photons and leptons is resolved by rejecting any photons found to be within $\Delta R < 0.4$ of an electron or a muon. Jets found within $\Delta R < 0.4$ of any photons are rejected.

Events are required to contain exactly two lepton candidates (electrons or muons) with the same flavour and opposite charge and at least one photon candidate satisfying the selection criteria described above. When there are two or more photons selected, the one with the highest E_T is used for further processing.

The invariant mass of the two leptons, $m_{\ell\ell}$, must be at least 40 GeV. The sum of the dilepton mass and the three-body $\ell\ell\gamma$ invariant mass ($m_{\ell\ell} + m_{\ell\ell\gamma}$) is required to be larger than 182 GeV, which is twice the Z boson mass. This requirement ensures that the three-body invariant mass is larger than the Z boson mass, thus suppressing cases where the Z boson decays into $\ell\ell\gamma$ [15, 64].

To select electroweak processes, events are further required to include at least two ‘VBS-tagging’ jets. A symmetric selection of $p_T > 50$ GeV is used to select both tagging jets, which are classified as leading and subleading in transverse momentum. These two jets are required to have an invariant mass $m_{jj} > 150$ GeV, in order to minimise the contamination from triboson background in which a hadronically decaying W or Z boson is produced in association with a Z boson and a photon, i.e. $Z\gamma + Z/W(\rightarrow jj)$.

The final VBS signal region (SR) is defined by requiring that the pseudorapidity difference between the two leading jets $|\Delta\eta(jj)|$ be larger than 1; that no b -tagged jet be present in the event; and that the centrality of the $\ell\ell\gamma$ system relative to the tagging jets, defined as

$$\zeta(\ell\ell\gamma) = \left| \frac{y_{\ell\ell\gamma} - (y_{j_1} + y_{j_2})/2}{(y_{j_1} - y_{j_2})} \right|, \quad (1)$$

be lower than 5, where y corresponds to the rapidity, and j_1 and j_2 label the selected leading and subleading jets.

5 Background estimation

Irreducible backgrounds are modelled kinematically by MC simulations, and their normalisation is evaluated from the data. Reducible backgrounds, in which a photon originates from a hadron decay, are determined using data-driven techniques. Events in which one or more leptons originate from a hadronic jet are suppressed by the stringent lepton selection. They are found to be negligible and are not considered here.

The main reducible background originates from Z -jets events, in which one hadronic jet is misidentified as a photon. This background is not well modelled by the MC simulation and, therefore, is estimated with data using a two-dimensional sideband method [65] similar to that applied in a previous analysis with Run 1 data [15]. The shapes of the distributions of Z -jets events are obtained using data, after applying all the signal requirements, but reversing the photon identification and isolation criteria [55]. The normalisation of this background is estimated in a control region designed to maximise the number of events available in the data while being close to the signal region; all signal region requirements are applied, except the transverse momentum requirement for the jets, which is lowered to 30 GeV, and the dijet invariant mass requirement, which is less than 150 GeV. The ratio of Z -jets to $Z\gamma jj$ -QCD events is computed in this region, since it is found to be the same in this control region and in the signal region, in both data and MC simulation, and used to extrapolate the normalisation of Z -jets events to the signal region. To estimate

both the shape and the normalisation of this background, the contamination from events containing real photons is estimated and corrected using MC predictions.

The most important background is irreducible and comes from the QCD-induced production of $Z\gamma$ events in association with two jets. The normalisation of this background is constrained by the data, as explained in Section 6.

The other main irreducible background arises from $t\bar{t} + \gamma$ events. This process is also constrained by the data in a dedicated control region which is referred to as b -Control Region (b -CR). This control region is obtained by imposing all SR selections but requiring the presence of at least one reconstructed b -tagged jet in the event.

The contribution of backgrounds due to the production of $Z+jets$ and $\gamma+jets$ events in two different overlaid interactions is evaluated using a data-driven estimate following the method described in Ref. [64] and found to be negligible.

Backgrounds from other sources are reducible and are evaluated using MC simulations. The most important contribution comes from WZ events, in which a charged lepton is misidentified as a photon, and from Wt events.

6 Signal extraction procedure

A boosted decision tree (BDT), as implemented in the TMVA package [66], is used to separate the electroweak signal from all the backgrounds. The BDT is trained and the set of variables retained as input to the BDT is optimised on simulated events to separate $Z\gamma jj$ –EW events from all background processes, excluding $Z+jets$, and to maximise the signal-to-background ratio. In total, 13 kinematic variables are combined into one discriminant that can take any value in the range $[-1, 1]$. The final binning of the BDT discriminant, or BDT score, is optimised to improve the sensitivity of the analysis.

Some of the variables used in the BDT training are related to the kinematic properties of the two tagging jets: the invariant mass of these two jets, m_{jj} , the difference in pseudorapidity between these two jets, $\Delta\eta_{jj}$, and the pseudorapidity and p_T of the leading jet. Other variables are related to the kinematic properties of the photon and the Z boson: the transverse momenta of the leading lepton, the $\ell\ell$ system and the $\ell\ell\gamma$ system, and the $\ell\ell$ and $\ell\ell\gamma$ invariant masses. Another set of variables is related to the correlation of the two tagging jets and the $Z\gamma$ system: the distance in the η – ϕ plane between the $Z\gamma$ system and the two-jet system, $\Delta R(Z\gamma, jj)$; the smallest distance in the η – ϕ plane between a photon and a jet, among all possible combinations, $\text{Min}(\Delta R(\gamma, j))$; the difference in azimuth between the $Z\gamma$ system and the two-jet system, $\Delta\phi(Z\gamma, jj)$ and the centrality $\zeta(\ell\ell\gamma)$ as defined in Eq. (1).

The modelling by MC simulations of the distribution shapes and the correlations between all input variables for the BDT is verified in the signal region. Compatibility within the uncertainties is observed for all distributions, as exemplified by Figures 2(a) and 2(b), except for the high-mass tail of m_{jj} as shown in Figure 2(c), as was also observed in previous analyses of electroweak processes [67–69]. This mismodelling does not impact the signal significance nor the uncertainty in the measurement reported in Section 9.

The BDT score distribution in the signal region is used to measure the $Z\gamma jj$ –EW signal fiducial cross-section with a maximum-likelihood fit, and to determine the significance of the signal. In this fit the $e\gamma jj$ and $\mu\gamma jj$ final states are combined. An extended likelihood function is built from the product of two likelihoods corresponding to the BDT score distribution in the $Z\gamma jj$ SR, and the multiplicity

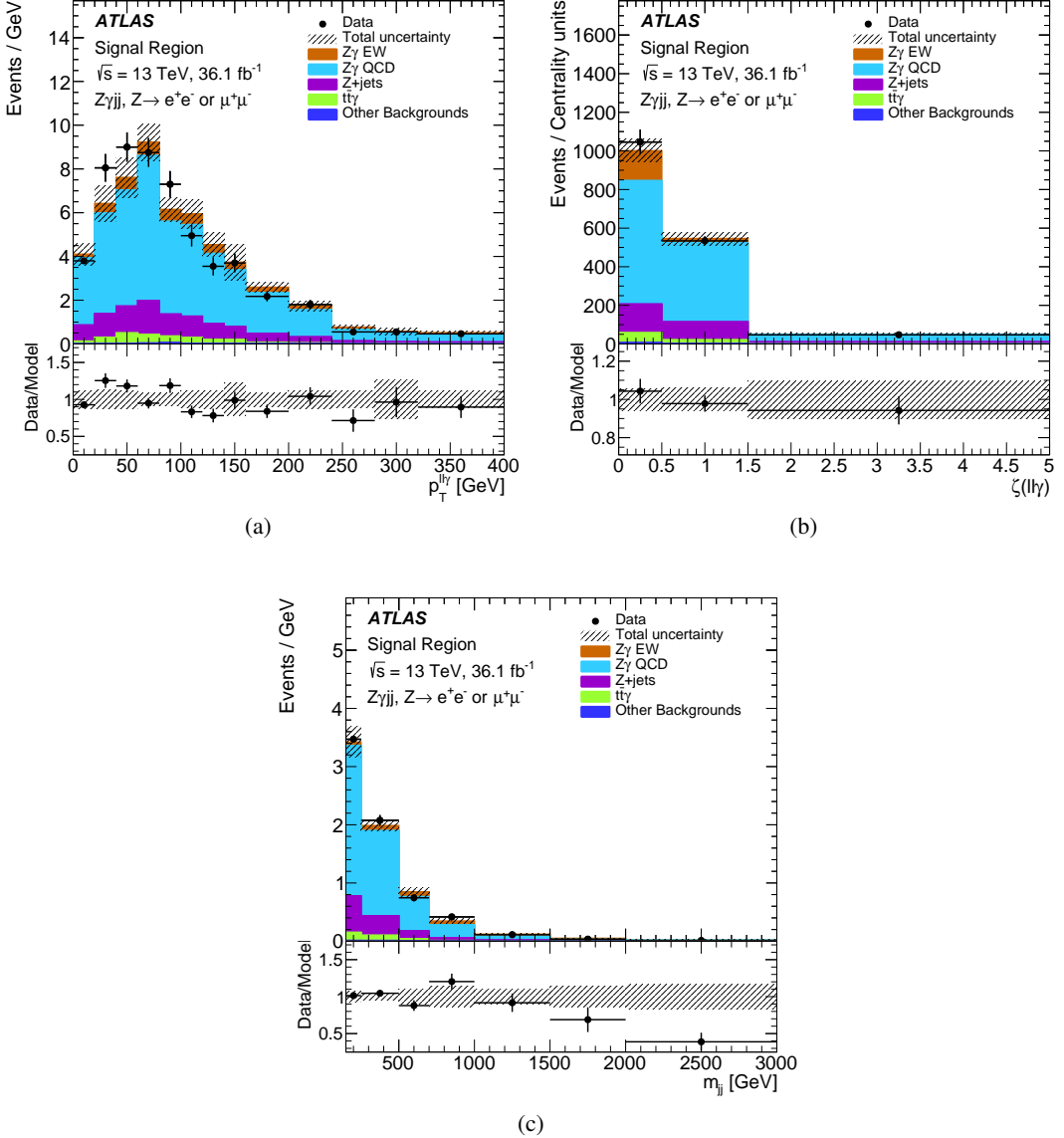


Figure 2: Post-fit distributions of (a) the transverse momentum of the $\ell\ell\gamma$ system, (b) the centrality of the $\ell\ell\gamma$ system relative to the tagging jets, and (c) m_{jj} in the signal region. The uncertainty band around the expectation includes all systematic uncertainties and takes into account their correlations as obtained from the fit. Events beyond the upper limit of the histogram are included in the last bin of the distribution.

of reconstructed b -jets in the b -CR. The yields of the $t\bar{t} + \gamma$ simulated events are constrained by data using this last distribution. The normalisation of the $Z\gamma jj$ -QCD sample is also constrained by the data, directly in the signal region, since this background dominates the distribution at low BDT score values. The normalisations of these backgrounds are introduced in the likelihood fit as unconstrained nuisance parameters, labelled as $\mu_{Z\gamma jj\text{-QCD}}$ and $\mu_{t\bar{t}+\gamma}$ for the $Z\gamma jj$ -QCD and $t\bar{t} + \gamma$ backgrounds, respectively. These parameters are relative normalisation factors, defined with respect to the SM predictions. For these backgrounds, the kinematic distributions are obtained from MC simulations. Both the shape and the normalisation distributions of $Z + \text{jets}$ background are estimated from data, as described in Section 5. The other irreducible backgrounds are determined from MC simulations. Background normalisations and shapes can vary within the uncertainties, constrained by Gaussian distributions as described in Section 7.

The fiducial cross-section is derived using the signal strength parameter $\mu_{Z\gamma jj\text{-EW}}$:

$$\mu_{Z\gamma jj\text{-EW}} = \frac{N_{Z\gamma jj\text{-EW}}^{\text{data}}}{N_{Z\gamma jj\text{-EW}}^{\text{MC}}} ,$$

where $N_{Z\gamma jj\text{-EW}}^{\text{data}}$ is the number of signal events measured in the data, while $N_{Z\gamma jj\text{-EW}}^{\text{MC}}$ is the number of signal events predicted by the `MADGRAPH5_AMC@NLO 2.3.3` MC simulation.

The observed cross-section ($\sigma_{Z\gamma jj\text{-EW}}^{\text{fid., data}}$) is then obtained by multiplying the signal strength $\mu_{Z\gamma jj\text{-EW}}$ by the `MADGRAPH5_AMC@NLO 2.3.3` MC cross-section prediction in the fiducial region ($\sigma_{Z\gamma jj\text{-EW}}^{\text{fid., MC}}$). Because the effect of interference between the $Z\gamma jj$ -QCD and the $Z\gamma jj$ -EW processes is not accounted for in the $Z\gamma jj$ -QCD contribution, the observed cross-section $\sigma_{Z\gamma jj\text{-EW}}^{\text{fid.}}$ formally corresponds to electroweak production plus the interference effects.

7 Systematic uncertainties

Several sources of systematic uncertainty in the signal and background processes can affect the cross-section measurement. For the background and signal processes, all systematic uncertainties that affect the shapes of the BDT score and $N_{b\text{-jets}}$ distributions are considered. In addition, all systematic uncertainties that affect the acceptance and normalisation of the distributions are considered for all processes, except for the theory uncertainties in the signal process, where only the effect on the acceptance is considered. Systematic uncertainties in the shapes of distributions are not applied if they are consistent with statistical fluctuations.

The uncertainties in the theoretical modelling of the signal and backgrounds that are estimated from MC simulations can affect the cross-section measurement. The uncertainties due to the knowledge of the PDF and the α_S value used in the generation of the MC samples are determined using the PDF4LHC prescription [70]. They are found to be of the order of 2% for the normalisation of the QCD and $t\bar{t}\gamma$ samples. The uncertainties due to missing higher-order QCD corrections are evaluated using an envelope of the largest deviations obtained by varying the renormalisation and factorisation scales independently by factors of two and one-half. These uncertainties are large for the $Z\gamma jj$ -QCD and $t\bar{t} + \gamma$ backgrounds and their impact on the normalisation is $^{+30}_{-20}\%$. The shape uncertainties due to the missing higher-order QCD corrections are of 2–4% for the signal and the $Z\gamma jj$ -QCD and $t\bar{t} + \gamma$ backgrounds.

For the signal and $t\bar{t} + \gamma$ background, uncertainties due to the parton shower and underlying-event modelling are evaluated using dedicated tune variations [33] and by re-showering events with Herwig 7.0.1 instead of PYTHIA 8.212. These uncertainties affect the shape of the distribution by at most 5% at large values of the BDT score and are negligible at low values of the BDT score. For the signal this uncertainty takes into account a problem with color flow connection in VBS-like topology that was observed and reported in Ref. [71, 72] in the parton shower models of PYTHIA 8.212 and SHERPA 2.2.4. For the $Z\gamma jj$ -QCD background, the modelling uncertainties due to the parton showers, underlying-event and matrix elements are estimated by comparing the predictions of the SHERPA 2.2.2 and MADGRAPH5_AMC@NLO 2.3.3 MC generators. The difference between these two predictions is taken as a systematic uncertainty applied as both a positive and a negative variation. The effects in the BDT score distribution and the $N_{b\text{-jets}}$ distribution due to these two set-ups are taken as uncertainties. The main impact is on the BDT score distribution with an effect ranging from -5% to 20% at low and high values of the BDT score, respectively.

As discussed in Section 6, the interference between the electroweak signal and the $Z\gamma jj$ -QCD process is not included in the fit. However, this interference can distort the shape of the $Z\gamma jj$ -EW template. This effect is estimated using the MADGRAPH5_AMC@NLO 2.3.3 MC generator at LO in QCD, and is taken as a systematic uncertainty in the shape of the signal. The size of this effect ranges from 5% to 2% at low and high values of the BDT score, respectively.

Another source of uncertainty arises from the sizes of the MC samples and data sample in the regions used in the analysis to model the BDT score and $N_{b\text{-jets}}$ distributions. The statistical uncertainty in the shape of the BDT score for $Z\gamma jj$ -QCD events ranges from 5% to 13% at low and high values of the BDT score, respectively, and is about 2% for $Z\gamma jj$ -EW events. For the Z +jets background, the statistical uncertainty dominates the shape uncertainty due to the size of the data sample; it is about 10% at low BDT score values, and up to 50% at high values, while uncertainties from other sources are negligible. The statistical uncertainty in the shape of $N_{b\text{-jets}}$ is about 25% for $Z\gamma jj$ -QCD and is about 3% for $t\bar{t}\gamma$ events.

Other systematic uncertainties originate from the reconstruction, identification, and energy calibration of electrons, photons, muons, and jets. The largest of these uncertainties is due to the jet energy scale calibration. The uncertainties due to the jet energy resolution and to the suppression of pile-up jets are also considered, as described in Ref. [73]. The total effect of the uncertainties related to jet reconstruction and calibration on the normalisation of the $Z\gamma jj$ -QCD background is about 8%, and it is about 4% for $Z\gamma jj$ -EW events in the signal region. The impact on the shape is largest for the $Z\gamma jj$ -QCD events and ranges from 2% to 18% at low and high BDT values, respectively. The uncertainty due to the heavy-flavour tagging efficiency amounts to 9% (2%) in normalisation in the signal (b -CR) region for the $t\bar{t} + \gamma$ background, whereas the impact on other backgrounds and on the shape of the template distributions is found to be negligible. Uncertainties in the lepton identification, reconstruction, isolation requirements, trigger efficiencies, energy scale and energy resolution are determined by using $Z \rightarrow \ell\ell$ events [27, 28, 74]. The largest experimental uncertainty associated with the photons is the photon identification efficiency [55]. The photon and lepton uncertainties affect only the normalisation of $Z\gamma jj$ -EW, $Z\gamma jj$ -QCD, and $t\bar{t} + \gamma$ processes. In total, these effects are of 3% to 4% in the signal region.

A 20% yield uncertainty is assigned to the Z +jets reducible background estimate. This uncertainty accounts for the number of events in the control regions used in the two-dimensional sideband measurement, and for the correlation between photon identification and isolation requirements. A 20% yield uncertainty is assigned to the other backgrounds estimated from simulations.

A variation in the pileup reweighting of MC samples is included to cover the uncertainty on the ratio between the predicted and measured inelastic cross-section [75]. The resulting uncertainty in the measured

fiducial cross-section is 5%.

The uncertainty in the combined 2015–2016 integrated luminosity is 2.1% [76], obtained using the LUCID-2 detector [77] for the primary luminosity measurements.

The effect of each of these uncertainties on the fiducial cross-section measurement is shown in Table 1. The individual sources are grouped into either theoretical or experimental categories. The largest uncertainties are due to the jet reconstruction and calibration, followed by the uncertainty arising from the sizes of the MC samples, and the theoretical uncertainties in the modelling of the $Z\gamma jj$ –EW signal and of the $Z\gamma jj$ –QCD background. Uncertainties affecting only the normalisation of the $Z\gamma jj$ –QCD and $t\bar{t}\gamma$ background have almost no impact on the $Z\gamma jj$ –EW cross-section measurement since the corresponding normalisation parameters are constrained by the fit to the data as explained in Section 6.

Table 1: Relative uncertainties in the measured fiducial cross-section $\sigma_{Z\gamma jj\text{--EW}}^{\text{fid}}$. The uncertainties are expressed in percentages. The correlations between these uncertainties are taken into account in the computation of the total uncertainty.

Source	Uncertainty [%]
Statistical	+19 -18
$Z\gamma jj$ –EW theory modelling	+10 -6
$Z\gamma jj$ –QCD theory modelling	± 6
$t\bar{t} + \gamma$ theory modelling	± 2
$Z\gamma jj$ –EW and $Z\gamma jj$ –QCD interference	+3 -2
Jets	± 8
Pile-up	± 5
Electrons	± 1
Muons	+3 -2
Photons	± 1
Electrons/photons energy scale	± 1
b -tagging	± 2
MC statistical uncertainties	± 8
Other backgrounds normalisation (including Z +jets)	+9 -8
Luminosity	± 2
Total uncertainty	± 26

8 Phase space for cross-section measurements

The $Z\gamma jj$ electroweak cross-section is measured in a fiducial phase space that is defined to closely follow the selection criteria of the signal region described in Section 4. This region is defined at the particle level, using stable particles (with a proper decay length $c\tau > 10$ mm) which are produced from the hard scattering, including those that are the products of hadronisation, before their interaction with the detector. Leptons produced in the decay of a hadron, a τ -lepton, or their descendants are not considered in the

definition of the fiducial phase space. Prompt-lepton four-momenta are obtained from a sum of the leptons four-momenta and the four-momenta of photons not originating from hadron decays within a cone of size $\Delta R = 0.1$ around the leptons ('dressed leptons'). Jets are reconstructed using the anti- k_t algorithm with radius parameter $R = 0.4$ using stable particles, excluding electrons, muons, neutrinos, and photons associated with the decay of a W or Z boson. Photon isolation is defined as the transverse momentum of the system of stable particles within a cone of size $\Delta R = 0.2$ around the photon, excluding muons, neutrinos, and the photon itself.

The following selection requirements are imposed to define the fiducial phase space. The charged leptons from the Z boson decay are required to have transverse momentum $p_T > 20$ GeV and $|\eta| < 2.5$, and the invariant mass of the two leptons must be larger than 40 GeV. The photon is required to have transverse momentum $p_T > 15$ GeV and $|\eta| < 2.37$. Photons isolated from any hadronic activity are selected by requiring that the photon isolation, as defined above, divided by the photon transverse momentum be less than 5%. The angular distance between each of the charged leptons from the Z decay and the photon is required to be $\Delta R > 0.4$. The sum of the two-lepton invariant mass and two-lepton plus photon invariant mass must satisfy $(m_{\ell\ell} + m_{\ell\ell\gamma}) > 182$ GeV in order to exclude final-state radiation events.

In addition to these requirements, at least two jets with $p_T > 50$ GeV and $|\eta| < 4.5$ are required. The angular distance between each of the charged leptons from the Z boson decay and each of the jets is required to be $\Delta R(j, \ell) > 0.3$. The angular distance between the photon and each of the jets is required to be $\Delta R(j, \gamma) > 0.4$. The invariant mass m_{jj} of the two highest- p_T jets is required to be $m_{jj} > 150$ GeV, and the difference between the pseudorapidities of these two leading jets is required to be $|\Delta\eta_{jj}| > 1$. Finally, the centrality of the $\ell\ell\gamma$ system relative to the tagging jets must satisfy $\zeta(\ell\ell\gamma) < 5$.

9 Cross-section measurements

A profile-likelihood-ratio test statistic [78] is used to measure the signal strength $\mu_{Z\gamma jj-\text{EW}}$ and its associated uncertainties. The systematic uncertainties are treated as nuisance parameters and are constrained with Gaussian distributions in the fit. The statistical uncertainty is determined after having fixed each nuisance parameter to the conditional maximum-likelihood estimator [78] also called profiled value. Figure 3 shows the BDT score distribution in the signal region, and the b -tagged jet multiplicity in the b -CR, after having applied the background and signal normalisations and having set the nuisance parameters to the values adjusted by the profile-likelihood fit. The yield of events obtained after the fit is detailed in Table 2.

The signal strength is measured to be:

$$\mu_{Z\gamma jj-\text{EW}} = 1.00 \pm 0.19 \text{ (stat.)} \pm 0.13 \text{ (syst.)}_{-0.10}^{+0.13} \text{ (mod.)} = 1.00 \pm 0.26 ,$$

with "stat." corresponding to the data statistical uncertainty, "syst." to the experimental systematic uncertainties and size of MC samples, and "mod." to the theoretical modelling of the signal and background MC samples. This corresponds to a statistical significance of 4.1 standard deviations both observed and expected. The expected significance is obtained after having applied the backgrounds normalisations, which are found to be $\mu_{Z\gamma jj-\text{QCD}} = 0.78_{-0.20}^{+0.26}$ and $\mu_{t\bar{t}+\gamma} = 1.49_{-0.34}^{+0.40}$. The uncertainty in the normalisation parameter values includes the theoretical uncertainties, such as uncertainties derived from QCD scale variations. The normalisation of the $t\bar{t} + \gamma$ background agrees with results from other studies performed with ATLAS Run 2 data [79] in this final state. The normalisation of the $Z\gamma jj$ -QCD background is

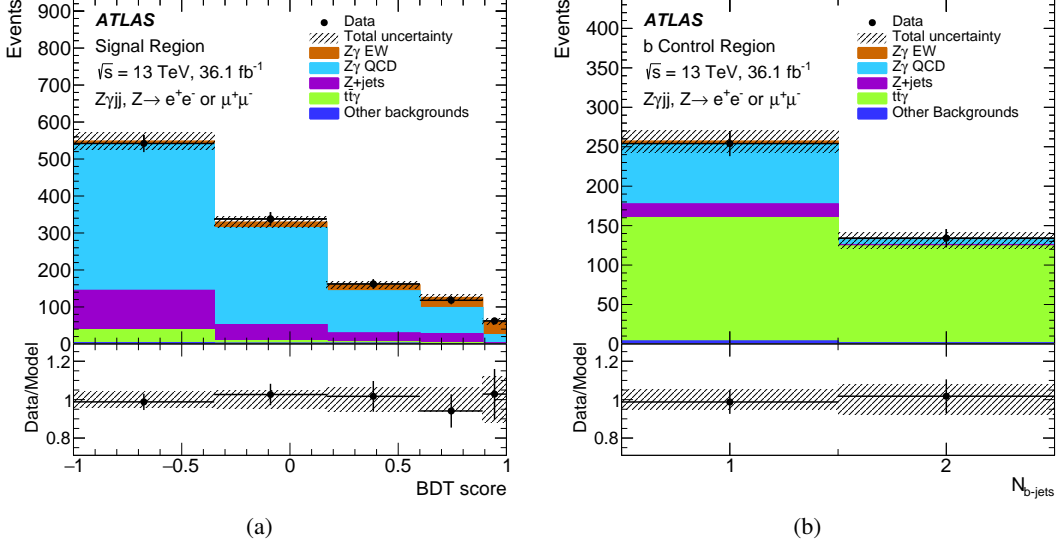


Figure 3: Post-fit distributions of (a) the BDT score in the signal region and of (b) $N_{b\text{-jets}}$ in the b -CR. The uncertainty band around the expectation includes all systematic uncertainties and takes into account their correlations as obtained from the fit. Events beyond the upper limit of the histogram are included in the last bin of the $N_{b\text{-jets}}$ distribution.

Table 2: Expected and observed numbers of events in the signal and control regions, after the fit. The expected number of $Z\gamma jj$ -EW events from `MADGRAPH5_AMC@NLO 2.3.3` and the estimated number of background events from the other processes are shown. Total post-fit uncertainties, as described in Section 7, are shown. The uncertainty in the total expected yield is smaller than the quadratic sum of the uncertainties in each process due to these being anti-correlated after the fit.

	SR		b -CR	
Data	1222		388	
Total expected	1222	± 35	389	± 19
$Z\gamma jj$ -EW (signal)	104	± 26	5	± 1
$Z\gamma jj$ -QCD	864	± 60	82	± 9
$Z+jets$	200	± 40	19	± 4
$t\bar{t} + \gamma$	48	± 10	280	± 21
Other backgrounds	7	± 1	4	± 1

compatible with results obtained in the $WZjj$ final state [7]. It was checked that the signal strength obtained in the combination of the $e\gamma jj$ and $\mu\gamma jj$ final states is consistent with the results obtained separately for each channel.

The fiducial cross-section is measured by computing the product of signal strength and the predicted cross-section used to define it:

$$\begin{aligned}\sigma_{Z\gamma jj-\text{EW}}^{\text{fid.}} &= 7.8 \pm 1.5 \text{ (stat.)} \pm 1.0 \text{ (syst.)} {}^{+1.0}_{-0.8} \text{ (mod.) fb} \\ &= 7.8 \pm 2.0 \text{ fb.}\end{aligned}$$

This cross-section corresponds to the electroweak $Z\gamma jj$ particle-level cross-section in the fiducial phase space defined in Section 8 using dressed leptons, and including constructive interference between the signal and the QCD-induced processes.

This measurement can be compared with the LO cross-section predicted by `MADGRAPH5_AMC@NLO` 2.3.3:

$$\sigma_{Z\gamma jj-\text{EW}}^{\text{fid., MADGRAPH}} = 7.75 \pm 0.03 \text{ (stat.)} \pm 0.20 \text{ (PDF + } \alpha_S \text{)} \pm 0.40 \text{ (scale) fb.}$$

The cross-section predicted by `SHERPA` 2.2.4 is somewhat larger than that predicted by `MADGRAPH5_AMC@NLO` 2.3.3:

$$\sigma_{Z\gamma jj-\text{EW}}^{\text{fid., SHERPA}} = 8.94 \pm 0.08 \text{ (stat.)} \pm 0.20 \text{ (PDF + } \alpha_S \text{)} \pm 0.50 \text{ (scale) fb.}$$

These predictions do not include the effects of interference, which are estimated with `MADGRAPH5_AMC@NLO` 2.3.3 to be 3% in this phase space.

To verify the results of the multivariate analysis, a cut-based approach is also used. The centrality of the $\ell\ell\gamma$ system, $\zeta(\ell\ell\gamma)$, is used as the sensitive variable for the extraction of the electroweak signal. In this alternative method, the signal region is further divided into two regions depending on the dijet invariant mass. The region with $m_{jj} < 500$ GeV is used to constrain the QCD background, while the region $m_{jj} > 500$ GeV is kept to extract the signal. The b -CR is also kept in this method as a second control region to constrain the $t\bar{t} + \gamma$ background normalisation. The profile-likelihood fit is applied in the same way as described above with the full treatment of systematic uncertainties, allowing exclusion of the background-only hypothesis with a statistical significance of 2.9σ (2.7σ) observed (expected). This is compatible with the result obtained with the multivariate approach and with the SM prediction.

The analysis is also used to measure the $Z\gamma jj$ cross-section in the same fiducial phase space. This measurement includes the electroweak-induced signal, the QCD-induced process and their interference. The extraction procedure is the same as for the electroweak $Z\gamma jj$ measurement. A template likelihood fit is performed, using the BDT score distribution in the signal region. For this measurement, the b -CR is not used, to simplify the statistical model. The omission of this control region in the fit does not change the result. The signal template corresponds to the sum of the $Z\gamma jj$ -EW and $Z\gamma jj$ -QCD templates, the relative amount being fixed to SM expectations. The cross-section is measured to be:

$$\begin{aligned}\sigma_{Z\gamma jj}^{\text{fid.}} &= 71 \pm 2 \text{ (stat.)} {}^{+9}_{-7} \text{ (syst.)} {}^{+21}_{-17} \text{ (mod.) fb} \\ &= 71 {}^{+23}_{-19} \text{ fb.}\end{aligned}$$

This agrees with the SM predictions obtained by summing the $Z\gamma jj$ –EW and $Z\gamma jj$ –QCD predictions obtained from **MADGRAPH5_AMC@NLO** 2.3.3 and **SHERPA** 2.2.2, respectively,

$$\sigma_{Z\gamma jj}^{\text{fid., MADGRAPH+SHERPA}} = 88.4 \pm 2.4 \text{ (stat.)} \pm 2.3 \text{ (PDF + } \alpha_S \text{)}^{+29.4}_{-19.1} \text{ (scale) fb.}$$

10 Conclusion

Evidence for electroweak production of two jets in association with a $Z\gamma$ pair is presented using 36.1 fb^{-1} of pp collision data at $\sqrt{s} = 13 \text{ TeV}$ collected with the ATLAS detector at the LHC. The production cross-section of this process is measured in a fiducial phase space approximating the acceptance of the analysis. This measurement uses the leptonic decay of the Z boson into e^+e^- or $\mu^+\mu^-$. The measurement is performed using a BDT to enhance the signal to background-ratio. The dominant backgrounds, $Z\gamma jj$ –QCD, $Z+jets$ and $t\bar{t} + \gamma$ are all estimated from the data. The background-only hypothesis is excluded with observed and expected significances of 4.1 standard deviations.

In the fiducial phase space the electroweak cross-section of the $Z\gamma jj$ process is measured to be:

$$\begin{aligned} \sigma_{Z\gamma jj-\text{EW}}^{\text{fid.}} &= 7.8 \pm 1.5 \text{ (stat.)} \pm 1.0 \text{ (syst.)}^{+1.0}_{-0.8} \text{ (mod.) fb,} \\ &= 7.8 \pm 2.0 \text{ fb} \end{aligned}$$

in good agreement with the Standard Model predictions at LO in perturbative QCD.

Acknowledgements

We thank CERN for the very successful operation of the LHC, as well as the support staff from our institutions without whom ATLAS could not be operated efficiently.

We acknowledge the support of ANPCyT, Argentina; YerPhI, Armenia; ARC, Australia; BMWFW and FWF, Austria; ANAS, Azerbaijan; SSTC, Belarus; CNPq and FAPESP, Brazil; NSERC, NRC and CFI, Canada; CERN; CONICYT, Chile; CAS, MOST and NSFC, China; COLCIENCIAS, Colombia; MSMT CR, MPO CR and VSC CR, Czech Republic; DNRF and DNSRC, Denmark; IN2P3-CNRS and CEA-DRF/IRFU, France; SRNSFG, Georgia; BMBF, HGF and MPG, Germany; GSRT, Greece; RGC and Hong Kong SAR, China; ISF and Benoziyo Center, Israel; INFN, Italy; MEXT and JSPS, Japan; CNRST, Morocco; NWO, Netherlands; RCN, Norway; MNiSW and NCN, Poland; FCT, Portugal; MNE/IFA, Romania; MES of Russia and NRC KI, Russia Federation; JINR; MESTD, Serbia; MSSR, Slovakia; ARRS and MIZŠ, Slovenia; DST/NRF, South Africa; MINECO, Spain; SRC and Wallenberg Foundation, Sweden; SERI, SNSF and Cantons of Bern and Geneva, Switzerland; MOST, Taiwan; TAEK, Turkey; STFC, United Kingdom; DOE and NSF, United States of America. In addition, individual groups and members have received support from BCKDF, CANARIE, Compute Canada and CRC, Canada; ERC, ERDF, Horizon 2020, Marie Skłodowska-Curie Actions and COST, European Union; Investissements d’Avenir Labex, Investissements d’Avenir Idex and ANR, France; DFG and AvH Foundation, Germany; Herakleitos, Thales and Aristeia programmes co-financed by EU-ESF and the Greek NSRF, Greece; BSF-NSF and GIF, Israel; CERCA Programme Generalitat de Catalunya and PROMETEO Programme Generalitat Valenciana, Spain; Göran Gustafssons Stiftelse, Sweden; The Royal Society and Leverhulme Trust, United Kingdom.

The crucial computing support from all WLCG partners is acknowledged gratefully, in particular from CERN, the ATLAS Tier-1 facilities at TRIUMF (Canada), NDGF (Denmark, Norway, Sweden), CC-IN2P3 (France), KIT/GridKA (Germany), INFN-CNAF (Italy), NL-T1 (Netherlands), PIC (Spain), ASGC (Taiwan), RAL (UK) and BNL (USA), the Tier-2 facilities worldwide and large non-WLCG resource providers. Major contributors of computing resources are listed in Ref. [80].

References

- [1] O. J. P. Éboli, M. C. Gonzalez-Garcia and S. M. Lietti, *Bosonic quartic couplings at CERN LHC*, *Phys. Rev. D* **69** (2004) 095005, arXiv: [hep-ph/0310141 \[hep-ph\]](#).
- [2] O. J. P. Éboli, M. C. Gonzalez-Garcia and J. K. Mizukoshi, *$pp \rightarrow jj e^\pm \mu^\pm vv$ and $jj e^\pm \mu^\mp vv$ at $O(\alpha_{em}^6)$ and $O(\alpha_{em}^4 \alpha_s^2)$ for the study of the quartic electroweak gauge boson vertex at CERN LHC*, *Phys. Rev. D* **74** (2006) 073005, arXiv: [hep-ph/0606118 \[hep-ph\]](#).
- [3] C. Degrande et al., *Effective field theory: A modern approach to anomalous couplings*, *Annals Phys.* **335** (2013) 21, arXiv: [1205.4231 \[hep-ph\]](#).
- [4] R. N. Cahn, S. D. Ellis, R. Kleiss and W. J. Stirling, *Transverse-momentum signatures for heavy Higgs bosons*, *Phys. Rev. D* **35** (1987) 1626.
- [5] E. Accomando, A. Ballestrero, A. Belhouari and E. Maina, *Isolating vector boson scattering at the CERN LHC: Gauge cancellations and the equivalent vector boson approximation versus complete calculations.*, *Phys. Rev. D* **74** (2006) 073010, arXiv: [hep-ph/0608019 \[hep-ph\]](#).
- [6] ATLAS Collaboration, *Observation of electroweak production of a same-sign W boson pair in association with two jets in pp collisions at $\sqrt{s} = 13$ TeV with the ATLAS detector*, *Phys. Rev. Lett.* **123** (2019) 161801, arXiv: [1906.03203 \[hep-ex\]](#).
- [7] ATLAS Collaboration, *Observation of electroweak $W^\pm Z$ boson pair production in association with two jets in pp collisions at $\sqrt{s} = 13$ TeV with the ATLAS detector*, *Phys. Lett. B* **793** (2019) 469, arXiv: [1812.09740 \[hep-ex\]](#).
- [8] CMS Collaboration, *Observation of Electroweak Production of Same-Sign W Boson Pairs in the Two Jet and Two Same-Sign Lepton Final State in Proton-Proton Collisions $\sqrt{s} = 13$ TeV*, *Phys. Rev. Lett.* **120** (2018) 081801, arXiv: [1709.05822 \[hep-ex\]](#).
- [9] CMS Collaboration, *Measurement of electroweak WZ boson production and search for new physics in $WZ +$ two jets events in pp collisions at $\sqrt{s} = 13$ TeV*, *Phys. Lett. B* **795** (2019) 281, arXiv: [1901.04060 \[hep-ex\]](#).
- [10] CMS Collaboration, *Measurement of the cross section for electroweak production of $Z\gamma$ in association with two jets and constraints on anomalous quartic gauge couplings in proton-proton collisions at $\sqrt{s} = 8$ TeV*, *Phys. Lett. B* **770** (2017) 380, arXiv: [1702.03025 \[hep-ex\]](#).
- [11] CMS Collaboration, *Measurement of vector boson scattering and constraints on anomalous quartic couplings from events with four leptons and two jets in proton-proton collisions at $\sqrt{s} = 13$ TeV*, *Phys. Lett. B* **774** (2017) 682, arXiv: [1708.02812 \[hep-ex\]](#).
- [12] CMS Collaboration, *Measurement of electroweak-induced production of $W\gamma$ with two jets in pp collisions at $\sqrt{s} = 8$ TeV and constraints on anomalous quartic gauge couplings*, *JHEP* **06** (2017) 106, arXiv: [1612.09256 \[hep-ex\]](#).

- [13] ATLAS Collaboration, *Search for the electroweak diboson production in association with a high-mass dijet system in semileptonic final states in pp collisions at $\sqrt{s} = 13$ TeV with the ATLAS detector*, *Phys. Rev. D* **100** (2019) 032007, arXiv: [1905.07714 \[hep-ex\]](#).
- [14] CMS Collaboration, *Search for anomalous electroweak production of vector boson pairs in association with two jets in proton-proton collisions at 13 TeV*, *Phys. Lett. B* **798** (2019) 134985, arXiv: [1905.07445 \[hep-ex\]](#).
- [15] ATLAS Collaboration, *Studies of $Z\gamma$ production in association with a high-mass dijet system in pp collisions at $\sqrt{s} = 8$ TeV with the ATLAS detector*, *JHEP* **07** (2017) 107, arXiv: [1705.01966 \[hep-ex\]](#).
- [16] F. Campanario, M. Kerner, L. D. Ninh and D. Zeppenfeld, *$Z\gamma$ production in association with two jets at next-to-leading order QCD*, *Eur. Phys. J. C* **74** (2014) 3085, arXiv: [1407.7857 \[hep-ph\]](#).
- [17] F. Campanario, M. Kerner and D. Zeppenfeld, *$Z\gamma$ production in vector-boson scattering at next-to-leading order QCD*, *JHEP* **01** (2018) 160, arXiv: [1704.01921 \[hep-ph\]](#).
- [18] ATLAS Collaboration, *The ATLAS Experiment at the CERN Large Hadron Collider*, *JINST* **3** (2008) S08003.
- [19] B. Abbott et al., *Production and integration of the ATLAS Insertable B-Layer*, *JINST* **13** (2018) T05008, arXiv: [1803.00844 \[physics.ins-det\]](#).
- [20] ATLAS Collaboration, *ATLAS Insertable B-Layer Technical Design Report*, ATLAS-TDR-19, 2010, URL: <https://cds.cern.ch/record/1291633>, Addendum: ATLAS-TDR-19-ADD-1, 2012, URL: <https://cds.cern.ch/record/1451888>.
- [21] ATLAS Collaboration, *Performance of the ATLAS trigger system in 2015*, *Eur. Phys. J. C* **77** (2017) 317, arXiv: [1611.09661 \[hep-ex\]](#).
- [22] S. Agostinelli et al., *GEANT4 — a simulation toolkit*, *Nucl. Instrum. Meth. A* **506** (2003) 250.
- [23] ATLAS Collaboration, *The ATLAS Simulation Infrastructure*, *Eur. Phys. J. C* **70** (2010) 823, arXiv: [1005.4568 \[physics.ins-det\]](#).
- [24] T. Sjöstrand, S. Mrenna and P. Skands, *A brief introduction to PYTHIA 8.1*, *Comput. Phys. Commun.* **178** (2008) 852, arXiv: [0710.3820 \[hep-ph\]](#).
- [25] A. D. Martin, W. J. Stirling, R. S. Thorne and G. Watt, *Parton distributions for the LHC*, *Eur. Phys. J. C* **63** (2009) 189, arXiv: [0901.0002 \[hep-ph\]](#).
- [26] ATLAS Collaboration, *Summary of ATLAS Pythia 8 tunes*, ATL-PHYS-PUB-2012-003, 2012, URL: <https://cds.cern.ch/record/1474107>.
- [27] ATLAS Collaboration, *Electron reconstruction and identification in the ATLAS experiment using the 2015 and 2016 LHC proton-proton collision data at $\sqrt{s} = 13$ TeV*, *Eur. Phys. J. C* **79** (2019) 639, arXiv: [1902.04655 \[physics.ins-det\]](#).
- [28] ATLAS Collaboration, *Muon reconstruction performance of the ATLAS detector in proton–proton collision data at $\sqrt{s} = 13$ TeV*, *Eur. Phys. J. C* **76** (2016) 292, arXiv: [1603.05598 \[hep-ex\]](#).
- [29] ATLAS Collaboration, *Electron and photon energy calibration with the ATLAS detector using 2015-2016 LHC proton-proton collision data*, *JINST* **14** (2019) P03017, arXiv: [1812.03848 \[hep-ex\]](#).
- [30] ATLAS Collaboration, *Multi-Boson Simulation for 13 TeV ATLAS Analyses*, ATL-PHYS-PUB-2017-005, 2017, URL: <https://cds.cern.ch/record/2261933>.

- [31] J. Alwall et al., *The automated computation of tree-level and next-to-leading order differential cross sections, and their matching to parton shower simulations*, *JHEP* **07** (2014) 079, arXiv: [1405.0301 \[hep-ph\]](#).
- [32] R. D. Ball et al., *Parton distributions for the LHC Run II*, *JHEP* **04** (2015) 040, arXiv: [1410.8849 \[hep-ph\]](#).
- [33] ATLAS Collaboration, *ATLAS Pythia 8 tunes to 7 TeV data*, ATL-PHYS-PUB-2014-021, 2014, URL: <https://cds.cern.ch/record/1966419>.
- [34] M. Bähr et al., *Herwig++ physics and manual*, *Eur. Phys. J. C* **58** (2008) 639, arXiv: [0803.0883 \[hep-ph\]](#).
- [35] J. Bellm et al., *Herwig 7.0/Herwig++ 3.0 release note*, *Eur. Phys. J. C* **76** (2016) 196, arXiv: [1512.01178 \[hep-ph\]](#).
- [36] S. Gieseke, C. Rohr and A. Siodmok, *Colour reconnections in Herwig++*, *Eur. Phys. J. C* **72** (2012) 2225, arXiv: [1206.0041 \[hep-ph\]](#).
- [37] M. H. Seymour and A. Siodmok, *Constraining MPI models using σ_{eff} and recent Tevatron and LHC Underlying Event data*, *JHEP* **10** (2013) 113, arXiv: [1307.5015 \[hep-ph\]](#).
- [38] J. Pumplin et al., *New generation of parton distributions with uncertainties from global QCD analysis*, *JHEP* **07** (2002) 012, arXiv: [hep-ph/0201195 \[hep-ph\]](#).
- [39] T. Gleisberg et al., *Event generation with SHERPA 1.1*, *JHEP* **02** (2009) 007, arXiv: [0811.4622 \[hep-ph\]](#).
- [40] T. Gleisberg and S. Höche, *Comix, a new matrix element generator*, *JHEP* **12** (2008) 039, arXiv: [0808.3674 \[hep-ph\]](#).
- [41] S. Schumann and F. Krauss, *A parton shower algorithm based on Catani-Seymour dipole factorisation*, *JHEP* **03** (2008) 038, arXiv: [0709.1027 \[hep-ph\]](#).
- [42] F. Cascioli, P. Maierhöfer and S. Pozzorini, *Scattering Amplitudes with Open Loops*, *Phys. Rev. Lett.* **108** (2012) 111601, arXiv: [1111.5206 \[hep-ph\]](#).
- [43] S. Höche, F. Krauss, M. Schönherr and F. Siegert, *QCD matrix elements + parton showers. The NLO case*, *JHEP* **04** (2013) 027, arXiv: [1207.5030 \[hep-ph\]](#).
- [44] R. Frederix and S. Frixione, *Merging meets matching in MC@NLO*, *JHEP* **12** (2012) 061, arXiv: [1209.6215 \[hep-ph\]](#).
- [45] ATLAS Collaboration, *Monte Carlo Generators for the Production of a W or Z/ γ^* Boson in Association with Jets at ATLAS in Run 2*, ATL-PHYS-PUB-2016-003, 2016, URL: <https://cds.cern.ch/record/2120133>.
- [46] C. Anastasiou, L. Dixon, K. Melnikov and F. Petriello, *High-precision QCD at hadron colliders: Electroweak gauge boson rapidity distributions at next-to-next-to-leading order*, *Phys. Rev. D* **69** (2004) 094008, arXiv: [hep-ph/0312266 \[hep-ph\]](#).
- [47] K. Melnikov, M. Schulze and A. Scharf, *QCD corrections to top quark pair production in association with a photon at hadron colliders*, *Phys. Rev. D* **83** (2011) 074013, arXiv: [1102.1967 \[hep-ph\]](#).
- [48] S. Frixione, P. Nason and C. Oleari, *Matching NLO QCD computations with parton shower simulations: the POWHEG method*, *JHEP* **11** (2007) 070, arXiv: [0709.2092 \[hep-ph\]](#).
- [49] P. Nason, *A new method for combining NLO QCD with shower Monte Carlo algorithms*, *JHEP* **11** (2004) 040, arXiv: [hep-ph/0409146 \[hep-ph\]](#).

- [50] S. Alioli, P. Nason, C. Oleari and E. Re, *A general framework for implementing NLO calculations in shower Monte Carlo programs: the POWHEG BOX*, *JHEP* **06** (2010) 043, arXiv: [1002.2581 \[hep-ph\]](#).
- [51] T. Sjöstrand, S. Mrenna and P. Z. Skands, *PYTHIA 6.4 Physics and Manual*, *JHEP* **05** (2006) 026, arXiv: [hep-ph/0603175](#).
- [52] P. Z. Skands, *Tuning Monte Carlo generators: The Perugia tunes*, *Phys. Rev. D* **82** (2010) 074018, arXiv: [1005.3457 \[hep-ph\]](#).
- [53] H.-L. Lai et al., *New parton distributions for collider physics*, *Phys. Rev. D* **82** (2010) 074024, arXiv: [1007.2241 \[hep-ph\]](#).
- [54] ATLAS Collaboration, *Performance of electron and photon triggers in ATLAS during LHC Run 2*, (2019), arXiv: [1909.00761 \[hep-ex\]](#).
- [55] ATLAS Collaboration, *Measurement of the photon identification efficiencies with the ATLAS detector using LHC Run 2 data collected in 2015 and 2016*, *Eur. Phys. J. C* **79** (2019) 205, arXiv: [1810.05087 \[hep-ex\]](#).
- [56] ATLAS Collaboration, *Topological cell clustering in the ATLAS calorimeters and its performance in LHC Run 1*, *Eur. Phys. J. C* **77** (2017) 490, arXiv: [1603.02934 \[hep-ex\]](#).
- [57] M. Cacciari, G. P. Salam and G. Soyez, *The anti- k_t jet clustering algorithm*, *JHEP* **04** (2008) 063, arXiv: [0802.1189 \[hep-ph\]](#).
- [58] M. Cacciari, G. P. Salam and G. Soyez, *FastJet user manual*, *Eur. Phys. J. C* **72** (2012) 1896, arXiv: [1111.6097 \[hep-ph\]](#).
- [59] ATLAS Collaboration, *Jet energy scale measurements and their systematic uncertainties in proton-proton collisions at $\sqrt{s} = 13$ TeV with the ATLAS detector*, *Phys. Rev. D* **96** (2017) 072002, arXiv: [1703.09665 \[hep-ex\]](#).
- [60] ATLAS Collaboration, *Selection of jets produced in 13 TeV proton–proton collisions with the ATLAS detector*, ATLAS-CONF-2015-029, 2015, URL: <https://cds.cern.ch/record/2037702>.
- [61] ATLAS Collaboration, *Performance of pile-up mitigation techniques for jets in pp collisions at $\sqrt{s} = 8$ TeV using the ATLAS detector*, *Eur. Phys. J. C* **76** (2016) 581, arXiv: [1510.03823 \[hep-ex\]](#).
- [62] ATLAS Collaboration, *Performance of b-jet identification in the ATLAS experiment*, *JINST* **11** (2016) P04008, arXiv: [1512.01094 \[hep-ex\]](#).
- [63] ATLAS Collaboration, *Optimisation of the ATLAS b-tagging performance for the 2016 LHC Run*, ATL-PHYS-PUB-2016-012, 2016, URL: <https://cds.cern.ch/record/2160731>.
- [64] ATLAS Collaboration, *Measurement of the $Z(\rightarrow \ell^+ \ell^-)\gamma$ production cross-section in pp collisions at $\sqrt{s} = 13$ TeV with the ATLAS detector*, (2019), arXiv: [1911.04813 \[hep-ex\]](#).
- [65] ATLAS Collaboration, *Measurement of the inclusive isolated prompt photon cross section in pp collisions at $\sqrt{s} = 7$ TeV with the ATLAS detector*, *Phys. Rev. D* **83** (2011) 052005, arXiv: [1012.4389 \[hep-ex\]](#).
- [66] A. Hoecker et al., *TMVA: Toolkit for Multivariate Data Analysis*, PoS ACAT (2007) 040, arXiv: [physics/0703039](#).
- [67] ATLAS Collaboration, *Measurement of the electroweak production of dijets in association with a Z-boson and distributions sensitive to vector boson fusion in proton-proton collisions at $\sqrt{s} = 8$ TeV using the ATLAS detector*, *JHEP* **04** (2014) 031, arXiv: [1401.7610 \[hep-ex\]](#).

- [68] ATLAS Collaboration, *Measurements of electroweak Wjj production and constraints on anomalous gauge couplings with the ATLAS detector*, *Eur. Phys. J. C* **77** (2017) 474, arXiv: [1703.04362 \[hep-ex\]](#).
- [69] ATLAS Collaboration, *Measurement of the cross-section for electroweak production of dijets in association with a Z boson in pp collisions at $\sqrt{s} = 13$ TeV with the ATLAS detector*, *Phys. Lett. B* **775** (2017) 206, arXiv: [1709.10264 \[hep-ex\]](#).
- [70] J. Butterworth et al., *PDF4LHC recommendations for LHC Run II*, *J. Phys. G* **43** (2016) 023001, arXiv: [1510.03865 \[hep-ph\]](#).
- [71] A. Ballestrero et al., *Precise predictions for same-sign W-boson scattering at the LHC*, *Eur. Phys. J. C* **78** (2018) 671, arXiv: [1803.07943 \[hep-ph\]](#).
- [72] ATLAS Collaboration, *Modelling of the vector boson scattering process $pp \rightarrow W^\pm W^\pm jj$ in Monte Carlo generators in ATLAS*, ATL-PHYS-PUB-2019-004, 2019, URL: <https://cds.cern.ch/record/2655303>.
- [73] ATLAS Collaboration, *Jet energy resolution in proton–proton collisions at $\sqrt{s} = 7$ TeV recorded in 2010 with the ATLAS detector*, *Eur. Phys. J. C* **73** (2013) 2306, arXiv: [1210.6210 \[hep-ex\]](#).
- [74] ATLAS Collaboration, *Electron and photon energy calibration with the ATLAS detector using LHC Run 1 data*, *Eur. Phys. J. C* **74** (2014) 3071, arXiv: [1407.5063 \[hep-ex\]](#).
- [75] ATLAS Collaboration, *Measurement of the Inelastic Proton–Proton Cross Section at $\sqrt{s} = 13$ TeV with the ATLAS Detector at the LHC*, *Phys. Rev. Lett.* **117** (2016) 182002, arXiv: [1606.02625 \[hep-ex\]](#).
- [76] ATLAS Collaboration, *Luminosity determination in pp collisions at $\sqrt{s} = 13$ TeV using the ATLAS detector at the LHC*, ATLAS-CONF-2019-021, 2019, URL: <https://cds.cern.ch/record/2677054>.
- [77] G. Avoni et al., *The new LUCID-2 detector for luminosity measurement and monitoring in ATLAS*, *JINST* **13** (2018) P07017.
- [78] G. Cowan, K. Cranmer, E. Gross and O. Vitells, *Asymptotic formulae for likelihood-based tests of new physics*, *Eur. Phys. J. C* **71** (2011) 1554, arXiv: [1007.1727 \[physics.data-an\]](#), Erratum: *Eur. Phys. J. C* **73** (2013) 2501.
- [79] ATLAS Collaboration, *Measurements of inclusive and differential fiducial cross-sections of $t\bar{t}\gamma$ production in leptonic final states at $\sqrt{s} = 13$ TeV in ATLAS*, *Eur. Phys. J. C* **79** (2019) 382, arXiv: [1812.01697 \[hep-ex\]](#).
- [80] ATLAS Collaboration, *ATLAS Computing Acknowledgements*, ATL-GEN-PUB-2016-002, URL: <https://cds.cern.ch/record/2202407>.

The ATLAS Collaboration

G. Aad¹⁰², B. Abbott¹²⁹, D.C. Abbott¹⁰³, A. Abed Abud^{71a,71b}, K. Abeling⁵³, D.K. Abhayasinghe⁹⁴, S.H. Abidi¹⁶⁷, O.S. AbouZeid⁴⁰, N.L. Abraham¹⁵⁶, H. Abramowicz¹⁶¹, H. Abreu¹⁶⁰, Y. Abulaiti⁶, B.S. Acharya^{67a,67b,n}, B. Achkar⁵³, S. Adachi¹⁶³, L. Adam¹⁰⁰, C. Adam Bourdarios⁵, L. Adamczyk^{84a}, L. Adamek¹⁶⁷, J. Adelman¹²¹, M. Adersberger¹¹⁴, A. Adiguzel^{12c}, S. Adorni⁵⁴, T. Adye¹⁴⁴, A.A. Affolder¹⁴⁶, Y. Afik¹⁶⁰, C. Agapopoulou⁶⁵, M.N. Agaras³⁸, A. Aggarwal¹¹⁹, C. Agheorghiesei^{27c}, J.A. Aguilar-Saavedra^{140f,140a,ag}, F. Ahmadov⁸⁰, W.S. Ahmed¹⁰⁴, X. Ai¹⁸, G. Aielli^{74a,74b}, S. Akatsuka⁸⁶, T.P.A. Åkesson⁹⁷, E. Akilli⁵⁴, A.V. Akimov¹¹¹, K. Al Khoury⁶⁵, G.L. Alberghini^{23b,23a}, J. Albert¹⁷⁶, M.J. Alconada Verzini¹⁶¹, S. Alderweireldt³⁶, M. Alekса³⁶, I.N. Aleksandrov⁸⁰, C. Alexa^{27b}, T. Alexopoulos¹⁰, A. Alfonsi¹²⁰, F. Alfonsi^{23b,23a}, M. Alhoob¹²⁹, B. Ali¹⁴², M. Aliev¹⁶⁶, G. Alimonti^{69a}, S.P. Alkire¹⁴⁸, C. Allaire⁶⁵, B.M.M. Allbrooke¹⁵⁶, B.W. Allen¹³², P.P. Allport²¹, A. Aloisio^{70a,70b}, A. Alonso⁴⁰, F. Alonso⁸⁹, C. Alpigiani¹⁴⁸, A.A. Alshehri⁵⁷, M. Alvarez Estevez⁹⁹, D. Álvarez Piqueras¹⁷⁴, M.G. Alvaggi^{70a,70b}, Y. Amaral Coutinho^{81b}, A. Ambler¹⁰⁴, L. Ambroz¹³⁵, C. Amelung²⁶, D. Amidei¹⁰⁶, S.P. Amor Dos Santos^{140a}, S. Amoroso⁴⁶, C.S. Amrouche⁵⁴, F. An⁷⁹, C. Anastopoulos¹⁴⁹, N. Andari¹⁴⁵, T. Andeen¹¹, C.F. Anders^{61b}, J.K. Anders²⁰, A. Andreazza^{69a,69b}, V. Andrei^{61a}, C.R. Anelli¹⁷⁶, S. Angelidakis³⁸, A. Angerami³⁹, A.V. Anisenkov^{122b,122a}, A. Annovi^{72a}, C. Antel⁵⁴, M.T. Anthony¹⁴⁹, E. Antipov¹³⁰, M. Antonelli⁵¹, D.J.A. Antrim¹⁷¹, F. Anulli^{73a}, M. Aoki⁸², J.A. Aparisi Pozo¹⁷⁴, L. Aperio Bella^{15a}, J.P. Araque^{140a}, V. Araujo Ferraz^{81b}, R. Araujo Pereira^{81b}, C. Arcangeletti⁵¹, A.T.H. Arce⁴⁹, F.A. Arduh⁸⁹, J-F. Arguin¹¹⁰, S. Argyropoulos⁷⁸, J.-H. Arling⁴⁶, A.J. Armbruster³⁶, A. Armstrong¹⁷¹, O. Arnaez¹⁶⁷, H. Arnold¹²⁰, Z.P. Arrubarrena Tame¹¹⁴, G. Artoni¹³⁵, S. Artz¹⁰⁰, S. Asai¹⁶³, T. Asawatavonvanich¹⁶⁵, N. Asbah⁵⁹, E.M. Asimakopoulou¹⁷², L. Asquith¹⁵⁶, J. Assahsah^{35d}, K. Assamagan²⁹, R. Astalos^{28a}, R.J. Atkin^{33a}, M. Atkinson¹⁷³, N.B. Atlay¹⁹, H. Atmani⁶⁵, K. Augsten¹⁴², G. Avolio³⁶, R. Avramidou^{60a}, M.K. Ayoub^{15a}, A.M. Azoulay^{168b}, G. Azuelos^{110,ar}, H. Bachacou¹⁴⁵, K. Bachas^{68a,68b}, M. Backes¹³⁵, F. Backman^{45a,45b}, P. Bagnaia^{73a,73b}, M. Bahmani⁸⁵, H. Bahrasemani¹⁵², A.J. Bailey¹⁷⁴, V.R. Bailey¹⁷³, J.T. Baines¹⁴⁴, M. Bajic⁴⁰, C. Bakalis¹⁰, O.K. Baker¹⁸³, P.J. Bakker¹²⁰, D. Bakshi Gupta⁸, S. Balaji¹⁵⁷, E.M. Baldin^{122b,122a}, P. Balek¹⁸⁰, F. Balli¹⁴⁵, W.K. Balunas¹³⁵, J. Balz¹⁰⁰, E. Banas⁸⁵, A. Bandyopadhyay²⁴, Sw. Banerjee^{181,i}, A.A.E. Bannoura¹⁸², L. Barak¹⁶¹, W.M. Barbe³⁸, E.L. Barberio¹⁰⁵, D. Barberis^{55b,55a}, M. Barbero¹⁰², G. Barbour⁹⁵, T. Barillari¹¹⁵, M-S. Barisits³⁶, J. Barkeloo¹³², T. Barklow¹⁵³, R. Barnea¹⁶⁰, S.L. Barnes^{60c}, B.M. Barnett¹⁴⁴, R.M. Barnett¹⁸, Z. Barnovska-Blenessy^{60a}, A. Baroncelli^{60a}, G. Barone²⁹, A.J. Barr¹³⁵, L. Barranco Navarro^{45a,45b}, F. Barreiro⁹⁹, J. Barreiro Guimarães da Costa^{15a}, S. Barsov¹³⁸, R. Bartoldus¹⁵³, G. Bartolini¹⁰², A.E. Barton⁹⁰, P. Bartos^{28a}, A. Basalaev⁴⁶, A. Basan¹⁰⁰, A. Bassalat^{65,am}, M.J. Basso¹⁶⁷, R.L. Bates⁵⁷, S. Batlamous^{35e}, J.R. Batley³², B. Batool¹⁵¹, M. Battaglia¹⁴⁶, M. Bauce^{73a,73b}, F. Bauer¹⁴⁵, K.T. Bauer¹⁷¹, H.S. Bawa^{31,l}, J.B. Beacham⁴⁹, T. Beau¹³⁶, P.H. Beauchemin¹⁷⁰, F. Becherer⁵², P. Bechtle²⁴, H.C. Beck⁵³, H.P. Beck^{20,r}, K. Becker⁵², M. Becker¹⁰⁰, C. Becot⁴⁶, A. Beddall^{12d}, A.J. Beddall^{12a}, V.A. Bednyakov⁸⁰, M. Bedognetti¹²⁰, C.P. Bee¹⁵⁵, T.A. Beermann¹⁸², M. Begalli^{81b}, M. Begel²⁹, A. Behera¹⁵⁵, J.K. Behr⁴⁶, F. Beisiegel²⁴, A.S. Bell⁹⁵, G. Bella¹⁶¹, L. Bellagamba^{23b}, A. Bellerive³⁴, P. Bellos⁹, K. Beloborodov^{122b,122a}, K. Belotskiy¹¹², N.L. Belyaev¹¹², D. Benchekroun^{35a}, N. Benekos¹⁰, Y. Benhammou¹⁶¹, D.P. Benjamin⁶, M. Benoit⁵⁴, J.R. Bensinger²⁶, S. Bentvelsen¹²⁰, L. Beresford¹³⁵, M. Beretta⁵¹, D. Berge⁴⁶, E. Bergeaas Kuutmann¹⁷², N. Berger⁵, B. Bergmann¹⁴², L.J. Bergsten²⁶, J. Beringer¹⁸, S. Berlendis⁷, G. Bernardi¹³⁶, C. Bernius¹⁵³, F.U. Bernlochner²⁴, T. Berry⁹⁴, P. Berta¹⁰⁰, C. Bertella^{15a}, I.A. Bertram⁹⁰, O. Bessidskaia Bylund¹⁸², N. Besson¹⁴⁵, A. Bethani¹⁰¹, S. Bethke¹¹⁵, A. Betti⁴², A.J. Bevan⁹³, J. Beyer¹¹⁵, D.S. Bhattacharya¹⁷⁷, P. Bhattacharai²⁶, R. Bi¹³⁹, R.M. Bianchi¹³⁹, O. Biebel¹¹⁴, D. Biedermann¹⁹, R. Bielski³⁶, K. Bierwagen¹⁰⁰, N.V. Biesuz^{72a,72b}, M. Biglietti^{75a}, T.R.V. Billoud¹¹⁰, M. Bindi⁵³, A. Bingul^{12d}, C. Bini^{73a,73b}, S. Biondi^{23b,23a}, M. Birman¹⁸⁰, T. Bisanz⁵³,

J.P. Biswal¹⁶¹, D. Biswas^{181,i}, A. Bitadze¹⁰¹, C. Bittrich⁴⁸, K. Bjørke¹³⁴, K.M. Black²⁵, T. Blazek^{28a}, I. Bloch⁴⁶, C. Blocker²⁶, A. Blue⁵⁷, U. Blumenschein⁹³, G.J. Bobbink¹²⁰, V.S. Bobrovnikov^{122b,122a}, S.S. Bocchetta⁹⁷, A. Bocci⁴⁹, D. Boerner⁴⁶, D. Bogavac¹⁴, A.G. Bogdanchikov^{122b,122a}, C. Bohm^{45a}, V. Boisvert⁹⁴, P. Bokan^{53,172}, T. Bold^{84a}, A.S. Boldyrev¹¹³, A.E. Bolz^{61b}, M. Bomben¹³⁶, M. Bona⁹³, J.S. Bonilla¹³², M. Boonekamp¹⁴⁵, C.D. Booth⁹⁴, H.M. Borecka-Bielska⁹¹, A. Borisov¹²³, G. Borissov⁹⁰, J. Bortfeldt³⁶, D. Bortoletto¹³⁵, D. Boscherini^{23b}, M. Bosman¹⁴, J.D. Bossio Sola¹⁰⁴, K. Bouaouda^{35a}, J. Boudreau¹³⁹, E.V. Bouhova-Thacker⁹⁰, D. Boumediene³⁸, S.K. Boutle⁵⁷, A. Boveia¹²⁷, J. Boyd³⁶, D. Boye^{33c,an}, I.R. Boyko⁸⁰, A.J. Bozson⁹⁴, J. Bracinik²¹, N. Brahimi¹⁰², G. Brandt¹⁸², O. Brandt³², F. Braren⁴⁶, B. Brau¹⁰³, J.E. Brau¹³², W.D. Breaden Madden⁵⁷, K. Brendlinger⁴⁶, L. Brenner⁴⁶, R. Brenner¹⁷², S. Bressler¹⁸⁰, B. Brickwedde¹⁰⁰, D.L. Briglin²¹, D. Britton⁵⁷, D. Britzger¹¹⁵, I. Brock²⁴, R. Brock¹⁰⁷, G. Brooijmans³⁹, W.K. Brooks^{147d}, E. Brost¹²¹, J.H. Broughton²¹, P.A. Bruckman de Renstrom⁸⁵, D. Bruncko^{28b}, A. Brun^{23b}, G. Brun^{23b}, L.S. Brun¹²⁰, S. Bruno^{74a,74b}, M. Bruschi^{23b}, N. Bruscino^{73a,73b}, P. Bryant³⁷, L. Bryngemark⁹⁷, T. Buanes¹⁷, Q. Buat³⁶, P. Buchholz¹⁵¹, A.G. Buckley⁵⁷, I.A. Budagov⁸⁰, M.K. Bugge¹³⁴, F. Bührer⁵², O. Bulekov¹¹², T.J. Burch¹²¹, S. Burdin⁹¹, C.D. Burgard¹²⁰, A.M. Burger¹³⁰, B. Burghgrave⁸, J.T.P. Burr⁴⁶, C.D. Burton¹¹, J.C. Burzynski¹⁰³, V. Büscher¹⁰⁰, E. Buschmann⁵³, P.J. Bussey⁵⁷, J.M. Butler²⁵, C.M. Buttar⁵⁷, J.M. Butterworth⁹⁵, P. Butti³⁶, W. Buttlinger³⁶, C.J. Buxo Vazquez¹⁰⁷, A. Buzatu¹⁵⁸, A.R. Buzykaev^{122b,122a}, G. Cabras^{23b,23a}, S. Cabrera Urbán¹⁷⁴, D. Caforio⁵⁶, H. Cai¹⁷³, V.M.M. Cairo¹⁵³, O. Cakir^{4a}, N. Calace³⁶, P. Calafiura¹⁸, A. Calandri¹⁰², G. Calderini¹³⁶, P. Calfayan⁶⁶, G. Callea⁵⁷, L.P. Caloba^{81b}, A. Caltabiano^{74a,74b}, S. Calvente Lopez⁹⁹, D. Calvet³⁸, S. Calvet³⁸, T.P. Calvet¹⁵⁵, M. Calvetti^{72a,72b}, R. Camacho Toro¹³⁶, S. Camarda³⁶, D. Camarero Munoz⁹⁹, P. Camarri^{74a,74b}, D. Cameron¹³⁴, R. Caminal Armadans¹⁰³, C. Camincher³⁶, S. Campana³⁶, M. Campanelli⁹⁵, A. Camplani⁴⁰, A. Campoverde¹⁵¹, V. Canale^{70a,70b}, A. Canesse¹⁰⁴, M. Cano Bret^{60c}, J. Cantero¹³⁰, T. Cao¹⁶¹, Y. Cao¹⁷³, M.D.M. Capeans Garrido³⁶, M. Capua^{41b,41a}, R. Cardarelli^{74a}, F. Cardillo¹⁴⁹, G. Carducci^{41b,41a}, I. Carli¹⁴³, T. Carli³⁶, G. Carlino^{70a}, B.T. Carlson¹³⁹, L. Carminati^{69a,69b}, R.M.D. Carney^{45a,45b}, S. Caron¹¹⁹, E. Carquin^{147d}, S. Carrá⁴⁶, J.W.S. Carter¹⁶⁷, M.P. Casado^{14,e}, A.F. Casha¹⁶⁷, D.W. Casper¹⁷¹, R. Castelijn¹²⁰, F.L. Castillo¹⁷⁴, V. Castillo Gimenez¹⁷⁴, N.F. Castro^{140a,140e}, A. Catinaccio³⁶, J.R. Catmore¹³⁴, A. Cattai³⁶, V. Cavaliere²⁹, E. Cavallaro¹⁴, M. Cavalli-Sforza¹⁴, V. Cavasinni^{72a,72b}, E. Celebi^{12b}, F. Ceradini^{75a,75b}, L. Cerdà Alberich¹⁷⁴, K. Cerny¹³¹, A.S. Cerqueira^{81a}, A. Cerri¹⁵⁶, L. Cerrito^{74a,74b}, F. Cerutti¹⁸, A. Cervelli^{23b,23a}, S.A. Cetin^{12b}, Z. Chadi^{35a}, D. Chakraborty¹²¹, W.S. Chan¹²⁰, W.Y. Chan⁹¹, J.D. Chapman³², B. Chargeishvili^{159b}, D.G. Charlton²¹, T.P. Charman⁹³, C.C. Chau³⁴, S. Che¹²⁷, S. Chekanov⁶, S.V. Chekulaev^{168a}, G.A. Chelkov⁸⁰, M.A. Chelstowska³⁶, B. Chen⁷⁹, C. Chen^{60a}, C.H. Chen⁷⁹, H. Chen²⁹, J. Chen^{60a}, J. Chen³⁹, S. Chen¹³⁷, S.J. Chen^{15c}, X. Chen^{15b}, Y-H. Chen⁴⁶, H.C. Cheng^{63a}, H.J. Cheng^{15a}, A. Cheplakov⁸⁰, E. Cheremushkina¹²³, R. Cherkaoui El Moursli^{35e}, E. Cheu⁷, K. Cheung⁶⁴, T.J.A. Chevaléries¹⁴⁵, L. Chevalier¹⁴⁵, V. Chiarella⁵¹, G. Chiarelli^{72a}, G. Chiodini^{68a}, A.S. Chisholm²¹, A. Chitan^{27b}, I. Chiu¹⁶³, Y.H. Chiu¹⁷⁶, M.V. Chizhov⁸⁰, K. Choi⁶⁶, A.R. Chomont^{73a,73b}, S. Chouridou¹⁶², Y.S. Chow¹²⁰, M.C. Chu^{63a}, X. Chu^{15a,15d}, J. Chudoba¹⁴¹, A.J. Chuinard¹⁰⁴, J.J. Chwastowski⁸⁵, L. Chytka¹³¹, D. Cieri¹¹⁵, K.M. Ciesla⁸⁵, D. Cinca⁴⁷, V. Cindro⁹², I.A. Cioară^{27b}, A. Ciocio¹⁸, F. Cirotto^{70a,70b}, Z.H. Citron^{180j}, M. Citterio^{69a}, D.A. Ciubotaru^{27b}, B.M. Ciungu¹⁶⁷, A. Clark⁵⁴, M.R. Clark³⁹, P.J. Clark⁵⁰, C. Clement^{45a,45b}, Y. Coadou¹⁰², M. Cobal^{67a,67c}, A. Coccaro^{55b}, J. Cochran⁷⁹, H. Cohen¹⁶¹, A.E.C. Coimbra³⁶, L. Colasurdo¹¹⁹, B. Cole³⁹, A.P. Colijn¹²⁰, J. Collot⁵⁸, P. Conde Muiño^{140a,140h}, S.H. Connell^{33c}, I.A. Connelly⁵⁷, S. Constantinescu^{27b}, F. Conventi^{70a,as}, A.M. Cooper-Sarkar¹³⁵, F. Cormier¹⁷⁵, K.J.R. Cormier¹⁶⁷, L.D. Corpe⁹⁵, M. Corradi^{73a,73b}, E.E. Corrigan⁹⁷, F. Corriveau^{104,ae}, A. Cortes-Gonzalez³⁶, M.J. Costa¹⁷⁴, F. Costanza⁵, D. Costanzo¹⁴⁹, G. Cowan⁹⁴, J.W. Cowley³², J. Crane¹⁰¹, K. Cranmer¹²⁵, S.J. Crawley⁵⁷, R.A. Creager¹³⁷, S. Crépé-Renaudin⁵⁸, F. Crescioli¹³⁶, M. Cristinziani²⁴, V. Croft¹²⁰, G. Crosetti^{41b,41a}, A. Cueto⁵, T. Cuhadar Donszelmann¹⁴⁹, A.R. Cukierman¹⁵³, W.R. Cunningham⁵⁷, S. Czekierda⁸⁵, P. Czodrowski³⁶,

M.J. Da Cunha Sargedas De Sousa^{60b}, J.V. Da Fonseca Pinto^{81b}, C. Da Via¹⁰¹, W. Dabrowski^{84a},
 F. Dachs³⁶, T. Dado^{28a}, S. Dahbi^{35e}, T. Dai¹⁰⁶, C. Dallapiccola¹⁰³, M. Dam⁴⁰, G. D'amen²⁹,
 V. D'Amico^{75a,75b}, J. Damp¹⁰⁰, J.R. Dandoy¹³⁷, M.F. Daneri³⁰, N.P. Dang^{181,i}, N.S. Dann¹⁰¹,
 M. Danninger¹⁷⁵, V. Dao³⁶, G. Darbo^{55b}, O. Dartsi⁵, A. Dattagupta¹³², T. Daubney⁴⁶, S. D'Auria^{69a,69b},
 C. David⁴⁶, T. Davidek¹⁴³, D.R. Davis⁴⁹, I. Dawson¹⁴⁹, K. De⁸, R. De Asmundis^{70a}, M. De Beurs¹²⁰,
 S. De Castro^{23b,23a}, S. De Cecco^{73a,73b}, N. De Groot¹¹⁹, P. de Jong¹²⁰, H. De la Torre¹⁰⁷, A. De Maria^{15c},
 D. De Pedis^{73a}, A. De Salvo^{73a}, U. De Sanctis^{74a,74b}, M. De Santis^{74a,74b}, A. De Santo¹⁵⁶,
 K. De Vasconcelos Corga¹⁰², J.B. De Vivie De Regie⁶⁵, C. Debenedetti¹⁴⁶, D.V. Dedovich⁸⁰,
 A.M. Deiana⁴², J. Del Peso⁹⁹, Y. Delabat Diaz⁴⁶, D. Delgove⁶⁵, F. Deliot^{145,q}, C.M. Delitzsch⁷,
 M. Della Pietra^{70a,70b}, D. Della Volpe⁵⁴, A. Dell'Acqua³⁶, L. Dell'Asta^{74a,74b}, M. Delmastro⁵,
 C. Delporte⁶⁵, P.A. Delsart⁵⁸, D.A. DeMarco¹⁶⁷, S. Demers¹⁸³, M. Demichev⁸⁰, G. Demontigny¹¹⁰,
 S.P. Denisov¹²³, L. D'Eramo¹³⁶, D. Derendarz⁸⁵, J.E. Derkaoui^{35d}, F. Derue¹³⁶, P. Dervan⁹¹, K. Desch²⁴,
 C. Deterre⁴⁶, K. Dette¹⁶⁷, C. Deutsch²⁴, M.R. Devesa³⁰, P.O. Deviveiros³⁶, A. Dewhurst¹⁴⁴,
 F.A. Di Bello⁵⁴, A. Di Ciaccio^{74a,74b}, L. Di Ciaccio⁵, W.K. Di Clemente¹³⁷, C. Di Donato^{70a,70b},
 A. Di Girolamo³⁶, G. Di Gregorio^{72a,72b}, B. Di Micco^{75a,75b}, R. Di Nardo¹⁰³, K.F. Di Petrillo⁵⁹,
 R. Di Sipio¹⁶⁷, D. Di Valentino³⁴, C. Diaconu¹⁰², F.A. Dias⁴⁰, T. Dias Do Vale^{140a}, M.A. Diaz^{147a},
 J. Dickinson¹⁸, E.B. Diehl¹⁰⁶, J. Dietrich¹⁹, S. Díez Cornell¹⁴⁶, A. Dimitrievska¹⁸, W. Ding^{15b},
 J. Dingfelder²⁴, F. Dittus³⁶, F. Djama¹⁰², T. Djobava^{159b}, J.I. Djuvoland¹⁷, M.A.B. Do Vale^{81c},
 M. Dobre^{27b}, D. Dodsworth²⁶, C. Doglioni⁹⁷, J. Dolejsi¹⁴³, Z. Dolezal¹⁴³, M. Donadelli^{81d}, B. Dong^{60c},
 J. Donini³⁸, A. D'onofrio^{15c}, M. D'Onofrio⁹¹, J. Dopke¹⁴⁴, A. Doria^{70a}, M.T. Dova⁸⁹, A.T. Doyle⁵⁷,
 E. Drechsler¹⁵², E. Dreyer¹⁵², T. Dreyer⁵³, A.S. Drobac¹⁷⁰, D. Du^{60b}, Y. Duan^{60b}, F. Dubinin¹¹¹,
 M. Dubovsky^{28a}, A. Dubreuil⁵⁴, E. Duchovni¹⁸⁰, G. Duckeck¹¹⁴, A. Ducourthial¹³⁶, O.A. Ducu¹¹⁰,
 D. Duda¹¹⁵, A. Dudarev³⁶, A.C. Dudder¹⁰⁰, E.M. Duffield¹⁸, L. Duflot⁶⁵, M. Dührssen³⁶, C. Dülsen¹⁸²,
 M. Dumancic¹⁸⁰, A.E. Dumitriu^{27b}, A.K. Duncan⁵⁷, M. Dunford^{61a}, A. Duperrin¹⁰², H. Duran Yildiz^{4a},
 M. Düren⁵⁶, A. Durghishvili^{159b}, D. Duschinger⁴⁸, B. Dutta⁴⁶, D. Duvnjak¹, G.I. Dyckes¹³⁷, M. Dyndal³⁶,
 S. Dysch¹⁰¹, B.S. Dziedzic⁸⁵, K.M. Ecker¹¹⁵, R.C. Edgar¹⁰⁶, M.G. Eggleston⁴⁹, T. Eifert³⁶, G. Eigen¹⁷,
 K. Einsweiler¹⁸, T. Ekelof¹⁷², H. El Jarrari^{35e}, M. El Kacimi^{35c}, R. El Kosseifi¹⁰², V. Ellajosyula¹⁷²,
 M. Ellert¹⁷², F. Ellinghaus¹⁸², A.A. Elliot⁹³, N. Ellis³⁶, J. Elmsheuser²⁹, M. Elsing³⁶, D. Emeliyanov¹⁴⁴,
 A. Emerman³⁹, Y. Enari¹⁶³, M.B. Epland⁴⁹, J. Erdmann⁴⁷, A. Ereditato²⁰, M. Errenst³⁶, M. Escalier⁶⁵,
 C. Escobar¹⁷⁴, O. Estrada Pastor¹⁷⁴, E. Etzion¹⁶¹, H. Evans⁶⁶, A. Ezhilov¹³⁸, F. Fabbri⁵⁷, L. Fabbri^{23b,23a},
 V. Fabiani¹¹⁹, G. Facini⁹⁵, R.M. Faisca Rodrigues Pereira^{140a}, R.M. Fakhrutdinov¹²³, S. Falciano^{73a},
 P.J. Falke⁵, S. Falke⁵, J. Faltova¹⁴³, Y. Fang^{15a}, Y. Fang^{15a}, G. Fanourakis⁴⁴, M. Fanti^{69a,69b},
 M. Faraj^{67a,67c,t}, A. Farbin⁸, A. Farilla^{75a}, E.M. Farina^{71a,71b}, T. Farooque¹⁰⁷, S. Farrell¹⁸,
 S.M. Farrington⁵⁰, P. Farthouat³⁶, F. Fassi^{35e}, P. Fassnacht³⁶, D. Fassouliotis⁹, M. Faucci Giannelli⁵⁰,
 W.J. Fawcett³², L. Fayard⁶⁵, O.L. Fedin^{138,o}, W. Fedorko¹⁷⁵, A. Fehr²⁰, M. Feickert⁴², L. Feligioni¹⁰²,
 A. Fell¹⁴⁹, C. Feng^{60b}, M. Feng⁴⁹, M.J. Fenton⁵⁷, A.B. Fenyuk¹²³, S.W. Ferguson⁴³, J. Ferrando⁴⁶,
 A. Ferrante¹⁷³, A. Ferrari¹⁷², P. Ferrari¹²⁰, R. Ferrari^{71a}, D.E. Ferreira de Lima^{61b}, A. Ferrer¹⁷⁴,
 D. Ferrere⁵⁴, C. Ferretti¹⁰⁶, F. Fiedler¹⁰⁰, A. Filipčič⁹², F. Filthaut¹¹⁹, K.D. Finelli²⁵,
 M.C.N. Fiolhais^{140a,140c,a}, L. Fiorini¹⁷⁴, F. Fischer¹¹⁴, W.C. Fisher¹⁰⁷, I. Fleck¹⁵¹, P. Fleischmann¹⁰⁶,
 R.R.M. Fletcher¹³⁷, T. Flick¹⁸², B.M. Flierl¹¹⁴, L. Flores¹³⁷, L.R. Flores Castillo^{63a}, F.M. Follega^{76a,76b},
 N. Fomin¹⁷, J.H. Foo¹⁶⁷, G.T. Forcolin^{76a,76b}, A. Formica¹⁴⁵, F.A. Förster¹⁴, A.C. Forti¹⁰¹, A.G. Foster²¹,
 M.G. Foti¹³⁵, D. Fournier⁶⁵, H. Fox⁹⁰, P. Francavilla^{72a,72b}, S. Francescato^{73a,73b}, M. Franchini^{23b,23a},
 S. Franchino^{61a}, D. Francis³⁶, L. Franconi²⁰, M. Franklin⁵⁹, A.N. Fray⁹³, P.M. Freeman²¹, B. Freund¹¹⁰,
 W.S. Freund^{81b}, E.M. Freundlich⁴⁷, D.C. Frizzell¹²⁹, D. Froidevaux³⁶, J.A. Frost¹³⁵, C. Fukunaga¹⁶⁴,
 E. Fullana Torregrosa¹⁷⁴, E. Fumagalli^{55b,55a}, T. Fusayasu¹¹⁶, J. Fuster¹⁷⁴, A. Gabrielli^{23b,23a},
 A. Gabrielli¹⁸, S. Gadatsch⁵⁴, P. Gadow¹¹⁵, G. Gagliardi^{55b,55a}, L.G. Gagnon¹¹⁰, C. Galea^{27b},
 B. Galhardo^{140a}, G.E. Gallardo¹³⁵, E.J. Gallas¹³⁵, B.J. Gallop¹⁴⁴, G. Galster⁴⁰, R. Gamboa Goni⁹³,

K.K. Gan¹²⁷, S. Ganguly¹⁸⁰, J. Gao^{60a}, Y. Gao⁵⁰, Y.S. Gao^{31,l}, C. García¹⁷⁴, J.E. García Navarro¹⁷⁴, J.A. García Pascual^{15a}, C. Garcia-Argos⁵², M. Garcia-Sciveres¹⁸, R.W. Gardner³⁷, N. Garelli¹⁵³, S. Gargiulo⁵², C.A. Garner¹⁶⁷, V. Garonne¹³⁴, S.J. Gasiorowski¹⁴⁸, P. Gaspar^{81b}, A. Gaudiello^{55b,55a}, G. Gaudio^{71a}, I.L. Gavrilenco¹¹¹, A. Gavrilyuk¹²⁴, C. Gay¹⁷⁵, G. Gaycken⁴⁶, E.N. Gazis¹⁰, A.A. Geanta^{27b}, C.M. Gee¹⁴⁶, C.N.P. Gee¹⁴⁴, J. Geisen⁵³, M. Geisen¹⁰⁰, C. Gemme^{55b}, M.H. Genest⁵⁸, C. Geng¹⁰⁶, S. Gentile^{73a,73b}, S. George⁹⁴, T. Geralis⁴⁴, L.O. Gerlach⁵³, P. Gessinger-Befurt¹⁰⁰, G. Gessner⁴⁷, S. Ghasemi¹⁵¹, M. Ghasemi Bostanabad¹⁷⁶, M. Ghneimat¹⁵¹, A. Ghosh⁶⁵, A. Ghosh⁷⁸, B. Giacobbe^{23b}, S. Giagu^{73a,73b}, N. Giangiacomi^{23b,23a}, P. Giannetti^{72a}, A. Giannini^{70a,70b}, G. Giannini¹⁴, S.M. Gibson⁹⁴, M. Gignac¹⁴⁶, D. Gillberg³⁴, G. Gilles¹⁸², D.M. Gingrich^{3,ar}, M.P. Giordani^{67a,67c}, F.M. Giorgi^{23b}, P.F. Giraud¹⁴⁵, G. Giugliarelli^{67a,67c}, D. Giugni^{69a}, F. Giulì^{74a,74b}, S. Gkaitatzis¹⁶², I. Gkialas^{9,g}, E.L. Gkougkousis¹⁴, P. Gkountoumis¹⁰, L.K. Gladilin¹¹³, C. Glasman⁹⁹, J. Glatzer¹⁴, P.C.F. Glaysher⁴⁶, A. Glazov⁴⁶, G.R. Gledhill¹³², M. Goblersch-Kolb²⁶, D. Godin¹¹⁰, S. Goldfarb¹⁰⁵, T. Golling⁵⁴, D. Golubkov¹²³, A. Gomes^{140a,140b}, R. Goncalves Gama⁵³, R. Gonçalo^{140a}, G. Gonella⁵², L. Gonella²¹, A. Gongadze⁸⁰, F. Gonnella²¹, J.L. Gonski³⁹, S. González de la Hoz¹⁷⁴, S. Gonzalez-Sevilla⁵⁴, G.R. Gonzalvo Rodriguez¹⁷⁴, L. Goossens³⁶, N.A. Gorasia²¹, P.A. Gorbounov¹²⁴, H.A. Gordon²⁹, B. Gorini³⁶, E. Gorini^{68a,68b}, A. Gorišek⁹², A.T. Goshaw⁴⁹, M.I. Gostkin⁸⁰, C.A. Gottardo¹¹⁹, M. Gouighri^{35b}, D. Goujdami^{35c}, A.G. Goussiou¹⁴⁸, N. Govender^{33c}, C. Goy⁵, E. Gozani¹⁶⁰, I. Grabowska-Bold^{84a}, E.C. Graham⁹¹, J. Gramling¹⁷¹, E. Gramstad¹³⁴, S. Grancagnolo¹⁹, M. Grandi¹⁵⁶, V. Gratchev¹³⁸, P.M. Gravila^{27f}, F.G. Gravili^{68a,68b}, C. Gray⁵⁷, H.M. Gray¹⁸, C. Grefe²⁴, K. Gregersen⁹⁷, I.M. Gregor⁴⁶, P. Grenier¹⁵³, K. Grevtsov⁴⁶, C. Grieco¹⁴, N.A. Grieser¹²⁹, A.A. Grillo¹⁴⁶, K. Grimm^{31,k}, S. Grinstein^{14,z}, J.-F. Grivaz⁶⁵, S. Groh¹⁰⁰, E. Gross¹⁸⁰, J. Grosse-Knetter⁵³, Z.J. Grout⁹⁵, C. Grud¹⁰⁶, A. Grummer¹¹⁸, L. Guan¹⁰⁶, W. Guan¹⁸¹, C. Gubbels¹⁷⁵, J. Guenther³⁶, A. Guerguichon⁶⁵, J.G.R. Guerrero Rojas¹⁷⁴, F. Guescini¹¹⁵, D. Guest¹⁷¹, R. Gugel⁵², T. Guillemin⁵, S. Guindon³⁶, U. Gul⁵⁷, J. Guo^{60c}, W. Guo¹⁰⁶, Y. Guo^{60a,s}, Z. Guo¹⁰², R. Gupta⁴⁶, S. Gurbuz^{12c}, G. Gustavino¹²⁹, M. Guth⁵², P. Gutierrez¹²⁹, C. Gutschow⁹⁵, C. Guyot¹⁴⁵, C. Gwenlan¹³⁵, C.B. Gwilliam⁹¹, A. Haas¹²⁵, C. Haber¹⁸, H.K. Hadavand⁸, N. Haddad^{35e}, A. Hadef^{60a}, S. Hageböck³⁶, M. Haleem¹⁷⁷, J. Haley¹³⁰, G. Halladjian¹⁰⁷, G.D. Hallewell¹⁰², K. Hamacher¹⁸², P. Hamal¹³¹, K. Hamano¹⁷⁶, H. Hamdaoui^{35e}, M. Hamer²⁴, G.N. Hamity⁵⁰, K. Han^{60a,y}, L. Han^{60a}, S. Han^{15a}, Y.F. Han¹⁶⁷, K. Hanagaki^{82,w}, M. Hance¹⁴⁶, D.M. Handl¹¹⁴, B. Haney¹³⁷, R. Hankache¹³⁶, E. Hansen⁹⁷, J.B. Hansen⁴⁰, J.D. Hansen⁴⁰, M.C. Hansen²⁴, P.H. Hansen⁴⁰, E.C. Hanson¹⁰¹, K. Hara¹⁶⁹, T. Harenberg¹⁸², S. Harkusha¹⁰⁸, P.F. Harrison¹⁷⁸, N.M. Hartmann¹¹⁴, Y. Hasegawa¹⁵⁰, A. Hasib⁵⁰, S. Hassani¹⁴⁵, S. Haug²⁰, R. Hauser¹⁰⁷, L.B. Havener³⁹, M. Havranek¹⁴², C.M. Hawkes²¹, R.J. Hawkings³⁶, D. Hayden¹⁰⁷, C. Hayes¹⁰⁶, R.L. Hayes¹⁷⁵, C.P. Hays¹³⁵, J.M. Hays⁹³, H.S. Hayward⁹¹, S.J. Haywood¹⁴⁴, F. He^{60a}, M.P. Heath⁵⁰, V. Hedberg⁹⁷, L. Heelan⁸, S. Heer²⁴, K.K. Heidegger⁵², W.D. Heidorn⁷⁹, J. Heilman³⁴, S. Heim⁴⁶, T. Heim¹⁸, B. Heinemann^{46,ao}, J.J. Heinrich¹³², L. Heinrich³⁶, J. Hejbal¹⁴¹, L. Helary^{61b}, A. Held¹⁷⁵, S. Hellesund¹³⁴, C.M. Helling¹⁴⁶, S. Hellman^{45a,45b}, C. Helsens³⁶, R.C.W. Henderson⁹⁰, Y. Heng¹⁸¹, L. Henkelmann^{61a}, S. Henkelmann¹⁷⁵, A.M. Henriques Correia³⁶, G.H. Herbert¹⁹, H. Herde²⁶, V. Herget¹⁷⁷, Y. Hernández Jiménez^{33e}, H. Herr¹⁰⁰, M.G. Herrmann¹¹⁴, T. Herrmann⁴⁸, G. Herten⁵², R. Hertenberger¹¹⁴, L. Hervas³⁶, T.C. Herwig¹³⁷, G.G. Hesketh⁹⁵, N.P. Hessey^{168a}, A. Higashida¹⁶³, S. Higashino⁸², E. Higón-Rodriguez¹⁷⁴, K. Hildebrand³⁷, E. Hill¹⁷⁶, J.C. Hill³², K.K. Hill²⁹, K.H. Hiller⁴⁶, S.J. Hillier²¹, M. Hils⁴⁸, I. Hincliffe¹⁸, F. Hinterkeuser²⁴, M. Hirose¹³³, S. Hirose⁵², D. Hirschbuehl¹⁸², B. Hiti⁹², O. Hladík¹⁴¹, D.R. Hlalučku^{33e}, X. Hoad⁵⁰, J. Hobbs¹⁵⁵, N. Hod¹⁸⁰, M.C. Hodgkinson¹⁴⁹, A. Hoecker³⁶, D. Hohn⁵², D. Hohov⁶⁵, T. Holm²⁴, T.R. Holmes³⁷, M. Holzbock¹¹⁴, L.B.A.H. Hommels³², S. Honda¹⁶⁹, T.M. Hong¹³⁹, J.C. Honig⁵², A. Hönl¹¹⁵, B.H. Hooberman¹⁷³, W.H. Hopkins⁶, Y. Horii¹¹⁷, P. Horn⁴⁸, L.A. Horyn³⁷, S. Hou¹⁵⁸, A. Hoummada^{35a}, J. Howarth¹⁰¹, J. Hoya⁸⁹, M. Hrabovsky¹³¹, J. Hrdinka⁷⁷, I. Hristova¹⁹, J. Hrivnac⁶⁵, A. Hrynevich¹⁰⁹, T. Hrynev'ova⁵, P.J. Hsu⁶⁴, S.-C. Hsu¹⁴⁸, Q. Hu²⁹, S. Hu^{60c}, Y.F. Hu^{15a,15d}, D.P. Huang⁹⁵, Y. Huang^{60a}, Y. Huang^{15a}, Z. Hubacek¹⁴², F. Hubaut¹⁰²,

M. Huebner²⁴, F. Huegging²⁴, T.B. Huffman¹³⁵, M. Huhtinen³⁶, R.F.H. Hunter³⁴, P. Huo¹⁵⁵, A.M. Hupe³⁴, N. Huseynov^{80,af}, J. Huston¹⁰⁷, J. Huth⁵⁹, R. Hyneman¹⁰⁶, S. Hyrych^{28a}, G. Iacobucci⁵⁴, G. Iakovidis²⁹, I. Ibragimov¹⁵¹, L. Iconomidou-Fayard⁶⁵, Z. Idrissi^{35e}, P. Iengo³⁶, R. Ignazzi⁴⁰, O. Igonkina^{120,ab,*}, R. Iguchi¹⁶³, T. Iizawa⁵⁴, Y. Ikegami⁸², M. Ikeno⁸², D. Iliadis¹⁶², N. Illic^{119,167,ae}, F. Iltzsche⁴⁸, G. Introzzi^{71a,71b}, M. Iodice^{75a}, K. Iordanidou^{168a}, V. Ippolito^{73a,73b}, M.F. Isacson¹⁷², M. Ishino¹⁶³, W. Islam¹³⁰, C. Issever^{19,46}, S. Istin¹⁶⁰, F. Ito¹⁶⁹, J.M. Iturbe Ponce^{63a}, R. Iuppa^{76a,76b}, A. Ivina¹⁸⁰, H. Iwasaki⁸², J.M. Izen⁴³, V. Izzo^{70a}, P. Jacka¹⁴¹, P. Jackson¹, R.M. Jacobs²⁴, B.P. Jaeger¹⁵², V. Jain², G. Jäkel¹⁸², K.B. Jakobi¹⁰⁰, K. Jakobs⁵², T. Jakoubek¹⁴¹, J. Jamieson⁵⁷, K.W. Janas^{84a}, R. Jansky⁵⁴, J. Janssen²⁴, M. Janus⁵³, P.A. Janus^{84a}, G. Jarlskog⁹⁷, N. Javadov^{80,af}, T. Javůrek³⁶, M. Javurkova¹⁰³, F. Jeanneau¹⁴⁵, L. Jeanty¹³², J. Jejelava^{159a}, A. Jelinskas¹⁷⁸, P. Jenni^{52,b}, J. Jeong⁴⁶, N. Jeong⁴⁶, S. Jézéquel⁵, H. Ji¹⁸¹, J. Jia¹⁵⁵, H. Jiang⁷⁹, Y. Jiang^{60a}, Z. Jiang^{153,p}, S. Jiggins⁵², F.A. Jimenez Morales³⁸, J. Jimenez Pena¹¹⁵, S. Jin^{15c}, A. Jinaru^{27b}, O. Jinnouchi¹⁶⁵, H. Jivan^{33e}, P. Johansson¹⁴⁹, K.A. Johns⁷, C.A. Johnson⁶⁶, K. Jon-And^{45a,45b}, R.W.L. Jones⁹⁰, S.D. Jones¹⁵⁶, S. Jones⁷, T.J. Jones⁹¹, J. Jongmanns^{61a}, P.M. Jorge^{140a}, J. Jovicevic³⁶, X. Ju¹⁸, J.J. Junggeburth¹¹⁵, A. Juste Rozas^{14,z}, A. Kaczmarska⁸⁵, M. Kado^{73a,73b}, H. Kagan¹²⁷, M. Kagan¹⁵³, A. Kahn³⁹, C. Kahra¹⁰⁰, T. Kaji¹⁷⁹, E. Kajomovitz¹⁶⁰, C.W. Kalderon⁹⁷, A. Kaluza¹⁰⁰, A. Kamenshchikov¹²³, M. Kaneda¹⁶³, N.J. Kang¹⁴⁶, L. Kanjir⁹², Y. Kano¹¹⁷, V.A. Kantserov¹¹², J. Kanzaki⁸², L.S. Kaplan¹⁸¹, D. Kar^{33e}, K. Karava¹³⁵, M.J. Kareem^{168b}, S.N. Karpov⁸⁰, Z.M. Karpova⁸⁰, V. Kartvelishvili⁹⁰, A.N. Karyukhin¹²³, L. Kashif¹⁸¹, R.D. Kass¹²⁷, A. Kastanas^{45a,45b}, C. Kato^{60d,60c}, J. Katzy⁴⁶, K. Kawade¹⁵⁰, K. Kawagoe⁸⁸, T. Kawaguchi¹¹⁷, T. Kawamoto¹⁶³, G. Kawamura⁵³, E.F. Kay¹⁷⁶, V.F. Kazanin^{122b,122a}, R. Keeler¹⁷⁶, R. Kehoe⁴², J.S. Keller³⁴, E. Kellermann⁹⁷, D. Kelsey¹⁵⁶, J.J. Kempster²¹, J. Kendrick²¹, K.E. Kennedy³⁹, O. Kepka¹⁴¹, S. Kersten¹⁸², B.P. Kerševan⁹², S. Ketabchi Haghigat¹⁶⁷, M. Khader¹⁷³, F. Khalil-Zada¹³, M. Khandoga¹⁴⁵, A. Khanov¹³⁰, A.G. Kharlamov^{122b,122a}, T. Kharlamova^{122b,122a}, E.E. Khoda¹⁷⁵, A. Khodinov¹⁶⁶, T.J. Khoo⁵⁴, E. Khramov⁸⁰, J. Khubua^{159b}, S. Kido⁸³, M. Kiehn⁵⁴, C.R. Kilby⁹⁴, Y.K. Kim³⁷, N. Kimura⁹⁵, O.M. Kind¹⁹, B.T. King^{91,*}, D. Kirchmeier⁴⁸, J. Kirk¹⁴⁴, A.E. Kiryunin¹¹⁵, T. Kishimoto¹⁶³, D.P. Kisliuk¹⁶⁷, V. Kitali⁴⁶, O. Kivernyk⁵, T. Klapdor-Kleingrothaus⁵², M. Klassen^{61a}, M.H. Klein¹⁰⁶, M. Klein⁹¹, U. Klein⁹¹, K. Kleinknecht¹⁰⁰, P. Klimek¹²¹, A. Klimentov²⁹, T. Klingl²⁴, T. Klioutchnikova³⁶, F.F. Klitzner¹¹⁴, P. Kluit¹²⁰, S. Kluth¹¹⁵, E. Kneringer⁷⁷, E.B.F.G. Knoops¹⁰², A. Knue⁵², D. Kobayashi⁸⁸, T. Kobayashi¹⁶³, M. Kobel⁴⁸, M. Kocian¹⁵³, P. Kodys¹⁴³, P.T. Koenig²⁴, T. Koffas³⁴, N.M. Köhler³⁶, T. Koi¹⁵³, M. Kolb¹⁴⁵, I. Koletsou⁵, T. Komarek¹³¹, T. Kondo⁸², K. Köneke⁵², A.X.Y. Kong¹, A.C. König¹¹⁹, T. Kono¹²⁶, R. Konoplich^{125,aj}, V. Konstantinides⁹⁵, N. Konstantinidis⁹⁵, B. Konya⁹⁷, R. Kopeliansky⁶⁶, S. Koperny^{84a}, K. Korcyl⁸⁵, K. Kordas¹⁶², G. Koren¹⁶¹, A. Korn⁹⁵, I. Korolkov¹⁴, E.V. Korolkova¹⁴⁹, N. Korotkova¹¹³, O. Kortner¹¹⁵, S. Kortner¹¹⁵, T. Kosek¹⁴³, V.V. Kostyukhin¹⁶⁶, A. Kotsokechagia⁶⁵, A. Kotwal⁴⁹, A. Koulouris¹⁰, A. Kourkoumeli-Charalampidi^{71a,71b}, C. Kourkoumelis⁹, E. Kourlitis¹⁴⁹, V. Kouskoura²⁹, A.B. Kowalewska⁸⁵, R. Kowalewski¹⁷⁶, C. Kozakai¹⁶³, W. Kozanecki¹⁴⁵, A.S. Kozhin¹²³, V.A. Kramarenko¹¹³, G. Kramberger⁹², D. Krasnovevtsev^{60a}, M.W. Krasny¹³⁶, A. Krasznahorkay³⁶, D. Krauss¹¹⁵, J.A. Kremer^{84a}, J. Kretzschmar⁹¹, P. Krieger¹⁶⁷, F. Krieter¹¹⁴, A. Krishnan^{61b}, K. Krizka¹⁸, K. Kroeninger⁴⁷, H. Kroha¹¹⁵, J. Kroll¹⁴¹, J. Kroll¹³⁷, K.S. Krowpman¹⁰⁷, J. Krstic¹⁶, U. Kruchonak⁸⁰, H. Krüger²⁴, N. Krumnack⁷⁹, M.C. Kruse⁴⁹, J.A. Krzysiak⁸⁵, T. Kubota¹⁰⁵, O. Kuchinskaia¹⁶⁶, S. Kuday^{4b}, J.T. Kuechler⁴⁶, S. Kuehn³⁶, A. Kugel^{61a}, T. Kuhl⁴⁶, V. Kukhtin⁸⁰, R. Kukla¹⁰², Y. Kulchitsky^{108,ah}, S. Kuleshov^{147d}, Y.P. Kulinich¹⁷³, M. Kuna⁵⁸, T. Kunigo⁸⁶, A. Kupco¹⁴¹, T. Kupfer⁴⁷, O. Kuprash⁵², H. Kurashige⁸³, L.L. Kurchaninov^{168a}, Y.A. Kurochkin¹⁰⁸, A. Kurova¹¹², M.G. Kurth^{15a,15d}, E.S. Kuwertz³⁶, M. Kuze¹⁶⁵, A.K. Kvam¹⁴⁸, J. Kvita¹³¹, T. Kwan¹⁰⁴, A. La Rosa¹¹⁵, L. La Rotonda^{41b,41a}, F. La Ruffa^{41b,41a}, C. Lacasta¹⁷⁴, F. Lacava^{73a,73b}, D.P.J. Lack¹⁰¹, H. Lacker¹⁹, D. Lacour¹³⁶, E. Ladygin⁸⁰, R. Lafaye⁵, B. Laforgue¹³⁶, T. Lagouri^{33e}, S. Lai⁵³, I.K. Lakomiec^{84a}, S. Lammers⁶⁶, W. Lampl⁷, C. Lampoudis¹⁶², E. Lançon²⁹, U. Landgraf⁵², M.P.J. Landon⁹³, M.C. Lanfermann⁵⁴, V.S. Lang⁴⁶,

J.C. Lange⁵³, R.J. Langenberg¹⁰³, A.J. Lankford¹⁷¹, F. Lanni²⁹, K. Lantzsch²⁴, A. Lanza^{71a},
 A. Lapertosa^{55b,55a}, S. Laplace¹³⁶, J.F. Laporte¹⁴⁵, T. Lari^{69a}, F. Lasagni Manghi^{23b,23a}, M. Lassnig³⁶,
 T.S. Lau^{63a}, A. Laudrain⁶⁵, A. Laurier³⁴, M. Lavorgna^{70a,70b}, S.D. Lawlor⁹⁴, M. Lazzaroni^{69a,69b}, B. Le¹⁰⁵,
 E. Le Guirriec¹⁰², M. LeBlanc⁷, T. LeCompte⁶, F. Ledroit-Guillon⁵⁸, A.C.A. Lee⁹⁵, C.A. Lee²⁹,
 G.R. Lee¹⁷, L. Lee⁵⁹, S.C. Lee¹⁵⁸, S.J. Lee³⁴, S. Lee⁷⁹, B. Lefebvre^{168a}, H.P. Lefebvre⁹⁴, M. Lefebvre¹⁷⁶,
 F. Legger¹¹⁴, C. Leggett¹⁸, K. Lehmann¹⁵², N. Lehmann¹⁸², G. Lehmann Miotto³⁶, W.A. Leight⁴⁶,
 A. Leisos^{162,x}, M.A.L. Leite^{81d}, C.E. Leitgeb¹¹⁴, R. Leitner¹⁴³, D. Lelouch^{180,*}, K.J.C. Leney⁴²,
 T. Lenz²⁴, R. Leone⁷, S. Leone^{72a}, C. Leonidopoulos⁵⁰, A. Leopold¹³⁶, C. Leroy¹¹⁰, R. Les¹⁶⁷,
 C.G. Lester³², M. Levchenko¹³⁸, J. Levêque⁵, D. Levin¹⁰⁶, L.J. Levinson¹⁸⁰, D.J. Lewis²¹, B. Li^{15b},
 B. Li¹⁰⁶, C-Q. Li^{60a}, F. Li^{60c}, H. Li^{60a}, H. Li^{60b}, J. Li^{60c}, K. Li¹⁵³, L. Li^{60c}, M. Li^{15a,15d}, Q. Li^{15a,15d},
 Q.Y. Li^{60a}, S. Li^{60d,60c}, X. Li⁴⁶, Y. Li⁴⁶, Z. Li^{60b}, Z. Liang^{15a}, B. Libert^{74a}, A. Liblong¹⁶⁷, K. Lie^{63c},
 S. Lim²⁹, C.Y. Lin³², K. Lin¹⁰⁷, T.H. Lin¹⁰⁰, R.A. Linck⁶⁶, J.H. Lindon²¹, A.L. Lioni⁵⁴, E. Lipeles¹³⁷,
 A. Lipniacka¹⁷, T.M. Liss^{173,aq}, A. Lister¹⁷⁵, A.M. Litke¹⁴⁶, J.D. Little⁸, B. Liu⁷⁹, B.L. Liu⁶, H.B. Liu²⁹,
 H. Liu¹⁰⁶, J.B. Liu^{60a}, J.K.K. Liu¹³⁵, K. Liu¹³⁶, M. Liu^{60a}, P. Liu¹⁸, Y. Liu^{15a,15d}, Y.L. Liu¹⁰⁶, Y.W. Liu^{60a},
 M. Livan^{71a,71b}, A. Lleres⁵⁸, J. Llorente Merino¹⁵², S.L. Lloyd⁹³, C.Y. Lo^{63b}, F. Lo Sterzo⁴²,
 E.M. Lobodzinska⁴⁶, P. Loch⁷, S. Loffredo^{74a,74b}, T. Lohse¹⁹, K. Lohwasser¹⁴⁹, M. Lokajicek¹⁴¹,
 J.D. Long¹⁷³, R.E. Long⁹⁰, L. Longo³⁶, K.A.Looper¹²⁷, J.A. Lopez^{147d}, I. Lopez Paz¹⁰¹,
 A. Lopez Solis¹⁴⁹, J. Lorenz¹¹⁴, N. Lorenzo Martinez⁵, A.M. Lory¹¹⁴, M. Losada^{22a}, P.J. Lösel¹¹⁴,
 A. Lösle⁵², X. Lou⁴⁶, X. Lou^{15a}, A. Lounis⁶⁵, J. Love⁶, P.A. Love⁹⁰, J.J. Lozano Bahilo¹⁷⁴, M. Lu^{60a},
 Y.J. Lu⁶⁴, H.J. Lubatti¹⁴⁸, C. Luci^{73a,73b}, A. Lucotte⁵⁸, C. Luedtke⁵², F. Luehring⁶⁶, I. Luise¹³⁶,
 L. Luminari^{73a}, B. Lund-Jensen¹⁵⁴, M.S. Lutz¹⁰³, D. Lynn²⁹, H. Lyons⁹¹, R. Lysak¹⁴¹, E. Lytken⁹⁷,
 F. Lyu^{15a}, V. Lyubushkin⁸⁰, T. Lyubushkina⁸⁰, H. Ma²⁹, L.L. Ma^{60b}, Y. Ma^{60b}, G. Maccarrone⁵¹,
 A. Macchiolo¹¹⁵, C.M. Macdonald¹⁴⁹, J. Machado Miguens¹³⁷, D. Madaffari¹⁷⁴, R. Madar³⁸,
 W.F. Mader⁴⁸, M. Madugoda Ralalage Don¹³⁰, N. Madysa⁴⁸, J. Maeda⁸³, T. Maeno²⁹, M. Maerker⁴⁸,
 A.S. Maevskiy¹¹³, V. Magerl⁵², N. Magini⁷⁹, D.J. Mahon³⁹, C. Maidantchik^{81b}, T. Maier¹¹⁴,
 A. Maio^{140a,140b,140d}, K. Maj^{84a}, O. Majersky^{28a}, S. Majewski¹³², Y. Makida⁸², N. Makovec⁶⁵,
 B. Malaescu¹³⁶, Pa. Malecki⁸⁵, V.P. Maleev¹³⁸, F. Malek⁵⁸, U. Mallik⁷⁸, D. Malon⁶, C. Malone³²,
 S. Maltezos¹⁰, S. Malyukov⁸⁰, J. Mamuzic¹⁷⁴, G. Mancini⁵¹, I. Mandić⁹²,
 L. Manhaes de Andrade Filho^{81a}, I.M. Maniatis¹⁶², J. Manjarres Ramos⁴⁸, K.H. Mankinen⁹⁷, A. Mann¹¹⁴,
 A. Manousos⁷⁷, B. Mansoulie¹⁴⁵, I. Manthos¹⁶², S. Manzoni¹²⁰, A. Marantis¹⁶², G. Marceca³⁰,
 L. Marchese¹³⁵, G. Marchiori¹³⁶, M. Marcisovsky¹⁴¹, L. Marcoccia^{74a,74b}, C. Marcon⁹⁷,
 C.A. Marin Tobon³⁶, M. Marjanovic¹²⁹, Z. Marshall¹⁸, M.U.F. Martensson¹⁷², S. Marti-Garcia¹⁷⁴,
 C.B. Martin¹²⁷, T.A. Martin¹⁷⁸, V.J. Martin⁵⁰, B. Martin dit Latour¹⁷, L. Martinelli^{75a,75b}, M. Martinez^{14,z},
 V.I. Martinez Outschoorn¹⁰³, S. Martin-Haugh¹⁴⁴, V.S. Martoiu^{27b}, A.C. Martyniuk⁹⁵, A. Marzin³⁶,
 S.R. Maschek¹¹⁵, L. Masetti¹⁰⁰, T. Mashimo¹⁶³, R. Mashinistov¹¹¹, J. Masik¹⁰¹, A.L. Maslennikov^{122b,122a},
 L. Massa^{74a,74b}, P. Massarotti^{70a,70b}, P. Mastrandrea^{72a,72b}, A. Mastroberardino^{41b,41a}, T. Masubuchi¹⁶³,
 D. Matakias¹⁰, A. Matic¹¹⁴, N. Matsuzawa¹⁶³, P. Mättig²⁴, J. Maurer^{27b}, B. Maček⁹²,
 D.A. Maximov^{122b,122a}, R. Mazini¹⁵⁸, I. Maznas¹⁶², S.M. Mazza¹⁴⁶, S.P. Mc Kee¹⁰⁶, T.G. McCarthy¹¹⁵,
 W.P. McCormack¹⁸, E.F. McDonald¹⁰⁵, J.A. McFayden³⁶, G. Mchedlidze^{159b}, M.A. McKay⁴²,
 K.D. McLean¹⁷⁶, S.J. McMahon¹⁴⁴, P.C. McNamara¹⁰⁵, C.J. Nicol¹⁷⁸, R.A. McPherson^{176,ae},
 J.E. Mdhluli^{33e}, Z.A. Meadows¹⁰³, S. Meehan³⁶, T. Megy⁵², S. Mehlhase¹¹⁴, A. Mehta⁹¹, T. Meideck⁵⁸,
 B. Meiroke⁴³, D. Melini¹⁶⁰, B.R. Mellado Garcia^{33e}, J.D. Mellenthin⁵³, M. Melo^{28a}, F. Meloni⁴⁶,
 A. Melzer²⁴, S.B. Menary¹⁰¹, E.D. Mendes Gouveia^{140a,140e}, L. Meng³⁶, X.T. Meng¹⁰⁶, S. Menke¹¹⁵,
 E. Meoni^{41b,41a}, S. Mergelmeyer¹⁹, S.A.M. Merkt¹³⁹, C. Merlassino²⁰, P. Mermod⁵⁴, L. Merola^{70a,70b},
 C. Meroni^{69a}, G. Merz¹⁰⁶, O. Meshkov^{113,111}, J.K.R. Meshreki¹⁵¹, A. Messina^{73a,73b}, J. Metcalfe⁶,
 A.S. Mete¹⁷¹, C. Meyer⁶⁶, J-P. Meyer¹⁴⁵, H. Meyer Zu Theenhausen^{61a}, F. Miano¹⁵⁶, M. Michetti¹⁹,
 R.P. Middleton¹⁴⁴, L. Mijovic⁵⁰, G. Mikenberg¹⁸⁰, M. Mikestikova¹⁴¹, M. Mikuž⁹², H. Mildner¹⁴⁹,

M. Milesi¹⁰⁵, A. Milic¹⁶⁷, D.A. Millar⁹³, D.W. Miller³⁷, A. Milov¹⁸⁰, D.A. Milstead^{45a,45b}, R.A. Mina¹⁵³, A.A. Minaenko¹²³, M. Miñano Moya¹⁷⁴, I.A. Minashvili^{159b}, A.I. Mincer¹²⁵, B. Mindur^{84a}, M. Mineev⁸⁰, Y. Minegishi¹⁶³, L.M. Mir¹⁴, A. Mirto^{68a,68b}, K.P. Mistry¹³⁷, T. Mitani¹⁷⁹, J. Mitrevski¹¹⁴, V.A. Mitsou¹⁷⁴, M. Mittal^{60c}, O. Miu¹⁶⁷, A. Miucci²⁰, P.S. Miyagawa¹⁴⁹, A. Mizukami⁸², J.U. Mjörnmark⁹⁷, T. Mkrtchyan^{61a}, M. Mlynarikova¹⁴³, T. Moa^{45a,45b}, K. Mochizuki¹¹⁰, P. Mogg⁵², S. Mohapatra³⁹, R. Moles-Valls²⁴, M.C. Mondragon¹⁰⁷, K. Mönig⁴⁶, J. Monk⁴⁰, E. Monnier¹⁰², A. Montalbano¹⁵², J. Montejo Berlingen³⁶, M. Montella⁹⁵, F. Monticelli⁸⁹, S. Monzani^{69a}, N. Morange⁶⁵, D. Moreno^{22a}, M. Moreno Llácer¹⁷⁴, C. Moreno Martinez¹⁴, P. Morettini^{55b}, M. Morgenstern¹²⁰, S. Morgenstern⁴⁸, D. Mori¹⁵², M. Mori⁵⁹, M. Morinaga¹⁷⁹, V. Morisbak¹³⁴, A.K. Morley³⁶, G. Mornacchi³⁶, A.P. Morris⁹⁵, L. Morvaj¹⁵⁵, P. Moschovakos³⁶, B. Moser¹²⁰, M. Mosidze^{159b}, T. Moskalets¹⁴⁵, H.J. Moss¹⁴⁹, J. Moss^{31,m}, E.J.W. Moyse¹⁰³, S. Muanza¹⁰², J. Mueller¹³⁹, R.S.P. Mueller¹¹⁴, D. Muenstermann⁹⁰, G.A. Mullier⁹⁷, D.P. Mungo^{69a,69b}, J.L. Munoz Martinez¹⁴, F.J. Munoz Sanchez¹⁰¹, P. Murin^{28b}, W.J. Murray^{178,144}, A. Murrone^{69a,69b}, M. Muškinja¹⁸, C. Mwewa^{33a}, A.G. Myagkov^{123,ak}, A.A. Myers¹³⁹, J. Myers¹³², M. Myska¹⁴², B.P. Nachman¹⁸, O. Nackenhorst⁴⁷, A.Nag Nag⁴⁸, K. Nagai¹³⁵, K. Nagano⁸², Y. Nagasaka⁶², J.L. Nagle²⁹, E. Nagy¹⁰², A.M. Nairz³⁶, Y. Nakahama¹¹⁷, K. Nakamura⁸², T. Nakamura¹⁶³, I. Nakano¹²⁸, H. Nanjo¹³³, F. Napolitano^{61a}, R.F. Naranjo Garcia⁴⁶, R. Narayan⁴², I. Naryshkin¹³⁸, T. Naumann⁴⁶, G. Navarro^{22a}, P.Y. Nechaeva¹¹¹, F. Nechansky⁴⁶, T.J. Neep²¹, A. Negri^{71a,71b}, M. Negrini^{23b}, C. Nellist⁵³, M.E. Nelson^{45a,45b}, S. Nemecek¹⁴¹, P. Nemethy¹²⁵, M. Nessi^{36,d}, M.S. Neubauer¹⁷³, M. Neumann¹⁸², R. Newhouse¹⁷⁵, P.R. Newman²¹, Y.S. Ng¹⁹, Y.W.Y. Ng¹⁷¹, B. Ngair^{35e}, H.D.N. Nguyen¹⁰², T. Nguyen Manh¹¹⁰, E. Nibigira³⁸, R.B. Nickerson¹³⁵, R. Nicolaïdou¹⁴⁵, D.S. Nielsen⁴⁰, J. Nielsen¹⁴⁶, N. Nikiforou¹¹, V. Nikolaenko^{123,ak}, I. Nikolic-Audit¹³⁶, K. Nikolopoulos²¹, P. Nilsson²⁹, H.R. Nindhito⁵⁴, Y. Ninomiya⁸², A. Nisati^{73a}, N. Nishu^{60c}, R. Nisius¹¹⁵, I. Nitsche⁴⁷, T. Nitta¹⁷⁹, T. Nobe¹⁶³, Y. Noguchi⁸⁶, I. Nomidis¹³⁶, M.A. Nomura²⁹, M. Nordberg³⁶, N. Norjoharuddeen¹³⁵, T. Novak⁹², O. Novgorodova⁴⁸, R. Novotny¹⁴², L. Nozka¹³¹, K. Ntekas¹⁷¹, E. Nurse⁹⁵, F.G. Oakham^{34,ar}, H. Oberlack¹¹⁵, J. Ocariz¹³⁶, A. Ochi⁸³, I. Ochoa³⁹, J.P. Ochoa-Ricoux^{147a}, K. O'Connor²⁶, S. Oda⁸⁸, S. Odaka⁸², S. Oerdekk⁵³, A. Ogrodnik^{84a}, A. Oh¹⁰¹, S.H. Oh⁴⁹, C.C. Ohm¹⁵⁴, H. Oide¹⁶⁵, M.L. Ojeda¹⁶⁷, H. Okawa¹⁶⁹, Y. Okazaki⁸⁶, M.W. O'Keefe⁹¹, Y. Okumura¹⁶³, T. Okuyama⁸², A. Olariu^{27b}, L.F. Oleiro Seabra^{140a}, S.A. Olivares Pino^{147a}, D. Oliveira Damazio²⁹, J.L. Oliver¹, M.J.R. Olsson¹⁷¹, A. Olszewski⁸⁵, J. Olszowska⁸⁵, D.C. O'Neil¹⁵², A.P. O'neill¹³⁵, A. Onofre^{140a,140e}, P.U.E. Onyisi¹¹, H. Oppen¹³⁴, M.J. Oreglia³⁷, G.E. Orellana⁸⁹, D. Orestano^{75a,75b}, N. Orlando¹⁴, R.S. Orr¹⁶⁷, V. O'Shea⁵⁷, R. Ospanov^{60a}, G. Otero y Garzon³⁰, H. Otomo⁸⁸, P.S. Ott^{61a}, M. Ouchrif^{35d}, J. Ouellette²⁹, F. Ould-Saada¹³⁴, A. Ouraou¹⁴⁵, Q. Ouyang^{15a}, M. Owen⁵⁷, R.E. Owen²¹, V.E. Ozcan^{12c}, N. Ozturk⁸, J. Pacalt¹³¹, H.A. Pacey³², K. Pachal⁴⁹, A. Pacheco Pages¹⁴, C. Padilla Aranda¹⁴, S. Pagan Griso¹⁸, M. Paganini¹⁸³, G. Palacino⁶⁶, S. Palazzo⁵⁰, S. Palestini³⁶, M. Palka^{84b}, D. Pallin³⁸, I. Panagoulias¹⁰, C.E. Pandini³⁶, J.G. Panduro Vazquez⁹⁴, P. Pani⁴⁶, G. Panizzo^{67a,67c}, L. Paolozzi⁵⁴, C. Papadatos¹¹⁰, K. Papageorgiou^{9,g}, S. Parajuli⁴³, A. Paramonov⁶, D. Paredes Hernandez^{63b}, S.R. Paredes Saenz¹³⁵, B. Parida¹⁶⁶, T.H. Park¹⁶⁷, A.J. Parker³¹, M.A. Parker³², F. Parodi^{55b,55a}, E.W. Parrish¹²¹, J.A. Parsons³⁹, U. Parzefall⁵², L. Pascual Dominguez¹³⁶, V.R. Pascuzzi¹⁶⁷, J.M.P. Pasner¹⁴⁶, F. Pasquali¹²⁰, E. Pasqualucci^{73a}, S. Passaggio^{55b}, F. Pastore⁹⁴, P. Pasuwan^{45a,45b}, S. Pataria¹⁰⁰, J.R. Pater¹⁰¹, A. Pathak^{181,i}, T. Pauly³⁶, J. Pearkes¹⁵³, B. Pearson¹¹⁵, M. Pedersen¹³⁴, L. Pedraza Diaz¹¹⁹, R. Pedro^{140a}, T. Peiffer⁵³, S.V. Peleganchuk^{122b,122a}, O. Penc¹⁴¹, H. Peng^{60a}, B.S. Peralva^{81a}, M.M. Perego⁶⁵, A.P. Pereira Peixoto^{140a}, D.V. Perepelitsa²⁹, F. Peri¹⁹, L. Perini^{69a,69b}, H. Pernegger³⁶, S. Perrella^{70a,70b}, A. Perrevoort¹²⁰, K. Peters⁴⁶, R.F.Y. Peters¹⁰¹, B.A. Petersen³⁶, T.C. Petersen⁴⁰, E. Petit¹⁰², A. Petridis¹, C. Petridou¹⁶², P. Petroff⁶⁵, M. Petrov¹³⁵, F. Petrucci^{75a,75b}, M. Pettee¹⁸³, N.E. Pettersson¹⁰³, K. Petukhova¹⁴³, A. Peyaud¹⁴⁵, R. Pezoa^{147d}, L. Pezzotti^{71a,71b}, T. Pham¹⁰⁵, F.H. Phillips¹⁰⁷, P.W. Phillips¹⁴⁴, M.W. Phipps¹⁷³, G. Piacquadio¹⁵⁵, E. Pianori¹⁸, A. Picazio¹⁰³, R.H. Pickles¹⁰¹, R. Piegaia³⁰, D. Pietreanu^{27b}, J.E. Pilcher³⁷, A.D. Pilkington¹⁰¹,

M. Pinamonti^{67a,67c}, J.L. Pinfold³, M. Pitt¹⁶¹, L. Pizzimento^{74a,74b}, M.-A. Pleier²⁹, V. Pleskot¹⁴³,
 E. Plotnikova⁸⁰, P. Podberezko^{122b,122a}, R. Poettgen⁹⁷, R. Poggi⁵⁴, L. Poggiali⁶⁵, I. Pogrebnyak¹⁰⁷,
 D. Pohl²⁴, I. Pokharel⁵³, G. Polesello^{71a}, A. Poley¹⁸, A. Policicchio^{73a,73b}, R. Polifka¹⁴³, A. Polini^{23b},
 C.S. Pollard⁴⁶, V. Polychronakos²⁹, D. Ponomarenko¹¹², L. Pontecorvo³⁶, S. Popa^{27a}, G.A. Popeneciu^{27d},
 L. Portales⁵, D.M. Portillo Quintero⁵⁸, S. Pospisil¹⁴², K. Potamianos⁴⁶, I.N. Potrap⁸⁰, C.J. Potter³²,
 H. Potti¹¹, T. Poulsen⁹⁷, J. Poveda³⁶, T.D. Powell¹⁴⁹, G. Pownall⁴⁶, M.E. Pozo Astigarraga³⁶,
 P. Pralavorio¹⁰², S. Prell⁷⁹, D. Price¹⁰¹, M. Primavera^{68a}, S. Prince¹⁰⁴, M.L. Proffitt¹⁴⁸, N. Proklova¹¹²,
 K. Prokofiev^{63c}, F. Prokoshin⁸⁰, S. Protopopescu²⁹, J. Proudfoot⁶, M. Przybycien^{84a}, D. Pudzha¹³⁸,
 A. Puri¹⁷³, P. Puzo⁶⁵, J. Qian¹⁰⁶, Y. Qin¹⁰¹, A. Quadri⁵³, M. Queitsch-Maitland³⁶, A. Qureshi¹,
 M. Racko^{28a}, F. Ragusa^{69a,69b}, G. Rahal⁹⁸, J.A. Raine⁵⁴, S. Rajagopalan²⁹, A. Ramirez Morales⁹³,
 K. Ran^{15a,15d}, T. Rashid⁶⁵, S. Raspopov⁵, D.M. Rauch⁴⁶, F. Rauscher¹¹⁴, S. Rave¹⁰⁰, B. Ravina¹⁴⁹,
 I. Ravinovich¹⁸⁰, J.H. Rawling¹⁰¹, M. Raymond³⁶, A.L. Read¹³⁴, N.P. Readoff⁵⁸, M. Reale^{68a,68b},
 D.M. Rebuzzi^{71a,71b}, A. Redelbach¹⁷⁷, G. Redlinger²⁹, K. Reeves⁴³, L. Rehnisch¹⁹, J. Reichert¹³⁷,
 D. Reikher¹⁶¹, A. Reiss¹⁰⁰, A. Rej¹⁵¹, C. Rembser³⁶, M. Renda^{27b}, M. Rescigno^{73a}, S. Resconi^{69a},
 E.D. Ressegue¹³⁷, S. Rettie¹⁷⁵, B. Reynolds¹²⁷, E. Reynolds²¹, O.L. Rezanova^{122b,122a}, P. Reznicek¹⁴³,
 E. Ricci^{76a,76b}, R. Richter¹¹⁵, S. Richter⁴⁶, E. Richter-Was^{84b}, O. Ricken²⁴, M. Ridel¹³⁶, P. Rieck¹¹⁵,
 O. Rifki⁴⁶, M. Rijssenbeek¹⁵⁵, A. Rimoldi^{71a,71b}, M. Rimoldi⁴⁶, L. Rinaldi^{23b}, G. Ripellino¹⁵⁴, I. Riu¹⁴,
 J.C. Rivera Vergara¹⁷⁶, F. Rizatdinova¹³⁰, E. Rizvi⁹³, C. Rizzi³⁶, R.T. Roberts¹⁰¹, S.H. Robertson^{104,ae},
 M. Robin⁴⁶, D. Robinson³², J.E.M. Robinson⁴⁶, C.M. Robles Gajardo^{147d}, A. Robson⁵⁷, A. Rocchi^{74a,74b},
 E. Rocco¹⁰⁰, C. Roda^{72a,72b}, S. Rodriguez Bosca¹⁷⁴, A. Rodriguez Perez¹⁴, D. Rodriguez Rodriguez¹⁷⁴,
 A.M. Rodríguez Vera^{168b}, S. Roe³⁶, O. Røhne¹³⁴, R. Röhrlig¹¹⁵, R.A. Rojas^{147d}, C.P.A. Roland⁶⁶,
 J. Roloff²⁹, A. Romanouk¹¹², M. Romano^{23b,23a}, N. Rompotis⁹¹, M. Ronzani¹²⁵, L. Roos¹³⁶, S. Rosati^{73a},
 G. Rosin¹⁰³, B.J. Rosser¹³⁷, E. Rossi⁴⁶, E. Rossi^{75a,75b}, E. Rossi^{70a,70b}, L.P. Rossi^{55b}, L. Rossini^{69a,69b},
 R. Rosten¹⁴, M. Rotaru^{27b}, J. Rothberg¹⁴⁸, D. Rousseau⁶⁵, G. Rovelli^{71a,71b}, A. Roy¹¹, D. Roy^{33e},
 A. Rozanov¹⁰², Y. Rozen¹⁶⁰, X. Ruan^{33e}, F. Rühr⁵², A. Ruiz-Martinez¹⁷⁴, A. Rummler³⁶, Z. Rurikova⁵²,
 N.A. Rusakovich⁸⁰, H.L. Russell¹⁰⁴, L. Rustige^{38,47}, J.P. Rutherford⁷, E.M. Rüttinger¹⁴⁹, M. Rybar³⁹,
 G. Rybkin⁶⁵, E.B. Rye¹³⁴, A. Ryzhov¹²³, J.A. Sabater Iglesias⁴⁶, P. Sabatini⁵³, G. Sabato¹²⁰, S. Sacerdoti⁶⁵,
 H.F-W. Sadrozinski¹⁴⁶, R. Sadykov⁸⁰, F. Safai Tehrani^{73a}, B. Safarzadeh Samani¹⁵⁶, P. Saha¹²¹, S. Saha¹⁰⁴,
 M. Sahinsoy^{61a}, A. Sahu¹⁸², M. Saimpert⁴⁶, M. Saito¹⁶³, T. Saito¹⁶³, H. Sakamoto¹⁶³, A. Sakharov^{125,aj},
 D. Salamani⁵⁴, G. Salamanna^{75a,75b}, J.E. Salazar Loyola^{147d}, A. Salnikov¹⁵³, J. Salt¹⁷⁴, D. Salvatore^{41b,41a},
 F. Salvatore¹⁵⁶, A. Salvucci^{63a,63b,63c}, A. Salzburger³⁶, J. Samarati³⁶, D. Sammel⁵², D. Sampsonidis¹⁶²,
 D. Sampsonidou¹⁶², J. Sánchez¹⁷⁴, A. Sanchez Pineda^{67a,36,67c}, H. Sandaker¹³⁴, C.O. Sander⁴⁶,
 I.G. Sanderswood⁹⁰, M. Sandhoff¹⁸², C. Sandoval^{22a}, D.P.C. Sankey¹⁴⁴, M. Sannino^{55b,55a}, Y. Sano¹¹⁷,
 A. Sansoni⁵¹, C. Santoni³⁸, H. Santos^{140a,140b}, S.N. Santpur¹⁸, A. Santra¹⁷⁴, A. Sapronov⁸⁰,
 J.G. Saraiva^{140a,140d}, O. Sasaki⁸², K. Sato¹⁶⁹, F. Sauerburger⁵², E. Sauvan⁵, P. Savard^{167,ar}, R. Sawada¹⁶³,
 C. Sawyer¹⁴⁴, L. Sawyer^{96,ai}, C. Sbarra^{23b}, A. Sbrizzi^{23a}, T. Scanlon⁹⁵, J. Schaarschmidt¹⁴⁸, P. Schacht¹¹⁵,
 B.M. Schachtner¹¹⁴, D. Schaefer³⁷, L. Schaefer¹³⁷, J. Schaeffer¹⁰⁰, S. Schaepe³⁶, U. Schäfer¹⁰⁰,
 A.C. Schaffer⁶⁵, D. Schaile¹¹⁴, R.D. Schamberger¹⁵⁵, N. Scharmberg¹⁰¹, V.A. Schegelsky¹³⁸,
 D. Scheirich¹⁴³, F. Schenck¹⁹, M. Schernau¹⁷¹, C. Schiavi^{55b,55a}, S. Schier¹⁴⁶, L.K. Schildgen²⁴,
 Z.M. Schillaci²⁶, E.J. Schioppa³⁶, M. Schioppa^{41b,41a}, K.E. Schleicher⁵², S. Schlenker³⁶,
 K.R. Schmidt-Sommerfeld¹¹⁵, K. Schmieden³⁶, C. Schmitt¹⁰⁰, S. Schmitt⁴⁶, S. Schmitz¹⁰⁰,
 J.C. Schmoeckel⁴⁶, U. Schnoor⁵², L. Schoeffel¹⁴⁵, A. Schoening^{61b}, P.G. Scholer⁵², E. Schopf¹³⁵,
 M. Schott¹⁰⁰, J.F.P. Schouwenberg¹¹⁹, J. Schovancova³⁶, S. Schramm⁵⁴, F. Schroeder¹⁸², A. Schulte¹⁰⁰,
 H-C. Schultz-Coulon^{61a}, M. Schumacher⁵², B.A. Schumm¹⁴⁶, Ph. Schune¹⁴⁵, A. Schwartzman¹⁵³,
 T.A. Schwarz¹⁰⁶, Ph. Schwemling¹⁴⁵, R. Schwienhorst¹⁰⁷, A. Sciandra¹⁴⁶, G. Sciolla²⁶, M. Scodeggio⁴⁶,
 M. Scornajenghi^{41b,41a}, F. Scuri^{72a}, F. Scutti¹⁰⁵, L.M. Scyboz¹¹⁵, C.D. Sebastiani^{73a,73b}, P. Seema¹⁹,
 S.C. Seidel¹¹⁸, A. Seiden¹⁴⁶, B.D. Seidlitz²⁹, T. Seiss³⁷, J.M. Seixas^{81b}, G. Sekhniaidze^{70a}, K. Sekhon¹⁰⁶,

S.J. Sekula⁴², N. Semprini-Cesari^{23b,23a}, S. Sen⁴⁹, C. Serfon⁷⁷, L. Serin⁶⁵, L. Serkin^{67a,67b}, M. Sessa^{60a}, H. Severini¹²⁹, S. Sevova¹⁵³, T. Šfiligoj⁹², F. Sforza^{55b,55a}, A. Sfyrla⁵⁴, E. Shabalina⁵³, J.D. Shahinian¹⁴⁶, N.W. Shaikh^{45a,45b}, D. Shaked Renous¹⁸⁰, L.Y. Shan^{15a}, J.T. Shank²⁵, M. Shapiro¹⁸, A. Sharma¹³⁵, A.S. Sharma¹, P.B. Shatalov¹²⁴, K. Shaw¹⁵⁶, S.M. Shaw¹⁰¹, M. Shehade¹⁸⁰, Y. Shen¹²⁹, A.D. Sherman²⁵, P. Sherwood⁹⁵, L. Shi^{158,ap}, S. Shimizu⁸², C.O. Shimmin¹⁸³, Y. Shimogama¹⁷⁹, M. Shimojima¹¹⁶, I.P.J. Shipsey¹³⁵, S. Shirabe¹⁶⁵, M. Shiyakova^{80,ac}, J. Shlomi¹⁸⁰, A. Shmeleva¹¹¹, M.J. Shochet³⁷, J. Shojaei¹⁰⁵, D.R. Shope¹²⁹, S. Shrestha¹²⁷, E.M. Shrif^{33e}, E. Shulga¹⁸⁰, P. Sicho¹⁴¹, A.M. Sickles¹⁷³, P.E. Sidebo¹⁵⁴, E. Sideras Haddad^{33e}, O. Sidiropoulou³⁶, A. Sidoti^{23b,23a}, F. Siegert⁴⁸, Dj. Sijacki¹⁶, M.Jr. Silva¹⁸¹, M.V. Silva Oliveira^{81a}, S.B. Silverstein^{45a}, S. Simion⁶⁵, R. Simoniello¹⁰⁰, S. Simsek^{12b}, P. Sinervo¹⁶⁷, V. Sinetckii¹¹³, N.B. Sinev¹³², S. Singh¹⁵², M. Sioli^{23b,23a}, I. Siral¹³², S.Yu. Sivoklokov¹¹³, J. Sjölin^{45a,45b}, E. Skorda⁹⁷, P. Skubic¹²⁹, M. Slawinska⁸⁵, K. Sliwa¹⁷⁰, R. Slovak¹⁴³, V. Smakhtin¹⁸⁰, B.H. Smart¹⁴⁴, J. Smiesko^{28a}, N. Smirnov¹¹², S.Yu. Smirnov¹¹², Y. Smirnov¹¹², L.N. Smirnova^{113,u}, O. Smirnova⁹⁷, J.W. Smith⁵³, M. Smizanska⁹⁰, K. Smolek¹⁴², A. Smykiewicz⁸⁵, A.A. Snesarev¹¹¹, H.L. Snoek¹²⁰, I.M. Snyder¹³², S. Snyder²⁹, R. Sobie^{176,ae}, A. Soffer¹⁶¹, A. Søgaard⁵⁰, F. Sohns⁵³, C.A. Solans Sanchez³⁶, E.Yu. Soldatov¹¹², U. Soldevila¹⁷⁴, A.A. Solodkov¹²³, A. Soloshenko⁸⁰, O.V. Solovyanov¹²³, V. Solovyev¹³⁸, P. Sommer¹⁴⁹, H. Son¹⁷⁰, W. Song¹⁴⁴, W.Y. Song^{168b}, A. Sopczak¹⁴², A.L. Sopio⁹⁵, F. Sopkova^{28b}, C.L. Sotiropoulou^{72a,72b}, S. Sottocornola^{71a,71b}, R. Soualah^{67a,67c,f}, A.M. Soukharev^{122b,122a}, D. South⁴⁶, S. Spagnolo^{68a,68b}, M. Spalla¹¹⁵, M. Spangenberg¹⁷⁸, F. Spanò⁹⁴, D. Sperlich⁵², T.M. Spieker^{61a}, R. Spighi^{23b}, G. Spigo³⁶, M. Spina¹⁵⁶, D.P. Spiteri⁵⁷, M. Spousta¹⁴³, A. Stabile^{69a,69b}, B.L. Stamas¹²¹, R. Stamen^{61a}, M. Stamenkovic¹²⁰, E. Stanecka⁸⁵, B. Stanislaus¹³⁵, M.M. Stanitzki⁴⁶, M. Stankaityte¹³⁵, B. Stapf¹²⁰, E.A. Starchenko¹²³, G.H. Stark¹⁴⁶, J. Stark⁵⁸, S.H. Stark⁴⁰, P. Staroba¹⁴¹, P. Starovoitov^{61a}, S. Stärz¹⁰⁴, R. Staszewski⁸⁵, G. Stavropoulos⁴⁴, M. Stegler⁴⁶, P. Steinberg²⁹, A.L. Steinhebel¹³², B. Stelzer¹⁵², H.J. Stelzer¹³⁹, O. Stelzer-Chilton^{168a}, H. Stenzel⁵⁶, T.J. Stevenson¹⁵⁶, G.A. Stewart³⁶, M.C. Stockton³⁶, G. Stoicea^{27b}, M. Stolarski^{140a}, S. Stonjek¹¹⁵, A. Straessner⁴⁸, J. Strandberg¹⁵⁴, S. Strandberg^{45a,45b}, M. Strauss¹²⁹, P. Strizenec^{28b}, R. Ströhmer¹⁷⁷, D.M. Strom¹³², R. Stroynowski⁴², A. Strubig⁵⁰, S.A. Stucci²⁹, B. Stugu¹⁷, J. Stupak¹²⁹, N.A. Styles⁴⁶, D. Su¹⁵³, S. Suchek^{61a}, V.V. Sulin¹¹¹, M.J. Sullivan⁹¹, D.M.S. Sultan⁵⁴, S. Sultansoy^{4c}, T. Sumida⁸⁶, S. Sun¹⁰⁶, X. Sun³, K. Suruliz¹⁵⁶, C.J.E. Suster¹⁵⁷, M.R. Sutton¹⁵⁶, S. Suzuki⁸², M. Svatos¹⁴¹, M. Swiatlowski³⁷, S.P. Swift², T. Swirski¹⁷⁷, A. Sydorenko¹⁰⁰, I. Sykora^{28a}, M. Sykora¹⁴³, T. Sykora¹⁴³, D. Ta¹⁰⁰, K. Tackmann^{46,aa}, J. Taenzer¹⁶¹, A. Taffard¹⁷¹, R. Tafirout^{168a}, H. Takai²⁹, R. Takashima⁸⁷, K. Takeda⁸³, T. Takeshita¹⁵⁰, E.P. Takeva⁵⁰, Y. Takubo⁸², M. Talby¹⁰², A.A. Talyshev^{122b,122a}, N.M. Tamir¹⁶¹, J. Tanaka¹⁶³, M. Tanaka¹⁶⁵, R. Tanaka⁶⁵, S. Tapia Araya¹⁷³, S. Tapprogge¹⁰⁰, A. Tarek Abouelfadl Mohamed¹³⁶, S. Tarem¹⁶⁰, K. Tariq^{60b}, G. Tarna^{27b,c}, G.F. Tartarelli^{69a}, P. Tas¹⁴³, M. Tasevsky¹⁴¹, T. Tashiro⁸⁶, E. Tassi^{41b,41a}, A. Tavares Delgado^{140a}, Y. Tayalati^{35e}, A.J. Taylor⁵⁰, G.N. Taylor¹⁰⁵, W. Taylor^{168b}, A.S. Tee⁹⁰, R. Teixeira De Lima¹⁵³, P. Teixeira-Dias⁹⁴, H. Ten Kate³⁶, J.J. Teoh¹²⁰, S. Terada⁸², K. Terashi¹⁶³, J. Terron⁹⁹, S. Terzo¹⁴, M. Testa⁵¹, R.J. Teuscher^{167,ae}, S.J. Thais¹⁸³, T. Theveneaux-Pelzer⁴⁶, F. Thiele⁴⁰, D.W. Thomas⁹⁴, J.O. Thomas⁴², J.P. Thomas²¹, A.S. Thompson⁵⁷, P.D. Thompson²¹, L.A. Thomsen¹⁸³, E. Thomson¹³⁷, E.J. Thorpe⁹³, R.E. Ticse Torres⁵³, V.O. Tikhomirov^{111,al}, Yu.A. Tikhonov^{122b,122a}, S. Timoshenko¹¹², P. Tipton¹⁸³, S. Tisserant¹⁰², K. Todome^{23b,23a}, S. Todorova-Nova⁵, S. Todt⁴⁸, J. Tojo⁸⁸, S. Tokár^{28a}, K. Tokushuku⁸², E. Tolley¹²⁷, K.G. Tomiwa^{33e}, M. Tomoto¹¹⁷, L. Tompkins^{153,p}, B. Tong⁵⁹, P. Tornambe¹⁰³, E. Torrence¹³², H. Torres⁴⁸, E. Torró Pastor¹⁴⁸, C. Toscirci¹³⁵, J. Toth^{102,ad}, D.R. Tovey¹⁴⁹, A. Traeet¹⁷, C.J. Treado¹²⁵, T. Trefzger¹⁷⁷, F. Tresoldi¹⁵⁶, A. Tricoli²⁹, I.M. Trigger^{168a}, S. Trincaz-Duvoid¹³⁶, D.T. Trischuk¹⁷⁵, W. Trischuk¹⁶⁷, B. Trocmé⁵⁸, A. Trofymov¹⁴⁵, C. Troncon^{69a}, M. Trovatelli¹⁷⁶, F. Trovato¹⁵⁶, L. Truong^{33c}, M. Trzebinski⁸⁵, A. Trzupek⁸⁵, F. Tsai⁴⁶, J.C.-L. Tseng¹³⁵, P.V. Tsiareshka^{108,ah}, A. Tsirigotis^{162,x}, V. Tsiskaridze¹⁵⁵, E.G. Tskhadadze^{159a}, M. Tsopoulou¹⁶², I.I. Tsukerman¹²⁴, V. Tsulaia¹⁸, S. Tsuno⁸², D. Tsybychev¹⁵⁵, Y. Tu^{63b}, A. Tudorache^{27b}, V. Tudorache^{27b}, T.T. Tulbure^{27a},

A.N. Tuna⁵⁹, S. Turchikhin⁸⁰, D. Turgeman¹⁸⁰, I. Turk Cakir^{4b,v}, R.J. Turner²¹, R.T. Turra^{69a}, P.M. Tuts³⁹,
 S. Tzamarias¹⁶², E. Tzovara¹⁰⁰, G. Ucchielli⁴⁷, K. Uchida¹⁶³, I. Ueda⁸², F. Ukegawa¹⁶⁹, G. Unal³⁶,
 A. Undrus²⁹, G. Unel¹⁷¹, F.C. Ungaro¹⁰⁵, Y. Unno⁸², K. Uno¹⁶³, J. Urban^{28b}, P. Urquijo¹⁰⁵, G. Usai⁸,
 Z. Uysal^{12d}, V. Vacek¹⁴², B. Vachon¹⁰⁴, K.O.H. Vadla¹³⁴, A. Vaidya⁹⁵, C. Valderanis¹¹⁴,
 E. Valdes Santurio^{45a,45b}, M. Valente⁵⁴, S. Valentineti^{23b,23a}, A. Valero¹⁷⁴, L. Valéry⁴⁶, R.A. Vallance²¹,
 A. Vallier³⁶, J.A. Valls Ferrer¹⁷⁴, T.R. Van Daalen¹⁴, P. Van Gemmeren⁶, I. Van Vulpen¹²⁰,
 M. Vanadia^{74a,74b}, W. Vandelli³⁶, M. Vandenbroucke¹⁴⁵, E.R. Vandewall¹³⁰, A. Vaniachine¹⁶⁶,
 D. Vannicola^{73a,73b}, R. Vari^{73a}, E.W. Varnes⁷, C. Varni^{55b,55a}, T. Varol¹⁵⁸, D. Varouchas⁶⁵, K.E. Varvell¹⁵⁷,
 M.E. Vasile^{27b}, G.A. Vasquez¹⁷⁶, F. Vazeille³⁸, D. Vazquez Furelos¹⁴, T. Vazquez Schroeder³⁶, J. Veatch⁵³,
 V. Vecchio^{75a,75b}, M.J. Veen¹²⁰, L.M. Veloce¹⁶⁷, F. Veloso^{140a,140c}, S. Veneziano^{73a}, A. Ventura^{68a,68b},
 N. Venturi³⁶, A. Verbytskyi¹¹⁵, V. Vercesi^{71a}, M. Verducci^{72a,72b}, C.M. Vergel Infante⁷⁹, C. Vergis²⁴,
 W. Verkerke¹²⁰, A.T. Vermeulen¹²⁰, J.C. Vermeulen¹²⁰, M.C. Vetterli^{152,ar}, N. Viaux Maira^{147d},
 M. Vicente Barreto Pinto⁵⁴, T. Vickey¹⁴⁹, O.E. Vickey Boeriu¹⁴⁹, G.H.A. Viehhauser¹³⁵, L. Vigani^{61b},
 M. Villa^{23b,23a}, M. Villaplana Perez^{69a,69b}, E. Vilucchi⁵¹, M.G. Vincter³⁴, G.S. Virdee²¹,
 A. Vishwakarma⁴⁶, C. Vittori^{23b,23a}, I. Vivarelli¹⁵⁶, M. Vogel¹⁸², P. Vokac¹⁴², S.E. von Buddenbrock^{33e},
 E. Von Toerne²⁴, V. Vorobel¹⁴³, K. Vorobev¹¹², M. Vos¹⁷⁴, J.H. Vossebeld⁹¹, M. Vozak¹⁰¹, N. Vranjes¹⁶,
 M. Vranjes Milosavljevic¹⁶, V. Vrba¹⁴², M. Vreeswijk¹²⁰, R. Vuillermet³⁶, I. Vukotic³⁷, P. Wagner²⁴,
 W. Wagner¹⁸², J. Wagner-Kuhr¹¹⁴, S. Wahdan¹⁸², H. Wahlberg⁸⁹, V.M. Walbrecht¹¹⁵, J. Walder⁹⁰,
 R. Walker¹¹⁴, S.D. Walker⁹⁴, W. Walkowiak¹⁵¹, V. Wallangen^{45a,45b}, A.M. Wang⁵⁹, C. Wang^{60c},
 F. Wang¹⁸¹, H. Wang¹⁸, H. Wang³, J. Wang^{63a}, J. Wang¹⁵⁷, J. Wang^{61b}, P. Wang⁴², Q. Wang¹²⁹,
 R.-J. Wang¹⁰⁰, R. Wang^{60a}, R. Wang⁶, S.M. Wang¹⁵⁸, W.T. Wang^{60a}, W. Wang^{15c}, W.X. Wang^{60a},
 Y. Wang^{60a}, Z. Wang^{60c}, C. Wanotayaroj⁴⁶, A. Warburton¹⁰⁴, C.P. Ward³², D.R. Wardrope⁹⁵, N. Warrack⁵⁷,
 A. Washbrook⁵⁰, A.T. Watson²¹, M.F. Watson²¹, G. Watts¹⁴⁸, B.M. Waugh⁹⁵, A.F. Webb¹¹, S. Webb¹⁰⁰,
 C. Weber¹⁸³, M.S. Weber²⁰, S.A. Weber³⁴, S.M. Weber^{61a}, A.R. Weidberg¹³⁵, J. Weingarten⁴⁷,
 M. Weirich¹⁰⁰, C. Weiser⁵², P.S. Wells³⁶, T. Wenaus²⁹, T. Wengler³⁶, S. Wenig³⁶, N. Wermes²⁴,
 M.D. Werner⁷⁹, M. Wessels^{61a}, T.D. Weston²⁰, K. Whalen¹³², N.L. Whallon¹⁴⁸, A.M. Wharton⁹⁰,
 A.S. White¹⁰⁶, A. White⁸, M.J. White¹, D. Whiteson¹⁷¹, B.W. Whitmore⁹⁰, W. Wiedenmann¹⁸¹, C. Wiel⁴⁸,
 M. Wielers¹⁴⁴, N. Wieseotte¹⁰⁰, C. Wiglesworth⁴⁰, L.A.M. Wiik-Fuchs⁵², F. Wilk¹⁰¹, H.G. Wilkens³⁶,
 L.J. Wilkins⁹⁴, H.H. Williams¹³⁷, S. Williams³², C. Willis¹⁰⁷, S. Willocq¹⁰³, J.A. Wilson²¹,
 I. Wingerter-Seez⁵, E. Winkels¹⁵⁶, F. Winklmeier¹³², O.J. Winston¹⁵⁶, B.T. Winter⁵², M. Wittgen¹⁵³,
 M. Wobisch⁹⁶, A. Wolf¹⁰⁰, T.M.H. Wolf¹²⁰, R. Wolff¹⁰², R. Wölker¹³⁵, J. Wollrath⁵², M.W. Wolter⁸⁵,
 H. Wolters^{140a,140c}, V.W.S. Wong¹⁷⁵, N.L. Woods¹⁴⁶, S.D. Worm²¹, B.K. Wosiek⁸⁵, K.W. Woźniak⁸⁵,
 K. Wraight⁵⁷, S.L. Wu¹⁸¹, X. Wu⁵⁴, Y. Wu^{60a}, T.R. Wyatt¹⁰¹, B.M. Wynne⁵⁰, S. Xella⁴⁰, Z. Xi¹⁰⁶,
 L. Xia¹⁷⁸, X. Xiao¹⁰⁶, I. Xiotidis¹⁵⁶, D. Xu^{15a}, H. Xu^{60a}, L. Xu²⁹, T. Xu¹⁴⁵, W. Xu¹⁰⁶, Z. Xu^{60b}, Z. Xu¹⁵³,
 B. Yabsley¹⁵⁷, S. Yacoob^{33a}, K. Yajima¹³³, D.P. Yallup⁹⁵, N. Yamaguchi⁸⁸, Y. Yamaguchi¹⁶⁵,
 A. Yamamoto⁸², M. Yamatani¹⁶³, T. Yamazaki¹⁶³, Y. Yamazaki⁸³, Z. Yan²⁵, H.J. Yang^{60c,60d}, H.T. Yang¹⁸,
 S. Yang⁷⁸, X. Yang^{60b,58}, Y. Yang¹⁶³, W-M. Yao¹⁸, Y.C. Yap⁴⁶, Y. Yasu⁸², E. Yatsenko^{60c,60d}, H. Ye^{15c},
 J. Ye⁴², S. Ye²⁹, I. Yeletskikh⁸⁰, M.R. Yexley⁹⁰, E. Yigitbasi²⁵, K. Yorita¹⁷⁹, K. Yoshihara¹³⁷,
 C.J.S. Young³⁶, C. Young¹⁵³, J. Yu⁷⁹, R. Yuan^{60b,h}, X. Yue^{61a}, S.P.Y. Yuen²⁴, M. Zaazoua^{35e},
 B. Zabinski⁸⁵, G. Zacharis¹⁰, E. Zaffaroni⁵⁴, J. Zahreddine¹³⁶, A.M. Zaitsev^{123,ak}, T. Zakareishvili^{159b},
 N. Zakharchuk³⁴, S. Zambito⁵⁹, D. Zanzi³⁶, D.R. Zaripovas⁵⁷, S.V. Zeißner⁴⁷, C. Zeitnitz¹⁸²,
 G. Zemaityte¹³⁵, J.C. Zeng¹⁷³, O. Zenin¹²³, T. Ženiš^{28a}, D. Zerwas⁶⁵, M. Zgubič¹³⁵, B. Zhang^{15c},
 D.F. Zhang^{15b}, G. Zhang^{15b}, H. Zhang^{15c}, J. Zhang⁶, L. Zhang^{15c}, L. Zhang^{60a}, M. Zhang¹⁷³, R. Zhang¹⁸¹,
 S. Zhang¹⁰⁶, X. Zhang^{60b}, Y. Zhang^{15a,15d}, Z. Zhang^{63a}, Z. Zhang⁶⁵, P. Zhao⁴⁹, Y. Zhao^{60b}, Z. Zhao^{60a},
 A. Zhemchugov⁸⁰, Z. Zheng¹⁰⁶, D. Zhong¹⁷³, B. Zhou¹⁰⁶, C. Zhou¹⁸¹, M.S. Zhou^{15a,15d}, M. Zhou¹⁵⁵,
 N. Zhou^{60c}, Y. Zhou⁷, C.G. Zhu^{60b}, C. Zhu^{15a,15d}, H.L. Zhu^{60a}, H. Zhu^{15a}, J. Zhu¹⁰⁶, Y. Zhu^{60a},
 X. Zhuang^{15a}, K. Zhukov¹¹¹, V. Zhulanov^{122b,122a}, D. Zieminska⁶⁶, N.I. Zimine⁸⁰, S. Zimmermann⁵²,

Z. Zinonos¹¹⁵, M. Ziolkowski¹⁵¹, L. Živković¹⁶, G. Zobernig¹⁸¹, A. Zoccoli^{23b,23a}, K. Zoch⁵³, T.G. Zorbas¹⁴⁹, R. Zou³⁷, L. Zwalski³⁶.

¹Department of Physics, University of Adelaide, Adelaide; Australia.

²Physics Department, SUNY Albany, Albany NY; United States of America.

³Department of Physics, University of Alberta, Edmonton AB; Canada.

^{4(a)}Department of Physics, Ankara University, Ankara; ^(b)Istanbul Aydin University, Istanbul; ^(c)Division of Physics, TOBB University of Economics and Technology, Ankara; Turkey.

⁵LAPP, Université Grenoble Alpes, Université Savoie Mont Blanc, CNRS/IN2P3, Annecy; France.

⁶High Energy Physics Division, Argonne National Laboratory, Argonne IL; United States of America.

⁷Department of Physics, University of Arizona, Tucson AZ; United States of America.

⁸Department of Physics, University of Texas at Arlington, Arlington TX; United States of America.

⁹Physics Department, National and Kapodistrian University of Athens, Athens; Greece.

¹⁰Physics Department, National Technical University of Athens, Zografou; Greece.

¹¹Department of Physics, University of Texas at Austin, Austin TX; United States of America.

^{12(a)}Bahcesehir University, Faculty of Engineering and Natural Sciences, Istanbul; ^(b)Istanbul Bilgi University, Faculty of Engineering and Natural Sciences, Istanbul; ^(c)Department of Physics, Bogazici University, Istanbul; ^(d)Department of Physics Engineering, Gaziantep University, Gaziantep; Turkey.

¹³Institute of Physics, Azerbaijan Academy of Sciences, Baku; Azerbaijan.

¹⁴Institut de Física d'Altes Energies (IFAE), Barcelona Institute of Science and Technology, Barcelona; Spain.

^{15(a)}Institute of High Energy Physics, Chinese Academy of Sciences, Beijing; ^(b)Physics Department, Tsinghua University, Beijing; ^(c)Department of Physics, Nanjing University, Nanjing; ^(d)University of Chinese Academy of Science (UCAS), Beijing; China.

¹⁶Institute of Physics, University of Belgrade, Belgrade; Serbia.

¹⁷Department for Physics and Technology, University of Bergen, Bergen; Norway.

¹⁸Physics Division, Lawrence Berkeley National Laboratory and University of California, Berkeley CA; United States of America.

¹⁹Institut für Physik, Humboldt Universität zu Berlin, Berlin; Germany.

²⁰Albert Einstein Center for Fundamental Physics and Laboratory for High Energy Physics, University of Bern, Bern; Switzerland.

²¹School of Physics and Astronomy, University of Birmingham, Birmingham; United Kingdom.

^{22(a)}Facultad de Ciencias y Centro de Investigaciones, Universidad Antonio Nariño,

Bogotá; ^(b)Departamento de Física, Universidad Nacional de Colombia, Bogotá, Colombia; Colombia.

^{23(a)}INFN Bologna and Universita' di Bologna, Dipartimento di Fisica; ^(b)INFN Sezione di Bologna; Italy.

²⁴Physikalisches Institut, Universität Bonn, Bonn; Germany.

²⁵Department of Physics, Boston University, Boston MA; United States of America.

²⁶Department of Physics, Brandeis University, Waltham MA; United States of America.

^{27(a)}Transilvania University of Brasov, Brasov; ^(b)Horia Hulubei National Institute of Physics and Nuclear Engineering, Bucharest; ^(c)Department of Physics, Alexandru Ioan Cuza University of Iasi, Iasi; ^(d)National Institute for Research and Development of Isotopic and Molecular Technologies, Physics Department, Cluj-Napoca; ^(e)University Politehnica Bucharest, Bucharest; ^(f)West University in Timisoara, Timisoara; Romania.

^{28(a)}Faculty of Mathematics, Physics and Informatics, Comenius University, Bratislava; ^(b)Department of Subnuclear Physics, Institute of Experimental Physics of the Slovak Academy of Sciences, Kosice; Slovak Republic.

²⁹Physics Department, Brookhaven National Laboratory, Upton NY; United States of America.

- ³⁰Departamento de Física, Universidad de Buenos Aires, Buenos Aires; Argentina.
- ³¹California State University, CA; United States of America.
- ³²Cavendish Laboratory, University of Cambridge, Cambridge; United Kingdom.
- ^{33(a)}Department of Physics, University of Cape Town, Cape Town;^(b)iThemba Labs, Western Cape;^(c)Department of Mechanical Engineering Science, University of Johannesburg, Johannesburg;^(d)University of South Africa, Department of Physics, Pretoria;^(e)School of Physics, University of the Witwatersrand, Johannesburg; South Africa.
- ³⁴Department of Physics, Carleton University, Ottawa ON; Canada.
- ^{35(a)}Faculté des Sciences Ain Chock, Réseau Universitaire de Physique des Hautes Energies - Université Hassan II, Casablanca;^(b)Faculté des Sciences, Université Ibn-Tofail, Kénitra;^(c)Faculté des Sciences Semlalia, Université Cadi Ayyad, LPHEA-Marrakech;^(d)Faculté des Sciences, Université Mohamed Premier and LPTPM, Oujda;^(e)Faculté des sciences, Université Mohammed V, Rabat; Morocco.
- ³⁶CERN, Geneva; Switzerland.
- ³⁷Enrico Fermi Institute, University of Chicago, Chicago IL; United States of America.
- ³⁸LPC, Université Clermont Auvergne, CNRS/IN2P3, Clermont-Ferrand; France.
- ³⁹Nevis Laboratory, Columbia University, Irvington NY; United States of America.
- ⁴⁰Niels Bohr Institute, University of Copenhagen, Copenhagen; Denmark.
- ^{41(a)}Dipartimento di Fisica, Università della Calabria, Rende;^(b)INFN Gruppo Collegato di Cosenza, Laboratori Nazionali di Frascati; Italy.
- ⁴²Physics Department, Southern Methodist University, Dallas TX; United States of America.
- ⁴³Physics Department, University of Texas at Dallas, Richardson TX; United States of America.
- ⁴⁴National Centre for Scientific Research "Demokritos", Agia Paraskevi; Greece.
- ^{45(a)}Department of Physics, Stockholm University;^(b)Oskar Klein Centre, Stockholm; Sweden.
- ⁴⁶Deutsches Elektronen-Synchrotron DESY, Hamburg and Zeuthen; Germany.
- ⁴⁷Lehrstuhl für Experimentelle Physik IV, Technische Universität Dortmund, Dortmund; Germany.
- ⁴⁸Institut für Kern- und Teilchenphysik, Technische Universität Dresden, Dresden; Germany.
- ⁴⁹Department of Physics, Duke University, Durham NC; United States of America.
- ⁵⁰SUPA - School of Physics and Astronomy, University of Edinburgh, Edinburgh; United Kingdom.
- ⁵¹INFN e Laboratori Nazionali di Frascati, Frascati; Italy.
- ⁵²Physikalisches Institut, Albert-Ludwigs-Universität Freiburg, Freiburg; Germany.
- ⁵³II. Physikalisches Institut, Georg-August-Universität Göttingen, Göttingen; Germany.
- ⁵⁴Département de Physique Nucléaire et Corpusculaire, Université de Genève, Genève; Switzerland.
- ^{55(a)}Dipartimento di Fisica, Università di Genova, Genova;^(b)INFN Sezione di Genova; Italy.
- ⁵⁶II. Physikalisches Institut, Justus-Liebig-Universität Giessen, Giessen; Germany.
- ⁵⁷SUPA - School of Physics and Astronomy, University of Glasgow, Glasgow; United Kingdom.
- ⁵⁸LPSC, Université Grenoble Alpes, CNRS/IN2P3, Grenoble INP, Grenoble; France.
- ⁵⁹Laboratory for Particle Physics and Cosmology, Harvard University, Cambridge MA; United States of America.
- ^{60(a)}Department of Modern Physics and State Key Laboratory of Particle Detection and Electronics, University of Science and Technology of China, Hefei;^(b)Institute of Frontier and Interdisciplinary Science and Key Laboratory of Particle Physics and Particle Irradiation (MOE), Shandong University, Qingdao;^(c)School of Physics and Astronomy, Shanghai Jiao Tong University, KLPPAC-MoE, SKLPPC, Shanghai;^(d)Tsung-Dao Lee Institute, Shanghai; China.
- ^{61(a)}Kirchhoff-Institut für Physik, Ruprecht-Karls-Universität Heidelberg, Heidelberg;^(b)Physikalisches Institut, Ruprecht-Karls-Universität Heidelberg, Heidelberg; Germany.
- ⁶²Faculty of Applied Information Science, Hiroshima Institute of Technology, Hiroshima; Japan.
- ^{63(a)}Department of Physics, Chinese University of Hong Kong, Shatin, N.T., Hong Kong;^(b)Department of

Physics, University of Hong Kong, Hong Kong;^(c)Department of Physics and Institute for Advanced Study, Hong Kong University of Science and Technology, Clear Water Bay, Kowloon, Hong Kong; China.

⁶⁴Department of Physics, National Tsing Hua University, Hsinchu; Taiwan.

⁶⁵IJCLab, Université Paris-Saclay, CNRS/IN2P3, 91405, Orsay; France.

⁶⁶Department of Physics, Indiana University, Bloomington IN; United States of America.

^{67(a)}INFN Gruppo Collegato di Udine, Sezione di Trieste, Udine;^(b)ICTP, Trieste;^(c)Dipartimento Politecnico di Ingegneria e Architettura, Università di Udine, Udine; Italy.

^{68(a)}INFN Sezione di Lecce;^(b)Dipartimento di Matematica e Fisica, Università del Salento, Lecce; Italy.

^{69(a)}INFN Sezione di Milano;^(b)Dipartimento di Fisica, Università di Milano, Milano; Italy.

^{70(a)}INFN Sezione di Napoli;^(b)Dipartimento di Fisica, Università di Napoli, Napoli; Italy.

^{71(a)}INFN Sezione di Pavia;^(b)Dipartimento di Fisica, Università di Pavia, Pavia; Italy.

^{72(a)}INFN Sezione di Pisa;^(b)Dipartimento di Fisica E. Fermi, Università di Pisa, Pisa; Italy.

^{73(a)}INFN Sezione di Roma;^(b)Dipartimento di Fisica, Sapienza Università di Roma, Roma; Italy.

^{74(a)}INFN Sezione di Roma Tor Vergata;^(b)Dipartimento di Fisica, Università di Roma Tor Vergata, Roma; Italy.

^{75(a)}INFN Sezione di Roma Tre;^(b)Dipartimento di Matematica e Fisica, Università Roma Tre, Roma; Italy.

^{76(a)}INFN-TIFPA;^(b)Università degli Studi di Trento, Trento; Italy.

⁷⁷Institut für Astro- und Teilchenphysik, Leopold-Franzens-Universität, Innsbruck; Austria.

⁷⁸University of Iowa, Iowa City IA; United States of America.

⁷⁹Department of Physics and Astronomy, Iowa State University, Ames IA; United States of America.

⁸⁰Joint Institute for Nuclear Research, Dubna; Russia.

^{81(a)}Departamento de Engenharia Elétrica, Universidade Federal de Juiz de Fora (UFJF), Juiz de Fora;^(b)Universidade Federal do Rio De Janeiro COPPE/EE/IF, Rio de Janeiro;^(c)Universidade Federal de São João del Rei (UFSJ), São João del Rei;^(d)Instituto de Física, Universidade de São Paulo, São Paulo; Brazil.

⁸²KEK, High Energy Accelerator Research Organization, Tsukuba; Japan.

⁸³Graduate School of Science, Kobe University, Kobe; Japan.

^{84(a)}AGH University of Science and Technology, Faculty of Physics and Applied Computer Science, Krakow;^(b)Marian Smoluchowski Institute of Physics, Jagiellonian University, Krakow; Poland.

⁸⁵Institute of Nuclear Physics Polish Academy of Sciences, Krakow; Poland.

⁸⁶Faculty of Science, Kyoto University, Kyoto; Japan.

⁸⁷Kyoto University of Education, Kyoto; Japan.

⁸⁸Research Center for Advanced Particle Physics and Department of Physics, Kyushu University, Fukuoka ; Japan.

⁸⁹Instituto de Física La Plata, Universidad Nacional de La Plata and CONICET, La Plata; Argentina.

⁹⁰Physics Department, Lancaster University, Lancaster; United Kingdom.

⁹¹Oliver Lodge Laboratory, University of Liverpool, Liverpool; United Kingdom.

⁹²Department of Experimental Particle Physics, Jožef Stefan Institute and Department of Physics, University of Ljubljana, Ljubljana; Slovenia.

⁹³School of Physics and Astronomy, Queen Mary University of London, London; United Kingdom.

⁹⁴Department of Physics, Royal Holloway University of London, Egham; United Kingdom.

⁹⁵Department of Physics and Astronomy, University College London, London; United Kingdom.

⁹⁶Louisiana Tech University, Ruston LA; United States of America.

⁹⁷Fysiska institutionen, Lunds universitet, Lund; Sweden.

⁹⁸Centre de Calcul de l’Institut National de Physique Nucléaire et de Physique des Particules (IN2P3), Villeurbanne; France.

⁹⁹Departamento de Física Teorica C-15 and CIAFF, Universidad Autónoma de Madrid, Madrid; Spain.

- ¹⁰⁰Institut für Physik, Universität Mainz, Mainz; Germany.
- ¹⁰¹School of Physics and Astronomy, University of Manchester, Manchester; United Kingdom.
- ¹⁰²CPPM, Aix-Marseille Université, CNRS/IN2P3, Marseille; France.
- ¹⁰³Department of Physics, University of Massachusetts, Amherst MA; United States of America.
- ¹⁰⁴Department of Physics, McGill University, Montreal QC; Canada.
- ¹⁰⁵School of Physics, University of Melbourne, Victoria; Australia.
- ¹⁰⁶Department of Physics, University of Michigan, Ann Arbor MI; United States of America.
- ¹⁰⁷Department of Physics and Astronomy, Michigan State University, East Lansing MI; United States of America.
- ¹⁰⁸B.I. Stepanov Institute of Physics, National Academy of Sciences of Belarus, Minsk; Belarus.
- ¹⁰⁹Research Institute for Nuclear Problems of Byelorussian State University, Minsk; Belarus.
- ¹¹⁰Group of Particle Physics, University of Montreal, Montreal QC; Canada.
- ¹¹¹P.N. Lebedev Physical Institute of the Russian Academy of Sciences, Moscow; Russia.
- ¹¹²National Research Nuclear University MEPhI, Moscow; Russia.
- ¹¹³D.V. Skobeltsyn Institute of Nuclear Physics, M.V. Lomonosov Moscow State University, Moscow; Russia.
- ¹¹⁴Fakultät für Physik, Ludwig-Maximilians-Universität München, München; Germany.
- ¹¹⁵Max-Planck-Institut für Physik (Werner-Heisenberg-Institut), München; Germany.
- ¹¹⁶Nagasaki Institute of Applied Science, Nagasaki; Japan.
- ¹¹⁷Graduate School of Science and Kobayashi-Maskawa Institute, Nagoya University, Nagoya; Japan.
- ¹¹⁸Department of Physics and Astronomy, University of New Mexico, Albuquerque NM; United States of America.
- ¹¹⁹Institute for Mathematics, Astrophysics and Particle Physics, Radboud University Nijmegen/Nikhef, Nijmegen; Netherlands.
- ¹²⁰Nikhef National Institute for Subatomic Physics and University of Amsterdam, Amsterdam; Netherlands.
- ¹²¹Department of Physics, Northern Illinois University, DeKalb IL; United States of America.
- ^{122(a)}Budker Institute of Nuclear Physics and NSU, SB RAS, Novosibirsk;^(b)Novosibirsk State University Novosibirsk; Russia.
- ¹²³Institute for High Energy Physics of the National Research Centre Kurchatov Institute, Protvino; Russia.
- ¹²⁴Institute for Theoretical and Experimental Physics named by A.I. Alikhanov of National Research Centre "Kurchatov Institute", Moscow; Russia.
- ¹²⁵Department of Physics, New York University, New York NY; United States of America.
- ¹²⁶Ochanomizu University, Otsuka, Bunkyo-ku, Tokyo; Japan.
- ¹²⁷Ohio State University, Columbus OH; United States of America.
- ¹²⁸Faculty of Science, Okayama University, Okayama; Japan.
- ¹²⁹Homer L. Dodge Department of Physics and Astronomy, University of Oklahoma, Norman OK; United States of America.
- ¹³⁰Department of Physics, Oklahoma State University, Stillwater OK; United States of America.
- ¹³¹Palacký University, RCPTM, Joint Laboratory of Optics, Olomouc; Czech Republic.
- ¹³²Institute for Fundamental Science, University of Oregon, Eugene, OR; United States of America.
- ¹³³Graduate School of Science, Osaka University, Osaka; Japan.
- ¹³⁴Department of Physics, University of Oslo, Oslo; Norway.
- ¹³⁵Department of Physics, Oxford University, Oxford; United Kingdom.
- ¹³⁶LPNHE, Sorbonne Université, Université de Paris, CNRS/IN2P3, Paris; France.
- ¹³⁷Department of Physics, University of Pennsylvania, Philadelphia PA; United States of America.
- ¹³⁸Konstantinov Nuclear Physics Institute of National Research Centre "Kurchatov Institute", PNPI, St.

Petersburg; Russia.

¹³⁹Department of Physics and Astronomy, University of Pittsburgh, Pittsburgh PA; United States of America.

^{140(a)}Laboratório de Instrumentação e Física Experimental de Partículas - LIP, Lisboa;^(b)Departamento de Física, Faculdade de Ciências, Universidade de Lisboa, Lisboa;^(c)Departamento de Física, Universidade de Coimbra, Coimbra;^(d)Centro de Física Nuclear da Universidade de Lisboa, Lisboa;^(e)Departamento de Física, Universidade do Minho, Braga;^(f)Departamento de Física Teórica y del Cosmos, Universidad de Granada, Granada (Spain);^(g)Dep Física and CEFITEC of Faculdade de Ciências e Tecnologia, Universidade Nova de Lisboa, Caparica;^(h)Instituto Superior Técnico, Universidade de Lisboa, Lisboa; Portugal.

¹⁴¹Institute of Physics of the Czech Academy of Sciences, Prague; Czech Republic.

¹⁴²Czech Technical University in Prague, Prague; Czech Republic.

¹⁴³Charles University, Faculty of Mathematics and Physics, Prague; Czech Republic.

¹⁴⁴Particle Physics Department, Rutherford Appleton Laboratory, Didcot; United Kingdom.

¹⁴⁵IRFU, CEA, Université Paris-Saclay, Gif-sur-Yvette; France.

¹⁴⁶Santa Cruz Institute for Particle Physics, University of California Santa Cruz, Santa Cruz CA; United States of America.

^{147(a)}Departamento de Física, Pontificia Universidad Católica de Chile, Santiago;^(b)Universidad Andres Bello, Department of Physics, Santiago;^(c)Instituto de Alta Investigación, Universidad de Tarapacá;^(d)Departamento de Física, Universidad Técnica Federico Santa María, Valparaíso; Chile.

¹⁴⁸Department of Physics, University of Washington, Seattle WA; United States of America.

¹⁴⁹Department of Physics and Astronomy, University of Sheffield, Sheffield; United Kingdom.

¹⁵⁰Department of Physics, Shinshu University, Nagano; Japan.

¹⁵¹Department Physik, Universität Siegen, Siegen; Germany.

¹⁵²Department of Physics, Simon Fraser University, Burnaby BC; Canada.

¹⁵³SLAC National Accelerator Laboratory, Stanford CA; United States of America.

¹⁵⁴Physics Department, Royal Institute of Technology, Stockholm; Sweden.

¹⁵⁵Departments of Physics and Astronomy, Stony Brook University, Stony Brook NY; United States of America.

¹⁵⁶Department of Physics and Astronomy, University of Sussex, Brighton; United Kingdom.

¹⁵⁷School of Physics, University of Sydney, Sydney; Australia.

¹⁵⁸Institute of Physics, Academia Sinica, Taipei; Taiwan.

^{159(a)}E. Andronikashvili Institute of Physics, Iv. Javakhishvili Tbilisi State University, Tbilisi;^(b)High Energy Physics Institute, Tbilisi State University, Tbilisi; Georgia.

¹⁶⁰Department of Physics, Technion, Israel Institute of Technology, Haifa; Israel.

¹⁶¹Raymond and Beverly Sackler School of Physics and Astronomy, Tel Aviv University, Tel Aviv; Israel.

¹⁶²Department of Physics, Aristotle University of Thessaloniki, Thessaloniki; Greece.

¹⁶³International Center for Elementary Particle Physics and Department of Physics, University of Tokyo, Tokyo; Japan.

¹⁶⁴Graduate School of Science and Technology, Tokyo Metropolitan University, Tokyo; Japan.

¹⁶⁵Department of Physics, Tokyo Institute of Technology, Tokyo; Japan.

¹⁶⁶Tomsk State University, Tomsk; Russia.

¹⁶⁷Department of Physics, University of Toronto, Toronto ON; Canada.

^{168(a)}TRIUMF, Vancouver BC;^(b)Department of Physics and Astronomy, York University, Toronto ON; Canada.

¹⁶⁹Division of Physics and Tomonaga Center for the History of the Universe, Faculty of Pure and Applied Sciences, University of Tsukuba, Tsukuba; Japan.

- ¹⁷⁰Department of Physics and Astronomy, Tufts University, Medford MA; United States of America.
- ¹⁷¹Department of Physics and Astronomy, University of California Irvine, Irvine CA; United States of America.
- ¹⁷²Department of Physics and Astronomy, University of Uppsala, Uppsala; Sweden.
- ¹⁷³Department of Physics, University of Illinois, Urbana IL; United States of America.
- ¹⁷⁴Instituto de Física Corpuscular (IFIC), Centro Mixto Universidad de Valencia - CSIC, Valencia; Spain.
- ¹⁷⁵Department of Physics, University of British Columbia, Vancouver BC; Canada.
- ¹⁷⁶Department of Physics and Astronomy, University of Victoria, Victoria BC; Canada.
- ¹⁷⁷Fakultät für Physik und Astronomie, Julius-Maximilians-Universität Würzburg, Würzburg; Germany.
- ¹⁷⁸Department of Physics, University of Warwick, Coventry; United Kingdom.
- ¹⁷⁹Waseda University, Tokyo; Japan.
- ¹⁸⁰Department of Particle Physics, Weizmann Institute of Science, Rehovot; Israel.
- ¹⁸¹Department of Physics, University of Wisconsin, Madison WI; United States of America.
- ¹⁸²Fakultät für Mathematik und Naturwissenschaften, Fachgruppe Physik, Bergische Universität Wuppertal, Wuppertal; Germany.
- ¹⁸³Department of Physics, Yale University, New Haven CT; United States of America.
- ^a Also at Borough of Manhattan Community College, City University of New York, New York NY; United States of America.
- ^b Also at CERN, Geneva; Switzerland.
- ^c Also at CPPM, Aix-Marseille Université, CNRS/IN2P3, Marseille; France.
- ^d Also at Département de Physique Nucléaire et Corpusculaire, Université de Genève, Genève; Switzerland.
- ^e Also at Departament de Fisica de la Universitat Autònoma de Barcelona, Barcelona; Spain.
- ^f Also at Department of Applied Physics and Astronomy, University of Sharjah, Sharjah; United Arab Emirates.
- ^g Also at Department of Financial and Management Engineering, University of the Aegean, Chios; Greece.
- ^h Also at Department of Physics and Astronomy, Michigan State University, East Lansing MI; United States of America.
- ⁱ Also at Department of Physics and Astronomy, University of Louisville, Louisville, KY; United States of America.
- ^j Also at Department of Physics, Ben Gurion University of the Negev, Beer Sheva; Israel.
- ^k Also at Department of Physics, California State University, East Bay; United States of America.
- ^l Also at Department of Physics, California State University, Fresno; United States of America.
- ^m Also at Department of Physics, California State University, Sacramento; United States of America.
- ⁿ Also at Department of Physics, King's College London, London; United Kingdom.
- ^o Also at Department of Physics, St. Petersburg State Polytechnical University, St. Petersburg; Russia.
- ^p Also at Department of Physics, Stanford University, Stanford CA; United States of America.
- ^q Also at Department of Physics, University of Adelaide, Adelaide; Australia.
- ^r Also at Department of Physics, University of Fribourg, Fribourg; Switzerland.
- ^s Also at Department of Physics, University of Michigan, Ann Arbor MI; United States of America.
- ^t Also at Dipartimento di Matematica, Informatica e Fisica, Università di Udine, Udine; Italy.
- ^u Also at Faculty of Physics, M.V. Lomonosov Moscow State University, Moscow; Russia.
- ^v Also at Giresun University, Faculty of Engineering, Giresun; Turkey.
- ^w Also at Graduate School of Science, Osaka University, Osaka; Japan.
- ^x Also at Hellenic Open University, Patras; Greece.
- ^y Also at IJCLab, Université Paris-Saclay, CNRS/IN2P3, 91405, Orsay; France.
- ^z Also at Institutio Catalana de Recerca i Estudis Avancats, ICREA, Barcelona; Spain.

- aa* Also at Institut für Experimentalphysik, Universität Hamburg, Hamburg; Germany.
- ab* Also at Institute for Mathematics, Astrophysics and Particle Physics, Radboud University Nijmegen/Nikhef, Nijmegen; Netherlands.
- ac* Also at Institute for Nuclear Research and Nuclear Energy (INRNE) of the Bulgarian Academy of Sciences, Sofia; Bulgaria.
- ad* Also at Institute for Particle and Nuclear Physics, Wigner Research Centre for Physics, Budapest; Hungary.
- ae* Also at Institute of Particle Physics (IPP), Vancouver; Canada.
- af* Also at Institute of Physics, Azerbaijan Academy of Sciences, Baku; Azerbaijan.
- ag* Also at Instituto de Fisica Teorica, IFT-UAM/CSIC, Madrid; Spain.
- ah* Also at Joint Institute for Nuclear Research, Dubna; Russia.
- ai* Also at Louisiana Tech University, Ruston LA; United States of America.
- aj* Also at Manhattan College, New York NY; United States of America.
- ak* Also at Moscow Institute of Physics and Technology State University, Dolgoprudny; Russia.
- al* Also at National Research Nuclear University MEPhI, Moscow; Russia.
- am* Also at Physics Department, An-Najah National University, Nablus; Palestine.
- an* Also at Physics Dept, University of South Africa, Pretoria; South Africa.
- ao* Also at Physikalisches Institut, Albert-Ludwigs-Universität Freiburg, Freiburg; Germany.
- ap* Also at School of Physics, Sun Yat-sen University, Guangzhou; China.
- aq* Also at The City College of New York, New York NY; United States of America.
- ar* Also at TRIUMF, Vancouver BC; Canada.
- as* Also at Universita di Napoli Parthenope, Napoli; Italy.

* Deceased